UNIVERSIDADE FEDERAL DE PERNAMBUCO
CENTRO DE BIOCIÊNCIAS
PROGRAMA DE PÓS-GRADUAÇÃO EM BIOLOGIA VEGETAL

MARIA JUCICLÉA DOS SANTOS MEDEIROS

FLUXO DE SEIVA E DINÂMICA DE CARBOIDRATOS NÃO ESTRUTURAIS EM ESPÉCIES LENHOSAS DA CAATINGA

Recife
2025

MARIA JUCICLÉA DOS SANTOS MEDEIROS

FLUXO DE SEIVA E DINÂMICA DE CARBOIDRATOS NÃO ESTRUTURAIS EM ESPÉCIES LENHOSAS DA CAATINGA

Tese apresentada ao Programa de Pós-Graduação em Biologia Vegetal da Universidade Federal de Pernambuco, como requisito parcial para obtenção do título de doutora em Biologia Vegetal. Área de concentração: Ecologia e Conservação

Orientador (a): Mauro Guida dos Santos

Coorientador (a): André Luiz Alves de Lima

Recife

2025

.Catalogação de Publicação na Fonte. UFPE - Biblioteca Central

Medeiros, Maria Jucicléa Dos Santos.
Fluxo de seiva e dinâmica de carboidratos não estruturais em espécies lenhosas da caatinga / Maria Jucicléa Dos Santos Medeiros. - Recife, 2025.
144f.: il.

Tese (Doutorado) - Universidade Federal de Pernambuco, Centro de Biociências, Programa de Pós-Graduação em Biologia Vegetal, 2025.
Orientação: Mauro Guida dos Santos.
Coorientação: André Luiz Alves de Lima.
Inclui referências e apêndices.

1. Açúcares; 2. Densidade de madeira; 3. Decíduas; 4. Sempre verdes; 5. Semiárido; 6. Trocas gasosas. I. Santos, Mauro Guida dos. II. Lima, André Luiz Alves de. III. Título.

UFPE-Biblioteca Central

MARIA JUCICLÉA DOS SANTOS MEDEIROS

FLUXO DE SEIVA E DINÂMICA DE CARBOIDRATOS NÃO ESTRUTURAIS EM ESPÉCIES LENHOSAS DA CAATINGA

Tese apresentada ao Programa de Pós-graduação em Biologia Vegetal da Universidade Federal de Pernambuco, como requisito parcial para a obtenção do título de Doutora em Biologia Vegetal. Área de concentração: Ecologia e Conservação

Aprovada em 10/04/2025.

BANCA EXAMINADORA

_____
Prof. Dr. Mauro Guida dos Santos (Orientador)
Universidade Federal de Pernambuco

_____
Prof. Dr. Rafael Vasconcelos Ribeiro (Examinador Externo)
Universidade Estadual de Campinas

_____
Prof. Dr. Rivete Silva de Lima (Examinador Externo)
Universidade Federal da Paraíba

_____
Dra. Camila Dias Barros Medeiros (Examinadora Externa)
University of California

_____
Prof. Dr. José Romualdo de Sousa Lima (Examinador Externo)
Universidade Federal do Agreste de Pernambuco

AGRADECIMENTOS

Agradeço à Deus por sempre me dar forças ao longo da caminhada e por me conceder a realização desse sonho.

Agradeço em especial a minha família por não medir esforços para me ajudar quando precisei. À minha avó Maria Julieta pela educação que me deu, ao meu pai Romão Florentino de Medeiros pelo apoio, investimento em meus estudos e por acreditar em meus sonhos, à minha mãe Juscilene Maria pelo incentivo e por sempre rezar por mim, à minhas irmãs Jussara e Jaciária pelo carinho e incentivo.

Ao programa de Pós-Graduação em Biologia Vegetal (PPGBV) da UFPE, pela oportunidade de cursar meu doutorado e aos professores que fizeram parte dessa jornada compartilhando seus conhecimentos. Em especial ao professor Dr. Marciel Oliveira por sua contribuição nas bancas de revisão dos manuscritos durante as disciplinas de Seminários do PPGBV.

Agradeço também ao Programa de Pós-Graduação em Produção Vegetal da UFRPE/UAST, pelo apoio recebido como aluna visitante. Inclusive, o apoio do setor de transportes da UAST para idas à campo.

À Fundação de Amparo à Ciência e Tecnologia (FACEPE), pela concessão da bolsa de doutorado.

À Embaixada Francesa no Brasil e Campus France pela concessão da bolsa TerrEE 2024 para realização do doutorado sanduíche.

Ao Laboratório Physique et Physiologie Intégratives de l'Arbre en environnement Fluctuant (UMR PIAF) - French National Research Institute for Agriculture, Food and Environment (INRAE), e ao meu supervisor professor Dr. Hervé Cochard pelo apoio recebido durante meu doutorado sanduíche.

Agradeço ao meu orientador professor Dr. Mauro Guida Santos pelos ensinamentos, incentivo e por todo esforço dedicado para que essa pesquisa fosse concretizada.

Ao meu coorientador professor Dr. André Luiz Alves de Lima (meu pai acadêmico) pelo suporte, ensinamentos e a amizade construída ao longo de minha jornada acadêmica.

Ao meu orientador do mestrado professor Dr. Eduardo Soares de Souza que continuou dando suporte a pesquisa e me incentivando durante meu doutorado.

Aos parceiros de pesquisa que estiveram comigo desde o início: professor Dr. José Raliuson Inácio da Silva (suporte técnico), a querida MSc. Angela Lucena de Jesus e a Dra. Cynthia Wright.

Aos integrantes do Laboratório de Fisiologia Vegetal (LFV) da UFPE e do Núcleo de Estudos em Ecologia Funcional de Plantas (NEFPlan) da UFRPE/UAST pela troca de conhecimentos, pela ajuda fornecida em campo ou laboratório, pela amizade e momentos de descontração em meio a vida acadêmica. Em especial, agradeço a Cíntia Amando, Gabriel Ramos, Wilma Roberta, Marcela Albuquerque, Gleyce Melo, Joana Nicodemos, Juliana Barreto, Cauane Assunção, Mariana Santos e Renato Vanderley.

Aos amigos que fiz durante o Curso de Campo em Ecologia e Conservação da Caatinga (XIII ECCA), pela troca e experiência vivida.

Agradeço ao meu professor de Inglês, Jeff Sobral e a SoEnglish por todo incentivo e apoio quando precisei para o intercâmbio.

Agradeço aos amigos e amigas que tenho fora da Universidade que sempre estiveram dispostos a me ajudar. Em especial à Brígida Leal e Thayline Leite.

Agradeço a todos que de forma direta ou indireta contribuíram para conclusão de minha tese.

Gratidão!

RESUMO

Os eventos de seca têm causando danos ao funcionamento das plantas, alterações morfofisiológicas e a morte de espécies florestais por todo o mundo. Nas Florestas Tropicais Sazonalmente Secas (FTSS), os efeitos tendem a ser mais acentuados, devido a irregularidade das chuvas e alta demanda evaporativa que podem resultar em diferentes respostas ecofisiológicas entre os grupos funcionais de plantas. Diante disso, são necessários estudos que avaliem os efeitos da seca nas respostas das espécies ao longo do tempo, abordando diferentes grupos funcionais. O objetivo foi avaliar a dinâmica do fluxo de seiva e de carboidratos não estruturais (CNE) em árvores de diferentes grupos funcionais da Caatinga sob o efeito da sazonalidade. O trabalho foi realizado em uma área de caatinga em Serra Talhada-PE. Foram selecionadas seis espécies arbóreas: três de baixa densidade de madeira decídua (BDM), duas de alta densidade de madeira decíduas (ADM), uma sempre verde (SV) para a instalação de sensores de fluxo de seiva, as quais foram avaliadas por dois anos (2022 e 2023). Também foram realizadas medidas de potencial hídrico, trocas gasosas e observações fenológicas. Para determinação de CNE foram coletadas amostras de folhas, caule e raiz nas estações chuvosa e seca. O estudo foi dividido em três capítulos: I. Fluxo de seiva e dinâmica CNE em uma espécie em espécies de diferentes grupos funcionais durante a estação chuvosa e seca; II. Relações entre fotossíntese e resistência hidráulica em espécies de diferentes grupos funcionais da Caatinga; III. El Niño e La Niña podem modular o fluxo de seiva das árvores e a dinâmica de carboidratos não estruturais em uma floresta tropical seca. Os resultados indicam que as espécies respondem de maneira diferente na dinâmica de CNE e fluxo de seiva e que embora não haja correlação direta entre fotossíntese e condutividade hidráulica em espécies de BDM e ADM, há correlação entre outras características anatômicas e fisiológicas que nos ajudam a entender as estratégias de espécies de floresta seca da Caatinga. Existe uma diversidade hidráulica entre espécies coexistentes da Caatinga, o que mantém o funcionamento dos serviços ecossistêmicos e os efeitos das mudanças climáticas podem alterar o funcionamento desses ecossistemas em decorrência da falha hidráulica e redução das trocas gasosas. Além disso, a intensificação da seca causada pelo fenômeno El Niño pode reduzir até 70% as reservas de CNE nas raízes de espécies de BDM. Os resultados desta tese contribuem para o avanço do conhecimento no campo de pesquisa e oferecem novas abordagens e evidências que ampliam a compreensão sobre como ocorre a dinâmica de uso da água e de CNE das espécies da Caatinga.

Palavras-chave: açúcares, densidade de madeira, decíduas, sempre verdes, semiárido, trocas gasosas

ABSTRACT

Drought events have caused damage to plant function, morphophysiological changes and the death of forest species worldwide. In Seasonally Dry Tropical Forests (SDTF), the effects tend to be more pronounced, due to irregular rainfall and high evaporative demand, which can result in different ecophysiological responses among plant functional groups. Therefore, studies are needed to evaluate the effects of drought on species responses over time, addressing different functional groups. The objective was to evaluate the dynamics of sap flow and non-structural carbohydrates (NSC) in trees of different functional groups of the Caatinga under the effect of seasonality. The study was carried out in a caatinga area in Serra Talhada-PE. Six tree species were selected: three low wood density deciduous (LWD), two high wood density deciduous wood (HWD), and one evergreen (EV) for the installation of sap flow sensors, which were evaluated for two years (2022 and 2023). Measurements of water potential, gas exchange, and phenological observations were also performed. Leaf, stem, and root samples were collected in the rainy and dry seasons to determine NSC. The study was divided into three chapters: I. Sap flow and NSC dynamics in a species from different functional groups during the rainy and dry seasons; II. Relationships between photosynthesis and hydraulic resistance in species from different functional groups of the Caatinga; III. El Niño and La Niña can modulate tree sap flow and nonstructural carbohydrate dynamics in a tropical dry forest. The results indicate that species respond differently in the dynamics of NSC and sap flow and that although there is no direct correlation between photosynthesis and hydraulic conductivity in LWD and HWD species, there is a correlation between other anatomical and physiological characteristics that help us understand the strategies of dry forest species in the Caatinga. There is hydraulic diversity among coexisting species in the Caatinga, which maintains the functioning of ecosystem services, and the effects of climate change can alter the functioning of these ecosystems due to hydraulic failure and reduced gas exchange. In addition, the intensification of drought caused by the El Niño phenomenon can reduce NSC reserves in the roots of LWD species by up to 70%. The results of this thesis contribute to the advancement of knowledge in the field of research and offer new approaches and evidence that broaden the understanding of how the dynamics of water use and NSC of Caatinga species occur.

Keywords: sugars, wood density, deciduous, evergreen, semiarid, gas exchange

LISTA DE FIGURAS

ARTIGO 1 – PHOTOSYNTHESIS AND HYDRAULIC RESISTANCE: RELATIONSHIPS IN TREES OF DIFFERENT FUNCTIONAL GROUPS IN THE CAATINGA DRY FOREST

LISTA DE TABELAS

LISTA DE ABREVIATURAS E SIGLAS

WD – Densidade de madeira

NSC – Carboidratos não-estruturais

SS – Açúcar solúvel

Js – Velocidade do fluxo de seiva

gs – Condutância estomática

Ψ_{xylem} – Potencial hídrico do xilema

Kh – Condutividade hidráulica teórica da planta

Ks – Condutividade hidráulica específica do xilema

A – Taxa de Assimilação de CO_2

As – Área de xilema ativo

D – Diâmetro do vaso

XWT – Espessura da parede do vaso

VD – Densidade de vasos

VEL – Comprimento do elemento de vaso

VPD – Déficit de pressão de vapor

ET – Evapotranspiração Real

ΔSWS – Variação de água no solo

P – Precipitação

Sumário

INTRODUÇÃO

Períodos de seca severa têm ocorrido com mais frequência em decorrência do cenário de mudanças climáticas e isso vem sendo uma ameaça para as espécies florestais (ALLEN et al., 2017; IPCC, 2023), causando falha hidráulica pelos processos de embolia e cavitação induzida pela seca, que pode levar a morte de órgãos ou da planta inteira (Scoffoni et al., 2017). Em Florestas Tropicais Sazonalmente Secas (FTSS), estima-se que os efeitos da seca se tornem mais intensos devido à irregularidade das chuvas e alta demanda evaporativa, resultando em diferentes respostas da vegetação entre grupos funcionais de plantas, as quais podem ser tanto de tolerância das espécies, quanto de vulnerabilidade à mortalidade induzida pela seca (ALLEN et al., 2017). Uma forma bastante eficaz de avaliar os impactos do estresse é a partir da dinâmica do fluxo de seiva e de carboidratos não estruturais, já que estão diretamente envolvidos na resposta fisiológica de plantas à seca (Granier, 1985; Zhang et al., 2015a), entretanto, estudos com essa abordagem ainda são escassos para os diferentes grupos funcionais de plantas em FTSS (Zhang et al., 2015; Lima; Rodal 2010).

A dinâmica do fluxo de seiva é fundamental para entender as respostas das plantas de diferentes grupos funcionais no sistema ecohidrológico, pois a partir desta medida pode-se estimar a transpiração das árvores (Bosch et al., 2014). Outras medidas como potencial hídrico, condutância estomática e capacidade fotossintética formam um conjunto de traços funcionais coordenados que também contribuem para a compreensão da resposta fisiológica de plantas a flutuações no ambiente, e, se analisados em conjunto com características morfológicas da planta ajuda a responder questões sobre o controle no transporte de água (Vico et al., 2014).

Associado ao fluxo de seiva, os carboidratos não estruturais (NSC), como o amido e açúcares solúveis, refletem nas respostas ecofisiológicas das plantas, pois a progressão da seca também pode influenciar no armazenamento dos NSC (Zhang et al., 2015), portanto, analisar esses traços em conjunto ajudam a explicar as diferentes estratégias das espécies para tolerar a seca. Os NSC são importantes para o ajustamento osmótico, eliminação de espécies reativas de oxigênio e atuam como moléculas sinalizadoras do estresse (Santana-Vieira et al., 2016). Alguns estudos têm demonstrado que a dinâmica sazonal de carboidratos pode diferir entre espécies coexistentes com diferentes fenologias, as que mantém as folhas durante o ano, sempre verdes, e as que perdem as folhas totalmente em alguns meses do ano, decíduas (Palacio et al., 2018a), no entanto, esse padrão ainda foi estabelecido para espécies de FTSS. Além disso,

segundo Hartmann e Trumbore (2016), a seca não é só responsável pela quantidade de NSC armazenado, mas também pela variação em diferentes órgãos das árvores, ou seja, pode causar alterações na alocação e partição de NSC em raízes grossas, caules e galhos. Durante períodos de seca, espécies tolerantes tendem a alocar preferencialmente NSC para órgãos estruturais, como raízes e caules, favorecendo a manutenção da respiração, a integridade celular e a capacidade de rebrota após o déficit hídrico.

Para facilitar a inclusão de características fisiológicas em modelos mecanísticos e/ou hidrológicos, muitas vezes as plantas são classificadas em grupos funcionais (Calbi et al., 2024). Esses grupos são classificados com base em características morfológicas, fisiológicas e fenológicas, como a densidade de madeira e fenologia foliar (Lima; Rodal, 2010; Oliveira et al., 2015). Espécies com alta densidade da madeira (DM) tendem a apresentar menor condutividade hidráulica, mas maior resistência à cavitação, ou que conferem maior segurança hidráulica sob condições de déficit hídrico prolongado (Poorter et al., 2010). Em contraste, espécies com baixa densidade da madeira apresentam maior eficiência na condução de água e taxas de crescimento mais elevadas, porém com maior vulnerabilidade à disfunção hidráulica (Pineda-García et al., 2012; Poorter et al., 2019). Paralelamente, as espécies sempre-verdes adotam uma estratégia conservadora de uso da água, mantendo folhas e atividade fotossintética mesmo sob limitações hídricas moderadas, enquanto as espécies decíduas exibem uma estratégia de evitar a seca (Pineda-García et al., 2012; Souza et al., 2015), promovendo a senescência foliar durante a estação seca como forma de minimizar perdas por transpiração e retomar a maior atividade fisiológica apenas em condições mais favoráveis (Wright et al., 2021). Portanto, espécies de alta DM possuem maior estabilidade mecânica que promove maior resistência a processos de cavitação, enquanto que as decíduas de baixa DM possuem alta capacitância do xilema e uso de água mais eficiente durante a seca em regiões semiáridas, sendo assim, uma adaptação de baixo custo em relação as espécies sempre verdes (Pineda-García et al., 2012; Poorter et al., 2010).

Diante desse contexto, é essencial compreender quais mecanismos das plantas podem revelar como as espécies respondem às condições de seca (Venturas et al., 2017). Portanto, o objetivo desse trabalho é compreender como a dinâmica do fluxo de seiva e de carboidratos não estruturais em árvores nativas de diferentes grupos funcionais da Caatinga em função da sazonalidade.

FUNDAMENTAÇÃO TEÓRICA

Efeitos da seca em árvores de Florestas Tropicais Sazonalmente Secas (FTSS)

Estima-se que nas próximas décadas ocorra um aumento na temperatura do ar e redução da umidade do solo e do ar, em decorrência principalmente da falta de chuvas, fatores que tem levado à morte de espécies florestais, especialmente em regiões áridas (Allen et al., 2017). Em ambientes áridos ou semiáridos, os efeitos são mais drásticos devido às condições edáficas, elevadas temperaturas, alto déficit de pressão de vapor (DPV) e poucas chuvas, que causam danos no funcionamento hidráulico das árvores (Brodribb e Cochard, 2009).

Vários fatores abióticos tais como a baixa pluviosidade, elevada variabilidade espacial das chuvas e alto DPV, se analisados juntamente aos traços funcionais das árvores ajudam a entender os processos fisiológicos e a relação da vegetação com a disponibilidade hídrica em regiões semiáridas (Jiao et al., 2018; Markesteijn et al., 2011). Nas regiões semiáridas as espécies possuem uma ampla variedade de traços funcionais que favorecem diferentes estratégias para melhor aquisição, armazenamento e uso de água em período de maior restrição hídrica (Oliveira et al., 2015). Os efeitos da seca nas plantas são inúmeros, entretanto, as plantas apresentam diferentes respostas de enfrentamento a seca, tais como redução da condutância estomática para reduzir a perda de água pela transpiração e a manutenção de um potencial hídrico mais negativo durante os períodos de seca (Vico et al., 2014).

As respostas das plantas à seca podem ser definidas em três estratégias principais: escape, resistência e sensibilidade, que são determinadas por especificações específicas de características funcionais (Fletcher et al., 2022). De acordo com Fletcher et al. (2022), uma estratégia de fuga à seca é caracterizada por ajustes fenológicos que permitem à planta completar seu ciclo de vida ou apresentar sua fenofase reprodutiva antes do início da seca (Lima et al., 2021), sendo comum em espécies anuais (Fletcher et al., 2022) ou em ambientes com forte sazonalidade (Brito et al., 2022). A resistência à seca envolve mecanismos fisiológicos e morfológicos que permitem à planta tolerar ou minimizar os efeitos da escassez hídrica, como a capacidade de desenvolver raízes profundas, reduzir a condutância estomática e aumentar a eficiência no uso da água (Oliveira et al., 2021). Em contraste, uma sensibilidade à seca caracteriza espécies que, devido à sua alta taxa de crescimento e elevado consumo de água, possuem uma baixa capacidade de adaptação ao estresse hídrico, tornando-se mais vulneráveis à escassez de água (Grossiord et al., 2017; Fletcher et al., 2022). Essas estratégias podem

ocorrer em diferentes graus nas espécies, refletindo a variabilidade adaptativa ao ambiente (Fletcher et al., 2022).

Grupos funcionais de plantas: Densidade de madeira e fenologia foliar

As espécies que possuem atributos funcionais semelhantes tendem a se agrupar e desempenhar função ecológica semelhante no ambiente, caracterizando os grupos funcionais de plantas (Reich et al., 2003). Dentre os atributos funcionais que podem ser medidos para caracterizar o funcionamento de espécies de plantas em resposta ao ambiente, estão características morfológicas foliares (e.g., área foliar específica, deciduidade e longevidade foliar), características da madeira (e.g., densidade da madeira e espessura da casca) e da semente (e.g., massa e modo de dispersão) (Westoby et al., 2002).

A densidade da madeira (DM) é uma importante característica para determinação desses grupos, pois este é um traço chave para crescimento, sobrevivência e a estocagem de carbono pelas plantas (Poorter et al., 2019) e reflete nas estratégias globais de plantas e espectro global de economia de madeira (Chave et al., 2009). A DM está relacionada com o armazenamento de carbono por unidade de volume do caule e aos aspectos da estrutura hidráulica da planta, portanto, convergindo para diferentes grupos funcionais (Chave et al., 2009). Plantas de baixa DM possuem maior facilidade em armazenar água no caule, desta forma, podem obter maiores taxas de assimilação de carbono (Poorter et al., 2018, 2010). Já as plantas de alta DM possuem maior estabilidade mecânica devido à uma maior resistência da parede celular dos vasos do xilema ao colapso em caso de cavitação e à redução da condutividade hidráulica, causada pela presença de vaso com diâmetro menor (Hacke et al., 2001), promovendo maior resistência a processos de cavitação dos vasos xilemáticos (Pineda-García et al., 2012; Poorter et al., 2010).

Segundo Oliveira et al. (2015), os grupos funcionais de plantas diferem nas respostas aos fatores abióticos devido à grande variedade de atributos específicos das espécies em cada grupo, apresentando diferentes padrões em suas fenofases, em traços como a DM e capacidade de armazenamento de água no caule de espécies lenhosas. A coexistência desses grupos funcionais é possível devido aos *trade-offs* entre a grande variedade de traços para aquisição de recursos em FTSS (Guzman et al., 2017; Oliveira et al., 2015).

De acordo com Thomas et al. (2018), a abordagem de grupos funcionais permite agrupar espécies não apenas com base em sua taxonomia, mas com foco em características funcionais

que determinam como elas interagem com o ambiente e com outras espécies. Isso torna os grupos funcionais uma ferramenta útil para compreender o funcionamento de comunidades ecológicas, pois possibilita a identificação de padrões e processos que não seriam evidentes ao considerar apenas a composição taxonômica (Thomas et al., 2018; Calbi et al., 2024). A análise da diversidade funcional proporciona uma perspectiva mais mecanicista e preditiva sobre a dinâmica das comunidades (Calbi et al., 2024).

Os grupos funcionais de plantas podem ser classificados com base na DM (baixa ou alta DM) e fenologia foliar (decíduas ou sempre verdes) (Lima e Rodal, 2010). Desta forma, os grupos são representados por espécies lenhosas como grupo funcional de: espécies decíduas com baixa DM, espécies decíduas com alta DM e espécies sempre verdes com alta DM (Brito et al. 2022). Esses grupos ajudam a entender questões sobre as respostas das espécies frente à efeitos adversos, como por exemplo, condições de seca (Lima e Rodal, 2010; Souza et al., 2020)

A preocupação em entender os aspectos funcionais das plantas levou à classificação funcional das plantas com base em características fenológicas, densidade de madeira e relações hídricas (Borchert, 1994; Lima; Rodal, 2010; Souza et al., 2020) em FTSS, e mais recentemente, outros aspectos fisiológicos (fotossíntese) (Kannenberg and Phillips, 2020) e bioquímicos (Piper, 2011; Santos et al., 2021) tem sido considerado nos trabalhos para compreensão das estratégias de resposta à seca. No entanto, os mecanismos envolvidos na dinâmica de fluxo hídrico e NSC de espécies de diferentes grupos funcionais ainda não está clara.

Transporte de água na planta: Fluxo de seiva

O percurso de água das raízes até as folhas das árvores é longo e é explicado pela Teoria da Coesão-Tensão, na qual a coluna de água é mantida pelas forças de ligação entre moléculas de água (coesão) e a ligação de moléculas de água com uma superfície sólida (adesão), nesse caso, as paredes dos vasos xilemáticos, os quais são interconectados por pontoações que funcionam como "válvulas de segurança", impedindo a passagem de bolhas de ar (Venturas et al., 2017). Desta forma, a água é absorvida pelas raízes e percorre o caminho até as paredes celulares do mesofilo foliar através do xilema, sendo subsequentemente perdida para a atmosfera por meio dos estômatos no processo de transpiração para captura de CO_2 (Tomasella et al., 2020). No entanto, para manter a fotossíntese sob baixa disponibilidade hídrica, a planta normalmente reduz seu potencial hídrico (Ψw) afim de gerar uma diferença de pressão negativa

entre a raiz e o solo para permitir a captação de água, causando um aumento da tensão nos vasos condutores (Venturas et al., 2017). Esse processo pode ocasionar a formação de embolia (acúmulo de nano bolhas de ar) em vasos xilemáticos e consequentemente, redução da condutividade hidráulica (Schenk et al., 2015).

Atributos hidráulicos como a eficiência do xilema no transporte de água (condutividade hidráulica específica, *Ks*), condutividade hidráulica da planta (*Kh*) e o fluxo de seiva (*Js*) são características funcionais-chave para entender as estratégias das plantas frente à disponibilidade hídrica (Bhusal et al., 2019; Steppe et al., 2015). Esses atributos refletem a capacidade das espécies de absorver e transportar água do solo até as folhas, influenciando diretamente seu desempenho fisiológico, crescimento e tolerância ao estresse hídrico (Markesteijn et al., 2011). Espécies com alta *Ks* e *Js* tendem a ter um transporte mais eficiente, em condições alta disponibilidade hídrica, mas geralmente apresentam maior vulnerabilidade à cavitação sob seca severa (Rosner et al., 2019). Por outro lado, espécies com baixa condutividade e fluxo de seiva geralmente adotam estratégias mais conservadoras, com maior segurança hidráulica, com maior tolerância a seca (Poorter et al., 2010). Assim, esses atributos hidráulicos permitem identificar diferentes estratégias adaptativas ao longo dos gradientes ambientais e são fundamentais para compreender as respostas funcionais das comunidades vegetais a eventos de seca (Markesteijn et al., 2011).

O transporte de seiva no xilema não é controlado somente pelas forças físicas, mas também por processos metabólicos, tal como o metabolismo carboidratos não estruturais (NSC) (Nardini et al., 2011). que contribuem para a regulação do potencial osmótico da seiva do xilema (O'Brien et al., 2014; Tomasella et al., 2020). Árvores tropicais, por exemplo, podem ser mais tolerantes à seca quando acumulam NSC em seus caules pois, desta forma, retém mais água devido a diferença de potenciais osmóticos, mantendo maiores Ψw (O'Brien et al., 2014; Tomasella et al., 2020).

Papel dos carboidratos não estruturais (NSC) nas relações hídricas das árvores

As árvores realizam o transporte de água a longa distância constantemente para obtenção de CO_2 que será usado na fotossíntese. Nesse momento, acabam perdendo muita água para atmosfera, o que pode causar a dessecação de seus tecidos, assim, as árvores precisam captar mais água para manter os tecidos hidratados e evitar colapso dos seus sistemas hidráulicos (Vico et al., 2014; Venturas; Sperry; Hacke, 2017). A fotossíntese é o principal processo responsável pela fixação de carbono atmosférico e produção de açúcares nas plantas,

os quais, quando não utilizados imediatamente para crescimento e respiração, são armazenados como NSC (Zhang et al., 2015). Desta forma, os NSC representam uma forma de reserva de carbono assimilado, sendo formados a partir de produtos da fotossíntese e acumulados em diferentes órgãos da planta (Smith et al., 2018). Em condições adequadas, a taxa fotossintética excede a demanda metabólica, promovendo o acúmulo de NSC; entretanto, sob efeito da seca, o fechamento estomático limita a absorção de CO_2 e reduz a fotossíntese, forçando a planta a mobilizar essas reservas para manter funções (Piper, 2011). Portanto, a dinâmica de NSC está intimamente relacionada à atividade fotossintética e a manutenção fisiológica da planta em diversos ambientes (Zhang et al., 2015a).

Os NSC compreendem principalmente açúcares solúveis de baixo peso molecular, como glicose, frutose e sacarose, além de polissacarídeos de reserva, como o amido (Hartmann e Trumbore, 2016). Esses compostos são metabolicamente disponíveis e acumulados em tecidos parenquimáticos de diferentes órgãos da planta, incluindo folhas, ramos, tronco e raízes (Piper, 2011). Os NSC desempenham um papel central na manutenção da homeostase metabólica, atuando como fonte de carbono e energia para processos fisiológicos essenciais, particularmente sob condições de déficit hídrico, quando a atividade fotossintética está comprometida (Tomasella et al., 2020).

Adicionalmente, os NSC são fundamentais para os processos metabólicos das plantas e desempenham diferentes papeis funcionais (Tomasella et al., 2020), tais como metabolismo energético, transporte e osmorregulação, além de fornecer substratos para produção de compostos de defesa ou aquisição de nutrientes (Hartmann e Trumbore, 2016). Porém a seca pode promover uma redução nas reservas de carboidratos devido a limitação da fotossíntese, a qual diminui o nível de fotoassimilados, levando a depleção de carbono. Desta forma, se a seca continuar, haverá uma demanda metabólica maior que não é mais atendida pela fotossíntese, resultando em um desequilíbrio de carbono que pode se tornar irreversível (Piper, 2011). Entretanto, mesmo que a redução de carbono continue, o esgotamento nem sempre irá ocorrer, pois alguns estudos demonstraram que espécies mais adaptadas à seca são capazes de acumular reservas de carbono (Piper, 2011).

As árvores adotam diferentes estratégias de armazenamento NSC em seus diferentes órgãos, o que influencia sua capacidade de tolerar e se recuperar da seca (Palacio et al., 2018). Enquanto algumas espécies concentram reservas principalmente em raízes, outras priorizam o tronco, os ramos ou até mesmo as folhas (Chuste et al., 2020). Essa variação reflete diferenças

na dinâmica de uso e acesso às reservas durante o déficit hídrico (Hartmann e Trumbore, 2016). Durante a seca, os NSC podem ser mobilizados dos tecidos de armazenamento, como o parênquima do caule ou das raízes para sustentar processos essenciais, como respiração, manutenção celular e crescimento de raízes (Piper, 2011). O órgão de armazenamento e a concentração de NSC reservada determinam em grande parte a resiliência da planta, permitindo que ela suporte a redução da fotossíntese e preserve funções afetadas até que as condições sejam favoráveis para a planta (Palacio et al., 2018; Rosell et al., 2021).

Alguns estudos por exemplo, sugerem que algumas espécies são mais susceptíveis ao esgotamento de carbono, pois fecham seus estômatos rapidamente frente às condições de déficit hídrico, evitando o baixo Ψw, enquanto outras espécies toleram mais às condições de estresse e fecham seus estômatos mais tarde, mantendo baixo Ψw (McDowell et al., 2008). No entanto, são necessárias mais pesquisas para uma melhor compreensão sobre as variações no armazenamento de carbono entre os diferentes grupos funcionais de plantas, pois o balanço do carbono é controlado por diversos mecanismos fisiológicos em resposta à seca e não apenas resultado de alguns mecanismos como a fotossíntese e o Ψw (Sala et al., 2010).

REFERÊNCIAS BIBLIOGRÁFICAS

ALLEN, K. et al. Will seasonally dry tropical forests be sensitive or resistant to future changes in rainfall regimes? **Environmental Research Letters**, v. 12, n. 2, 2017.

BHUSAL, N.; HAN, S. G.; YOON, T. M. Impact of drought stress on photosynthetic response, leaf water potential, and stem sap flow in two cultivars of bi-leader apple trees (Malus × domestica Borkh.). **Scientia Horticulturae**, v. 246, n. July 2018, p. 535–543, 2019.

BOSCH, D. D.; MARSHALL, L. K.; TESKEY, R. Forest transpiration from sap flux density measurements in a Southeastern Coastal Plain riparian buffer system. **Agricultural and Forest Meteorology**, v. 187, p. 72–82, 2014.

BRITO, N. D. DA S. et al. Drought response strategies for deciduous species in the semiarid Caatinga derived from the interdependence of anatomical, phenological and bio-hydraulic attributes. **Flora: Morphology, Distribution, Functional Ecology of Plants**, v. 288, 1 mar. 2022.

BRODRIBB, T. J.; COCHARD, H. Hydraulic failure defines the recovery and point of death in water-stressed conifers. **Plant Physiology**, v. 149, n. 1, p. 575–584, 2009.

CALBI, M. et al. A novel framework to generate plant functional groups for ecological modelling. **Ecological Indicators**, v. 166, n. March, p. 112370, 2024.

CHAVE, J. et al. Towards a worldwide wood economics spectrum. **Ecology Letters**, v. 12, n. 4, p. 351–366, 2009.

CHUSTE, P. A. et al. Sacrificing growth and maintaining a dynamic carbohydrate storage are key processes for promoting beech survival under prolonged drought conditions. **Trees - Structure and Function**, v. 34, n. 2, p. 381–394, 2020.

DE GUZMAN, M. E. et al. Trade-offs between water transport capacity and drought resistance in neotropical canopy liana and tree species. **Tree Physiology**, v. 37, n. 10, p. 1404–1414, 2017.

DE OLIVEIRA, C. C. et al. Functional groups of woody species in semi-arid regions at low latitudes. **Austral Ecology**, v. 40, n. 1, p. 40–49, 1 fev. 2015.

FLETCHER, L. R. et al. Testing the association of relative growth rate and adaptation to climate across natural ecotypes of Arabidopsis. **New Phytologist**, v. 236, n. 2, p. 413–432, 2022.

GRANIER, A. Une nouvelle méthode pour la mesure du flux de sève brute dans le tronc des arbres. **Annales des Sciences Forestières**, v. 42, n. 2, p. 193–200, 1985.

GROSSIORD, C. et al. Tree water dynamics in a drying and warming world. **Plant Cell and Environment**, v. 40, n. 9, p. 1861–1873, 2017.

HARTMANN, H.; TRUMBORE, S. Understanding the roles of nonstructural carbohydrates in forest trees - from what we can measure to what we want to know. **The New phytologist**, v. 211, n. 2, p. 386–403, 2016.

IPCC (Intergovernmental Panel on Climate Change). 2024.

JIAO, L. et al. Evapotranspiration partitioning and its implications for plant water use strategy: Evidence from a black locust plantation in the semi-arid Loess Plateau, China. **Forest Ecology and Management**, v. 424, p. 428–438, set. 2018.

KANNENBERG, S. A.; PHILLIPS, R. P. Non-structural carbohydrate pools not linked to hydraulic strategies or carbon supply in tree saplings during severe drought and subsequent recovery. **Tree Physiology**, v. 40, n. 2, p. 259–271, 2020.

LIMA, A. L. A. DE et al. Phenology of high- and low-density wood deciduous species responds differently to water supply in tropical semiarid regions. **Journal of Arid Environments**, v. 193, n. July, 2021.

MARKESTEIJN, L. et al. Hydraulics and life history of tropical dry forest tree species: Coordination of species' drought and shade tolerance. **New Phytologist**, v. 191, n. 2, p. 480–495, 2011a.

MARKESTEIJN, L. et al. Ecological differentiation in xylem cavitation resistance is associated with stem and leaf structural traits. **Plant, Cell and Environment**, v. 34, n. 1, p. 137–148, 2011b.

MCDOWELL, N. et al. Mechanisms of plant survival and mortality during drought: why do some plants survive while others succumb to drought? **New Phytologist**, v. 178, n. 4, p. 719–739, 14 jun. 2008.

NARDINI, A.; SALLEO, S.; JANSEN, S. More than just a vulnerable pipeline: xylem physiology in the light of ion-mediated regulation of plant water transport. **Journal of Experimental Botany**, v. 62, n. 14, p. 4701–4718, 2011.

O'BRIEN, M. J. et al. Drought survival of tropical tree seedlings enhanced by non-structural carbohydrate levels. **Nature Climate Change**, v. 4, n. 8, p. 710–714, 2014.

OLIVEIRA, C. C. DE et al. Functional groups of woody species in semi-arid regions at low latitudes. **Austral Ecology**, v. 40, n. 1, p. 40–49, 1 fev. 2015.

OLIVEIRA, R. S. et al. Linking plant hydraulics and the fast–slow continuum to understand resilience to drought in tropical ecosystems. **New Phytologist**, v. 230, n. 3, p. 904–923, 2021.

PALACIO, S. et al. Are storage and tree growth related? Seasonal nutrient and carbohydrate dynamics in evergreen and deciduous Mediterranean oaks. **Trees - Structure and Function**, v. 32, n. 3, p. 777–790, 2018a.

PALACIO, S. et al. Are storage and tree growth related? Seasonal nutrient and carbohydrate dynamics in evergreen and deciduous Mediterranean oaks. v. 32, p. 777–790, 2018b.

PINEDA-GARCÍA, F.; PAZ, H.; MEINZER, F. C. Drought resistance in early and late secondary successional species from a tropical dry forest: The interplay between xylem resistance to embolism, sapwood water storage and leaf shedding. **Plant, Cell and Environment**, v. 36, n. 2, p. 405–418, 2012.

PIPER, F. I. Drought induces opposite changes in the concentration of non-structural carbohydrates of two evergreen Nothofagus species of differential drought resistance. **Annals of Forest Science**, v. 68, n. 2, p. 415–424, 2011.

POORTER, L. et al. The importance of wood traits and hydraulic conductance for the performance and life history strategies of 42 rainforest tree species - Poorter - 2009 - New Phytologist - Wiley Online Library. **New Phytologist**, n. 185, p. 481–492, 2010.

POORTER, L. et al. Can traits predict individual growth performance? A test in a hyperdiverse tropical forest. **New Phytologist**, v. 219, n. 1, p. 109–121, 1 jul. 2018.

POORTER, L. et al. Wet and dry tropical forests show opposite successional pathways in wood density but converge over time. **Nature Ecology and Evolution**, v. 3, n. 6, p. 928–934, 2019.

REICH, P. B. et al. The evolution of plant functional variation: Traits, spectra, and strategies. **International Journal of Plant Sciences**, v. 164, n. SUPPL. 3, 2003.

ROSELL, J. A. et al. Inner bark as a crucial tissue for non-structural carbohydrate storage across three tropical woody plant communities. **Plant Cell and Environment**, v. 44, n. 1, p. 156–170,

2021.

ROSNER, S. et al. Prediction of hydraulic conductivity loss from relative water loss: new insights into water storage of tree stems and branches. **Physiologia Plantarum**, v. 165, n. 4, p. 843–854, 2019.

SALA, A.; PIPER, F.; HOCH, G. Physiological mechanisms of drought-induced tree mortality are far from being resolved. **New Phytologist**, v. 186, n. 2, p. 274–281, 25 abr. 2010.

SANTOS, M. et al. Whole plant water status and non-structural carbohydrates under progressive drought in a Caatinga deciduous woody species. **Trees**, n. 0123456789, 2021.

SCHENK, H. J.; STEPPE, K.; JANSEN, S. Nanobubbles: A new paradigm for air-seeding in xylem. **Trends in Plant Science**, v. 20, n. 4, p. 199–205, 2015.

SCOFFONI, C. et al. Leaf vein xylem conduit diameter influences susceptibility to embolism and hydraulic decline. **New Phytologist**, v. 213, n. 3, p. 1076–1092, 2017.

SMITH, M. G. et al. Whole-tree distribution and temporal variation of non-structural carbohydrates in broadleaf evergreen trees. **Tree Physiology**, v. 38, n. 4, p. 570–581, 2018.

SOUZA, B. C. DE et al. Divergências funcionais e estratégias de resistência à seca entre espécies decíduas e sempre verdes tropicais. **Rodriguesia**, v. 66, n. 1, p. 21–32, 2015.

STEPPE, K. et al. Sap flow as a key trait in the understanding of plant hydraulic functioning. **Tree Physiology**, v. 35, n. 4, p. 341–345, 2015.

TOMASELLA, M. et al. The possible role of non-structural carbohydrates in the regulation of tree hydraulics. **International Journal of Molecular Sciences**, v. 21, n. 1, 2020.

VENTURAS, M. D.; SPERRY, J. S.; HACKE, U. G. Plant xylem hydraulics: What we understand, current research, and future challenges. **Journal of Integrative Plant Biology**, v. 59, n. 6, p. 356–389, 2017.

VICO, G. et al. Climatic, ecophysiological, and phenological controls on plant ecohydrological strategies in seasonally dry ecosystems. **Ecohydrology**, v. 8, n. 4, p. 660–681, 2014.

WESTOBY, M. et al. Plant ecological strategies: Some leading dimensions of variation between species. **Annual Review of Ecology and Systematics**, v. 33, p. 125–159, 2002.

WRIGHT, C. L. et al. Plant functional types broadly describe water use strategies in the

Caatinga, a seasonally dry tropical forest in northeast Brazil. **Ecology and Evolution**, v. 11, n. 17, p. 11808–11825, 2021.

ZHANG, T. et al. Non-structural carbohydrate dynamics in Robinia pseudoacacia saplings under three levels of continuous drought stress. **Trees - Structure and Function**, v. 29, n. 6, p. 1837–1849, 2015.

Artigo 1 - Photosynthesis and hydraulic resistance: Relationships in trees of different functional groups in the Caatinga dry forest

Authors:*Maria Medeiros[1]; Angela Lucena Nascimento de Jesus[2]; José Raliuson Inácio Silva[2]; Cíntia Amando[1]; Maria Marceliane da Silva[2]; Hugo Rafael Bentzen Santos[2]; Sérgio Luiz Ferreira-Silva[2]; Eduardo Souza[2]; André Luiz Alves de Lima[2]; Hervé Cochard[3]; Mauro Guida Santos[1]

[1]Department of Botany, Bioscience Center, Federal University of Pernambuco, Recife, PE, Brazil.

[2]Federal Rural University of Pernambuco, Serra Talhada Academic Unit, Serra Talhada, PE, Brazil.

[3]Université Clermont Auvergne, INRAE, PIAF, 63000 Clermont-Ferrand, France.

*Corresponding author: *Maria Jucicléa dos S. Medeiros*, maria.juciclea@ufpe.br

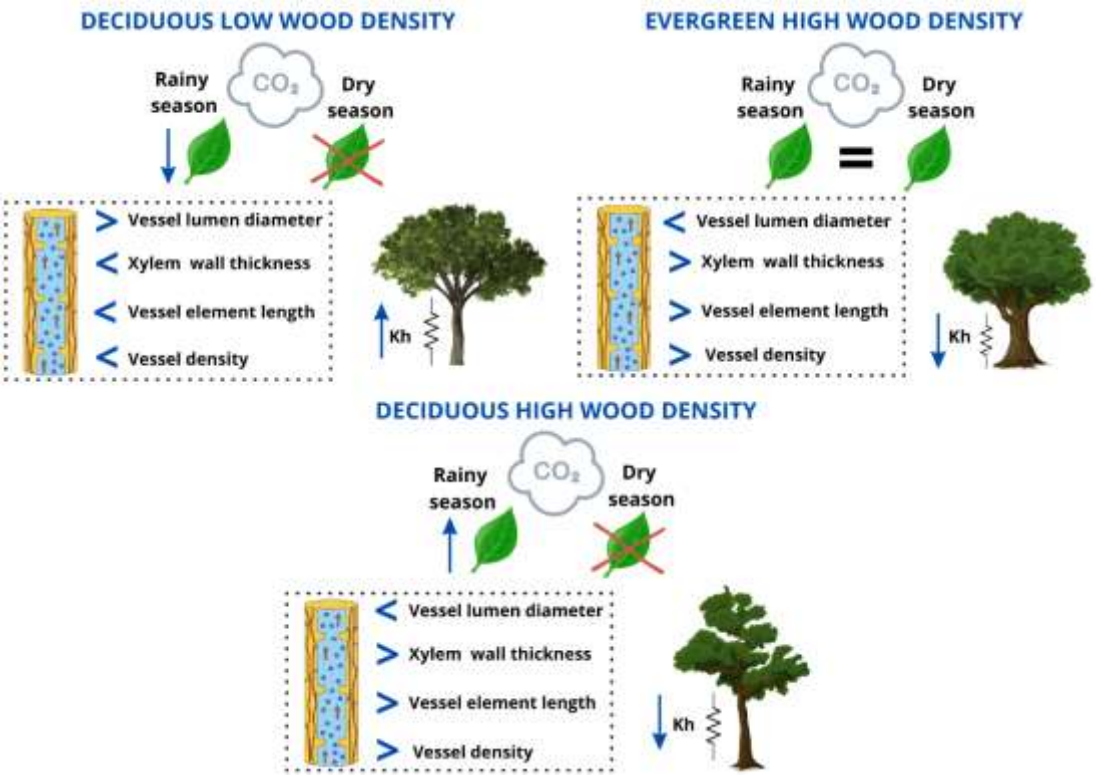

Graphical abstract. Representation of functional groups. Kh: theoretical hydraulic conductivity, *A*: CO_2 assimilation rate. Upward arrows indicate increase and downward arrows indicate decrease, > means greater, < means less, = means equal.

Abstract

Drought has put the survival of forest species at risk due to hydraulic failure and reduced photosynthetic rates. Our objective was to characterize the relationship between photosynthesis and the hydraulic characteristics of the stem xylem of species belonging to different functional groups: low deciduous wood density (LWD); high deciduous wood density (HWD); evergreen (EH), in a dry forest from Brazil. We hypothesized that LWD species have high theoretical hydraulic conductivity (K_h) and rate of CO_2 assimilation (*A*) in the rainy season; HWD have greater resistance to embolism and lower *A*; EH species have high resistance to embolism and maintain moderate *A* in both rainy and dry seasons. We measured *A*, wood anatomy, and sap flow to calculate K_h. The *A* carried out in the rainy season was highest in *C. pyramidale* (HWD) (14.90±0.48 µmol CO_2 m^{-2} s^{-1}), while *S. joazeiro* (EH), presented the lowest mean value (8.94±2.80 µmol CO_2 m^{-2} s^{-1}). The K_h was higher in the LWD ($1.31E^{-06}$±$1.59E^{-06}$ cm^2 h^{-1} MPa^{-1}) and lower in EH ($3.81E^{-07}$±$3.96E^{-07}$ cm^2 h^{-1} MPa^{-1}) e HWD ($9.37E^{-08}$±$1.07E^{-07}$ cm^2 h^{-1} MPa^{-1}). The correlation matrix showed that there is no correlation between the *A* and K_h in the functional groups. However, there is a correlation between other anatomical and physiological traits that help us understand the strategies of the species. Species LWD may not present high *A* even in the rainy season, to avoid damage to the hydraulic system. The EH has moderate *A* throughout the year and anatomical and physiological traits, such as greater xylem wall thickness and smaller diameter vessel lumen that promote high tolerance to drought. Therefore, there is hydraulic diversity between coexisting species, which maintains the functioning of ecosystem services. The effects of climate change can change the functioning of these ecosystems as a result of hydraulic failure and reduced gas exchange.

Keywords: deciduous, evergreen, hydraulic conductivity, phenology, seasonality, wood density

Introduction

Tropical dry forests present a challenging environment for plants due to water scarcity, and climate forecasts indicate that drought in these forests is likely to intensify (Anderegg et al. 2017, Intergovernmental Panel on Climate Change (IPCC) 2023). This puts the survival of forest species at risk, as they face the difficulty of overcoming hydraulic failure during periods of water deficit (Bréda et al. 2006, Brodribb and Cochard 2009, Allen et al. 2017). The lack of available water in the soil compromises the ability of trees to maintain water flow through the

xylem, resulting in reduced rates of transpiration and photosynthesis (Wang et al. 2016). To cope with drought conditions, trees have developed adaptation strategies, including changes in morphological and physiological traits that can promote hydraulic safety (Meinzer et al. 2009, Markesteijn, Poorter, Bongers, et al. 2011). Thus, plants can present drought resistance mechanisms, such as control of gas exchange and investment in anatomical characteristics of xylem vessels that promote efficiency and safety in water transport (Sperry 2000, Mcdowell et al. 2008, Janssen et al. 2020).

Water transport and photosynthetic activity are intrinsically linked processes, although they are distinct in nature (Brodribb 2009). Photosynthesis leads to significant loss of water by leaves through transpiration, in exchange for CO_2 uptake (Xu et al. 2021). It is critical that this water loss is compensated by the continuous supply of water from the soil, otherwise there will be desiccation and damage to the photosynthetic apparatus (Eamus 1999, Ryan et al. 2006), as well as, damage to the hydraulic system (Brunner et al. 2015). The transport of water through the vascular system of plants encounters resistance to flow, and to overcome this resistance the leaves create a tension in the water column of the xylem, driven by capillary forces and the cohesive properties of water (Blackman et al. 2009, Brodribb and Cochard 2009). However, drought can cause the entry of air bubbles that are capable of forming embolism, interrupting the continuous flow of water (Sperry and Tyree, 1988). Therefore, hydraulics also play a limiting role in the photosynthesis of trees, because hydraulic characteristics are related to the rate of carbon assimilation, since there is control of stomatal conductance to prevent embolism, there is also a reduction in CO_2 uptake (Venturas et al. 2017). However, the mechanisms involved in this process have not yet been fully elucidated, especially in different species of dry forests.

One functional trait that is linked to xylem characteristics is wood density (Chave et al. 2009, Poorter et al. 2010). This trait is associated with growth, survival, and carbon storage (Chave et al. 2009). In addition, it is an important trait for determining the functional groups of plants, in which species tend to group together and perform a similar ecological function in the environment (Reich et al. 2003). In this way, the plants can be classified as being of low or high wood density (Poorter et al. 2010, 2019). Plants with low density have more acquisitive strategies when resources are available and it is easier to store water in the stem, obtaining higher rates of carbon assimilation (Wright et al. 2004, Chave et al. 2009, Poorter et al. 2018). On the other hand, plants with high density are considered conservative, have greater

mechanical stability and greater resistance to cavitation processes of the xylem vessels (Markesteijn, Poorter, Paz, et al. 2011, Pineda-García et al. 2012).

The characteristics of xylem are typically related to the hydraulic conductivity of the plant (Janssen et al. 2020), xylem capacitance (Carrasco et al. 2014), and consequently, they also relate to wood density (Lima et al. 2018). Trees with low wood density have xylem vessels with thinner cell walls and large lumen areas and may have low resistance to embolism (Choat et al. 2005, Johnson and Brodribb 2023), however, the larger lumen area may contribute to higher xylem capacitance (Hacke et al. 2001). On the other hand, trees with a higher wood density have xylem vessels with thicker cell walls and smaller lumen areas (Hajek et al. 2014), however, they have a higher density of vessels that promote greater resistance to embolism (support more negative xylem water potential) and have low xylem capacitance (Sperry et al. 2003, Hoeber et al. 2014, Johnson and Brodribb 2023).

In addition to the characteristics of wood that help us understand the strategies of species for drought tolerance, there are phenological strategies, in which trees can be classified as deciduous (lose their leaves at the beginning of the dry season) or evergreen (remain with leaves throughout the year) (Eamus 1999, Choat et al. 2005). Deciduous species are considered drought “avoiding”, as they lose their leaves to prevent transpiration, conserving water during the dry season. In contrast, evergreen plants, which retain their leaves throughout the year, possess the ability to "tolerate" drought while maintaining photosynthetic activity and optimizing water absorption even under conditions of low water availability (Wright et al. 2004, Choat et al. 2005, Markesteijn, Poorter, Bongers, et al. 2011). Considering phenological and morphophysiological data, the species, forest species can be classified as: low density of deciduous wood (LWD); high density deciduous wood (HWD) and high density evergreen wood (EH) (Lima et al. 2021, Souza et al. (2020).

Although some studies have shown that there is a trade-off between embolism resistance and xylem capacitance or growth (Pineda-García et al. 2012, Mencuccini et al. 2019, Johnson and Brodribb 2023), only a few studies have linked resistance to embolism to traits such as photosynthesis of forest species (Xu et al. 2021, Wei et al. 2023), there is no link between hydraulic traits and the photosynthesis of different functional groups, especially when conducting field experiments with adult plants from dry forests.

Dry forests are ideal ecosystems for assessing ecophysiological responses to climate change (Corlett 2016), in particular, the Brazilian Caatinga is a dry forest marked by the strong

seasonality of rainfall, in which trees are always facing a dilemma to maintain hydraulic safety (Lima et al. 2018, Pinho et al. 2019). Our objective was to characterize the relationship between photosynthesis and hydraulic characteristics of the stem xylem of species belonging to different functional groups: LWD, HWD and EH in a dry forest in Brazil. We hypothesized that LWD species have high hydraulic conductivity and high photosynthetic rate in the rainy season; HWD species have higher resistance to embolism and lower photosynthetic rate; EH species has high resistance to embolism and maintains moderate photosynthetic rate in both rainy and dry seasons.

Material and methods

Study Site

The experiment was conducted at Fazenda Buenos Aires (07° 56'50" S e 38° 23'29" W), Serra Talhada, Pernambuco, Brazil (Fig 1). According to Köppen, the local climate is of the BSh' type (hot semi-arid climate). The average annual rainfall is around 632 mm, with the rainy period concentrated in the months of January to April and is responsible for 65% of annual rainfall. Average monthly air temperatures range between 23.6 and 27.7 °C and maximum temperatures reach values above 32 °C (Pereira et al. 2015).

Meteorological variables

We obtained rainfall and vapor pressure deficit (VPD) data provided by an 11 m high flow tower (3 m above the tree canopy) installed in the study area. Relative humidity and air temperature were measured by (EE181-L, Cambpell Scientific). Total rainfall was measured with a rain gauge (model TE 525 WS-L, Texas Electronics, Dallas, TX, USA). Data were recorded by a data logger (model CR1000, Campbell Scientific Inc., Logan, UT, USA) every 1 minute (Silva et al. 2017).

Soil water storage (SWS)

TDR-type sensors (CS616, Campbell Scientific) (Silva et al., 2017) introduced horizontally in the soil profile allowed the measurement of the volumetric soil water content up to 40 cm deep, being used to determine soil water storage (SWS, mm):

$$SWS = \sum(\theta_n \Delta Z_n) \qquad \text{Eq 1}$$

here θ is the volumetric water content of the soil, ΔZ is the soil depth interval, and the subscript n indicates the number of soil layers (up to 5).

Species selection

The low-density deciduous wood functional group (LWD) was composed of the following species: *Commiphora leptophloeos*; *Amburana cearensis, Spondias tuberosa* and the high-density group of deciduous wood (HWD): *Cenostigma pyramidale* and *Aspidosperma pyrifolium*; high density of evergreen wood (EH): *Sarcomphalus joazeiro*, with four trees of each species (Table 1), in which gas exchange and anatomical measurements were performed. Gas exchange measurements were performed in the rainy season for all species and in the dry season they were performed for the evergreen species. The collection of material for the anatomical measurements of the stem was carried out only once during the 2023 rainy season.

Wood density

At the ends of the tree branches, samples of branches were collected with approximately 2 cm thickness and 2 cm in length. These samples were peeled off and immersed in distilled water until saturated over a 24-hour period (Pérez-Harguindeguy et al. 2013).

Subsequently, the twig samples were dried in an oven at a temperature of 70 °C for a period of 72 hours. The determination of wood density (WD) was performed by means of the dipping method, which is based on Archimedes' principle. This involved measuring the dry mass of the wood sample (m, g) by weighing, and determining its volume (v, cm^3) by immersing the sample in a container with distilled water, kept at rest on a digital scale with an accuracy of 0.001 g. The density of the wood was calculated as WD = m/v, following the procedure established by Pérez-Harguindeguy et al. (2013).

Gas exchange measurements

We measured net photosynthesis (*A*) with an infrared gas analyzer (IRGA) model CI-340, manufacturer CID Bio-Science. Measurements were made on two days under full sun, between 9 and 10 am on 3 fully expanded and healthy leaves of each tree of all species in the rainy season, and during the dry season measurements were made on the evergreen species. We measured stomatal conductance (gs) on two fully expanded leaves of each tree in the morning (9–10 am) using a porometer (Decagon Devices, Inc. 2365 NE Hopkins Court Pullman WA 99163).

Xylem water potential

We measured xylem water potential (Ψ_x) before dawn (4–5 am, predawn) and at noon (12–13 pm, midday) using a Scholander chamber (PMS Instrument Company, 1505D).

Xylem anatomy

We collected three samples from the stem of each species using an incremental auger to determine the anatomical characteristics of the xylem (Fig. SI) (Vieira and Lisi 2019). The auger was inserted just before the first fork of the trunk in order to collect a sample that included the bark, sapwood and heartwood of the main trunk (Vieira and Lisi 2019). The samples were stored in microtubes with 50% FAA solution for 72 hours, and then placed in a 70% alcoholic solution (Johansen 1940).

The stored samples were subjected to a dehydration process using alcohol at concentrations of 80%, 85%, 90% and 95%, as described by Johansen in 1940. Then, the pre-infiltration stage was performed, in which the samples were prepared for resin infiltration. They were placed on a magnetic stirrer along with a base resin and an activator powder for fixation, and then stored in a desiccator to allow the activator powder to act. In the polymerization phase, aiming at the hardening of the product, the resin was mixed again in a magnetic stirrer and the hardener was added to the mixture. Subsequently, this mixture was deposited in Histomold molds made of polyethylene, following the protocol established in the Historesina kit.

After this process, the molds were placed in an oven with air circulation and kept at a temperature of 103°C for 24 hours for drying. The historesin blocks were fixed on wooden bases and then cut in a semi-automatic microtome (CUT-5062) to obtain sections with a thickness of 6 μm. The sections obtained were stained with toluidine blue for structural analysis purposes and then fixed using "Entellan" medium assembly from MERCK (Johansen 1940, Parker et al. 1982) From these sections, permanent slides were prepared, as described by Parker et al. 1982.

Then, the samples were photographed using a digital camera coupled to an LX 50 optical microscope, and the images were evaluated with the aid of the Image-pro Plus 4.5.0.29 software (Danuser 1999). Thus, anatomical measurements of the xylem were performed: diameter of the vessels, length of the vessel elements, wall thickness and frequency of the conductive vessels.

Sapwood area

We made two holes with a 5 mm diameter drill just below the bifurcation point of the main stem, in opposite positions of each tree. The radial holes reached a depth of 5 cm, and

through them, the methylene blue dye was introduced using a syringe. This allowed the dye to move through the conducting vessels, following the flow of the xylem (Andrade et al. 2005). After a period of two hours, a wood sample with a diameter of 5 mm and a radial length of 5 cm was collected, using an increment auger, at a distance of 5 cm above the perforation where the dye was inserted (Figure SI), as described by Chave (2005). To determine the area of the active xylem, the circumference of the tree stem was also measured. The collected samples were documented by means of photographs and, subsequently, the cross-sectional area marked by the dye was measured using a ruler graduated in millimeters as a reference. Then, the images were analyzed using the Image-pro Plus 4.5.0.29 software. Based on the calculated values for the total area of the active xylem, it was possible to obtain the area of the active xylem in proportional terms, through the relationship between the areas of the active xylem and the total xylem.

Theoretical hydraulic conductivity

The theoretical hydraulic conductivity (k_h) was determined through the velocity of sap flow, difference in xylem water potential and length of the xylem segment.

$$k_h = \frac{J_s}{\frac{\Delta\Psi_x}{L_x}} \qquad \text{Eq 2}$$

Js is the velocity of the sap flow, which was measured according to the methodology (Granier 1985) and adaptation of Wright et al. (2023), and $\Delta\Psi_x$ is the xylem water potential gradient.

For Js measurements, one sensor was installed in the main stem of the tree (at approximately 50 cm height). Js was calculated using Grainer's original equations and the average sap velocity, Js (cm h^{-1}), is calculated as:

$$Js = 119 * 10^{-6} * K^{1.23} \quad ; \qquad \text{Eq 3}$$

where

$$K = (\Delta T_{Max} - \Delta T) / \Delta T \quad ; \qquad \text{Eq 4}$$

Where, ΔT_{Max} is the maximum temperature difference between the two probes at zero sap velocity, and ΔT is the difference between the probes when the tree is transpiring.

$\Delta\Psi_x$ is the change in xylem water potential (Ψ_x) before dawn (predawn) and midday and L_x is the mean xylem length. The measurements of Ψ_x used in the equation 2 were performed with a Scholander chamber on the same day that the gas exchange measurements were performed.

We also calculate the sapwood-specific hydraulic conductance (k_s):

$$k_s = \frac{k_h}{A_s} \quad \text{Eq 5}$$

Where A_s is the sapwood area.

Statistical analysis

We performed an analysis of variance (ANOVA) and Student-Newman-Keuls (SNK) test to compare the means of *A* and K_h between species and functional groups. We performed the Shapiro–Wilk normality test, when the assumptions were met, we performed the ANOVA and subsequent SNK test. For K_h, we transformed it due to not meeting the normality of the data, we transformed the values into Log for later SNK tests. We performed Pearson Correlations between physiological and anatomical variables for functional groups. In addition, we also performed a Principal Component Analysis (PCA) for possible grouping of variables between the LWD, EH, and HWH groups.

Results

Environmental variables

During the experimental year it rained 472.45 mm, with March being the wettest month (178.82 mm) and the driest months were August (8.38 mm), September and October with no recorded precipitation (Fig 2). Soil water storage (SWS) was highest in April and May, 46.78 mm and 46.76 mm, respectively (Fig 2). While the lowest SWS was recorded in October (21.62 mm) corresponding to the highest VPD and no precipitation recorded (Fig 2). The VPD was lowest in June (0.89 kPa) and highest in the dry months, from August (1.71 kPa), September (2.06 kPa), October (2.57 kPa), November (2.59 kPa) and December (2.26 kPa) (Fig 2).

Photosynthesis of deciduous and evergreen species in rainy and dry seasons

The rate of CO_2 assimilation (*A*) carried out in the rainy season was different between some species (Fig 3). The HWD species *Cenostigma pyramidale* presented the highest mean value (14.90±0.48 µmol CO_2 m^{-2} s^{-1}), while the evergreen species, *Sarcomphalus joazeiro* presented the lowest mean value (8.94±2.80 µmol CO_2 m^{-2} s^{-1}), followed by the LWD species *Spondias tuberosa* (9.87±1.76 µmol CO_2 m^{-2} s^{-1}) (Fig 3). The CO_2 assimilation rate in the evergreen species did not show a significant difference between the rainy (8.94±2.80 µmol CO_2 m^{-2} s^{-1}) and dry (8.60±1.20 µmol CO_2 m^{-2} s^{-1}) seasons (Fig 3).

Theoretical hydraulic conductivity and photosynthesis in LWD, HWD and EH species

Theoretical hydraulic conductivity was higher in the LWD group ($1.31E^{-06}$±$1.59E^{-06}$ cm^2 h^{-1} MPa^{-1}) and lower in EH species ($3.81E^{-07}$±$3.96E^{-07}$ cm^2 h^{-1} MPa^{-1}) e HWD ($9.37E^{-08}$±$1.07E^{-07}$ cm^2 h^{-1} MPa^{-1}) (Fig. 5). The correlation matrix showed that there is no correlation between the net photosynthesis rate and theoretical hydraulic conductivity in the functional groups (Fig. 6, 7 and 8). However, when we correlated with other anatomical and physiological traits, the correlation matrix revealed that there is a positive correlation of photosynthesis with xylem vessel diameter (0.67, $p<0.05$) and a negative correlation with active xylem area (- 0.71, $p<0.05$) in the LWD group (Fig. 6). Regarding the evergreen species, there was a significant positive correlation between photosynthesis and Ψ_x (0.95 $p<0.05$) and a negative correlation with the active xylem area (-0.99, $p<0.01$) (Fig. 7). Furthermore, the EH species showed a negative relationship between K_h and xylem vessel length (-1, $p<0.01$), vessel density (-1, $p<0.01$) and water potential (-0.95, $p<0.05$), and a positive correlation of K_h with stomatal conductance (0.99, $p<0.01$) (Fig. 7). While in the HWD functional group, there is a positive correlation between photosynthesis and vessel diameter (0.92, $p<0.01$) (Fig. 8).

Water and anatomical traits of wood in species with high and low wood density and evergreen

The relationship between water traits (water potential and gs) and anatomical traits was different between functional groups (Fig. 6 and 10). In the LWD group – Active xylem area was positively related to vessel density (0.94, $p<0.01$) and negatively to vessel element length (-0.86, $p<0.01$), xylem wall thickness (-0.86, $p<0.01$), vessel diameter (-0.81, $p<0.01$) and gs (-0.84, $p<0.05$) (Fig. 6). Vessel density was negatively related to vessel element length (-0.95, $p<0.01$), xylem wall thickness (-0.91, $p<0.01$) and vessel diameter (-0.79, $p<0.01$) (Fig. 6). While vessel element length was positively related to xylem wall thickness (0.96, $p<0.01$) and vessel diameter (0.77, $p<0.01$) (Fig. 6).

In the EH group – there was a positive correlation between the length of the vessel element and the vessel diameter (1, $p<0.01$) and gs (0.99, $p<0.01$) (Fig. 7), and a negative correlation with water potential (-0.95, $p<0.05$), vessel density (-1, $p<0.01$) and xylem wall thickness (-1, $p<0.01$) (Fig. 7). Vessel diameter was positively related to gs and negatively to Ψ_x (-0.95, $p<0.01$), vessel density (-1, $p<0.01$) and xylem wall thickness (-1, $p<0.01$). Ψ_x showed a positive correlation with vessel density (0.95, $p<0.01$) (Fig. 7).

The HWD group only showed a positive correlation of gs with Ψ_x (0.86, p<0.05) and a negative correlation of vessel diameter with vessel density (-0.89, p<0.05) (Fig. 8).

Principal component analysis (PCA)

PCA indicated the separation of functional groups determined by anatomical and physiological traits (Fig. 9). Axis 1 explained 36.3% of the variables and axis 2 explained 27.1%. The variables on axis 1 were most related to the species belonging to the LWD functional group: A, gs, VEL, D, PD, Ks, Kh and As (Fig. 9). While axis 2 variables: XWT, WD and VD were more related to species belonging to the HWD and EH groups (Fig. 9).

Discussion

Our results show that deciduous species with low wood density (LWD) in the Caatinga dry forest have a strategy to "avoid" drought, as they are possibly more vulnerable to embolism. Therefore, to avoid cavitation of xylem vessels, these species do not present high rates of CO_2 assimilation even during the rainy season. However, they maintain high hydraulic conductivity throughout the rainy and dry seasons. While deciduous species with high wood density (HWD) present greater CO_2 assimilation during the rainy season, but present low hydraulic conductivity. The evergreen species (EH), *S. joazeiro*, maintains moderate rates of CO_2 assimilation and hydraulic conductivity throughout the rainy and dry seasons.

Variation and correlation for anatomical hydraulic traits, photosynthesis and water transport efficiency in LWD HWD and EH species

The results of our study showed that there is no direct relationship between hydraulic conductivity (K_h) and net photosynthesis (*A*) in LWD and HWD species, however, there is a relationship between some anatomical traits with photosynthesis, such as the positive relationship of photosynthesis with xylem vessel lumen diameter in the LWD group. Indicating that the larger the vessel diameter, the greater the photosynthesis (Hacke et al. 2017, Xu et al. 2021). There are also other relationships between the anatomical traits themselves and physiological traits. The EH species showed more relationships between its traits and a moderate photosynthetic rate between seasons, confirming our hypothesis that the evergreen species with high wood density can maintain its photosynthetic rates without suffering many hydraulic failures.

However, our results do not corroborate the results found by Wei et al. (2023), in which species with high capacitance of the stem sapwood maintain high photosynthetic rates, that is,

they store water in the stem, such as the LWD species in our study. In the study by Wei et al. (2023) evaluated species from two biomes: seasonal tropical forest and savanna and species with high capacitance maintained higher leaf photosynthetic rates and high stomatal conductance in the rainy season. This different response found in our study is possibly due to the fact that LWD species, despite being in a favorable condition for transpiration (rainy season), have a strategy to "avoid" drought, so to avoid cavitation of their vessels who are often more vulnerable to embolism (Carrasco et al. 2014, Wright et al. 2021), these species keep water stored in the stem, as in *Commiphora leptophloeos* and *Amburana cearensis*, or roots, in the case of *Spondias tuberosa* (Lima et al. 2012, Yu et al. 2019, Wright et al. 2021). Therefore, possibly existing in a trade-off, in which LWD species from the Caatinga dry forest had to close their stomata more frequently at the expense of significantly reduced carbon assimilation (Hajek et al. 2016, Brito et al. 2022). Furthermore, possibly the species *Commiphora leptophloeos*, *Amburana cearensis* and *Spondias tuberosa* have low wood density with the main purpose of storing water, therefore, for this to happen, these species need to have low density, corroborating with the results of Wright et al. (2023).

Deciduous trees are often more vulnerable to embolisms (Choat et al. 2005), Furthermore, there may be greater mortality in trees with low wood density, as they normally have high P50 values (Phillips et al. 2010, Liang et al. 2021). Possibly to avoid higher rates of hydraulic failure, Caatinga plants must use strategies that favor their survival (Medeiros et al., 2024), in this way, species avoid risks by reducing CO_2 assimilation (Hajek et al. 2016). However, we must take into account that the LWD species evaluated in our study have a high leaf area index (Brito et al. 2022, Medeiros et al. 2024), their canopies are large in relation to those of the HWD species evaluated. Thus, leading us to infer that the photosynthetic rate carried out at the canopy level during the short rainy season is sufficient to maintain their survival and reproduction for a long time. Furthermore, Smith-Martin et al. (2023) state that there is a trade-off between drought avoidance (species that store water in the stem) and drought tolerance (embolism-resistant species). These divergent hydraulic characteristics between groups of species result in high hydraulic diversity in the forests in which they coexist (Oliveira et al. 2021, Martin et al. 2023, Smith-Martin et al. 2023). Therefore, it is important that there is coexistence of these species for greater hydraulic diversity in a seasonally dry ecosystem such as the Caatinga. However, climate change can lead to changes in the composition of plant communities, as the effects of drought tend to be intensified, determining which species will be dominant in a hotter and drier climate (Smith-Martin et al. 2023). Thus, the future scenario of

plant composition in dry forests is still uncertain, as we do not know which species may become extinct due to drought-induced mortality.

Differences between photosynthesis of deciduous and evergreen species in rainy and dry seasons

Leaves are the most vulnerable organs of the plant to xylem cavitation and lead to canopy mortality, which is the first sign that the plant will die (Brodribb et al. 2020, Tonet et al. 2024). Most plants in seasonally dry forests, such as the Caatinga, lose their leaves in the dry season to avoid loss of water and consequently avoid further damage due to hydraulic failure (Lima and Rodal 2010, Wright et al. 2023). However, there are evergreen species that tolerate dry conditions and remain leafy throughout the dry season (da Silva e Teodoro et al. 2022).

The evergreen species studied managed to maintain its moderate photosynthetic rates throughout the year due to its ability to transport sap flow even under low soil humidity, as *S. joazeiro* possibly has a deep root system that allows it to obtain water from deeper areas of the soil (Oliveira et al. 2005, Souza et al. 2015). Evergreen trees in a seasonally dry tropical forest had deeper roots than deciduous species (Xu et al. 2021, Martin et al. 2023). Furthermore, the EH species has a high wood density that provides high hydraulic resistance, supports more negative xylem water potentials and may be less vulnerable to suffering embolism processes (Markesteijn, Poorter, Bongers, et al. 2011, Janssen et al. 2020).

Another explanation for photosynthesis throughout the year in this species is that evergreen species lose the leaves that are most vulnerable to water deficit, that is, the evergreen species lose leaves and produce new leaves during the dry season (Lima et al. 2012), in which the plant loses some of the most vulnerable leaves that have suffered greater cavitation, while others more resistant to cavitation, remain in the canopy (Tonet et al. 2024). This process may be an adaptation of hydraulic diversity so that simultaneous xylem cavitation does not occur in all leaves (Cardoso et al. 2020). The gradual loss of leaves in evergreen species also reduces the amount of water that the canopy demands, reducing the tree's drying time (Tonet et al. 2024). Although we do not follow the gradual loss of leaves, we observe the phenology of the trees in the wettest month (April) and the driest month (September) of each season in 2023, so we can show that there was a drastic reduction of leaves in the canopy cover of the tree evergreen species, *S. joazeiro* (42% of leaf fall) according to the classification of phenophases intensity (Fournier 1974) (Fig. SII). According to Tonet et al. (2024), despite the death of leaves

with cavitation >35%, it does not cause rapid damage to the tree canopy level in an evergreen species, therefore, leaf cavitation at the canopy level and the dynamics must be taken into account regulation of canopy death due to drought over time.

High stem xylem capacitance associated with low embolism resistance in LWD species

The LWD species presented greater area of active xylem, which contributed to the greater hydraulic conductivity and capacitance of the sapwood, and this has been associated with wood density (Hacke et al. 2001). Low wood density is associated with low resistance to xylem embolism and has high capacitance, unlike species with high density that are considered more resistant to embolism (Poorter et al. 2019). LWD species have a large vessel diameter that promotes greater hydraulic vulnerability due to the formation of embolisms and this leads to the hypothesis of a trade-off, in which the plant invests in the efficiency of water transport at the expense of lower hydraulic safety (Johnson and Brodribb 2023). Moreover, LWD species had wide vessels and thin walls, which leads to higher K_h, however, it puts hydraulic safety at risk, consequently causing more cavitation (Janssen et al. 2020, Brito et al. 2022).

On the other hand, loss of hydraulic conductivity has been linked to drought-induced tree mortality (Brodribb and Cochard 2009). Water deficit leads to a reduction in water potential, especially in HWD species that support more tension along the xylem, leading to the formation of embolisms and thus reducing hydraulic conductivity (Liang et al. 2021). For this reason, it is essential that HWD species have mechanisms to withstand negative xylem pressures, such as thicker vessel walls, smaller vessel diameters and greater vessel density (Poorter et al. 2010, Janssen et al. 2020). Our findings also corroborate Poorter et al (2010), in which some species with high wood density showed a strong trade-off between vessel density and xylem vessel lumen diameter, in which many xylem vessels with small lumen diameter and compacted in the same area are associated with less risk of cavitation. On the other hand, low wood density may be related to fast growth, but with low construction costs, resulting in lakes with large xylem vessel lumen diameters and high xylem specific hydraulic conductivity (Poorter et al. 2010, Janssen et al. 2020).

Conclusion

Our results indicate that although there is no direct correlation between photosynthesis and theoretical hydraulic conductivity in LWD and HWD species, there is a correlation between other anatomical and physiological traits that help us understand the strategies of Caatinga dry

forest species. Among the studied species with low deciduous density may not present high photosynthetic rates even in the rainy season, to avoid damage to the hydraulic system, however, we must take into account photosynthesis at the level of the tree canopy. The evergreen species has moderate photosynthetic rates throughout the year and anatomical and physiological traits, such as stomatal control, that promote high tolerance to drought, proving to be more resistant to embolisms in future scenarios. Therefore, there is hydraulic diversity between coexisting Caatinga species, which maintains the functioning of ecosystem services and the effects of climate change can change the functioning of these ecosystems as a result of hydraulic failure and reduced gas exchange.

Acknowledgements

We would like to thank the scientific initiation students from the Plant Physiology laboratory (LFV), Department of Botany at UFPE, for their assistance with laboratory analyses, the Study Group on Semiarid Ecohydrology and the Center for Functional Ecology of Plants (NEFPlan), Universidade Federal Rural de Pernambuco, Serra Talhada Academic Unit (UFRPE/UAST) for assistance in fieldwork. We also thank the Postgraduate Program in Plant Production at UFRPE/UAST for the availability of equipment and laboratories. We would like to thank Senhor Homem Bom Magalhães for access to the study field. The first author would like to thank the members of Laboratoire de Physique et Physiologie intégratives de l'Arbre en environnement Fluctuant (PIAF, INRAE) for their support during the sandwich doctoral stay.

Funding

This work had financial support from FACEPE (Facepe-Pronem-APQ-0336-2.03/14). MM is funded by (FACEPE Fellow-IBPG-0330-2.07/21) and Sandwich PhD Scholarship Program by the French Embassy in Brazil, Campus France Brazil (BGF-160421Y-TerrEE Scholarship, 2024). The work was also supported by INCT: National Observatory of Water and Carbon Dynamics in the Caatinga Biome – ONDACBC, contributing with meteorological data from the flow tower installed in the study area.

Authors' Contributions

MM and MGS conceived the study. MM, ALNJ, JRIS, HRBS, CA and MMS collected the data. MM analyzed the data. MM, ALAL, HC, and MGS wrote the first draft with edits from all authors. ALAL, ES, HC and MGS provided supervision and resources.

Conflict of Interest

None declared.

References

Allen K, Dupuy JM, Gei MG, Hulshof C, Medvigy D, Pizano C, Salgado-Negret B, Smith CM, Trierweiler A, Van Bloem SJ, Waring BG, Xu X, Powers JS (2017) Will seasonally dry tropical forests be sensitive or resistant to future changes in rainfall regimes? Environ Res Lett 12:023001. http://dx.doi.org/10.1088/1748-9326/aa5968.

Anderegg WRL, Wolf A, Arango-Velez A, Choat B, Chmura DJ, Jansen S, Kolb T, Li S, Meinzer F, Pita P, Resco de Dios V, Sperry JS, Wolfe BT, Pacala S (2017) Plant water potential improves prediction of empirical stomatal models. PLoS One 12. https://doi.org/10.1371/journal.pone.0185481.

Andrade JL, Meinzer FC, Goldstein G, Schnitzer SA (2005) Water uptake and transport in lianas and co-occurring trees of a seasonally dry tropical forest. Trees - Struct Funct 19:282–289. http://dx.doi.org/10.1007/s00468-004-0388-x.

Blackman CJ, Brodribb TJ, Jordan GJ (2009) Leaf hydraulics and drought stress: Response, recovery and survivorship in four woody temperate plant species. Plant, Cell Environ 32:1584–1595. https://doi.org/10.1111/j.1365-3040.2009.02023.x.

Bréda N, Huc R, Granier A, Dreyer E (2006) Temperate forest trees and stands under severe drought: a review of ecophysiological responses, adaptation processes and long-term consequences. Ann For Sci 63:625–644. http://dx.doi.org/10.1051/forest:2006042.

Brito ND da S, Medeiros MJ dos S, Souza ES de, Lima ALA de (2022) Drought response strategies for deciduous species in the semiarid Caatinga derived from the interdependence of anatomical, phenological and bio-hydraulic attributes. Flora Morphol Distrib Funct Ecol Plants 288:152009. http://dx.doi.org/10.1016/j.flora.2022.152009.

Brodribb TJ (2009) Xylem hydraulic physiology: The functional backbone of terrestrial plant productivity. Plant Sci 177:245–251. http://dx.doi.org/10.1016/j.plantsci.2009.06.001.

Brodribb TJ, Cochard H (2009) Hydraulic failure defines the recovery and point of death in water-stressed conifers. Plant Physiol 149:575–584. http://dx.doi.org/10.1104/pp.108.129783.

Brodribb TJ, Powers J, Cochard H, Choat B (2020) Hanging by a thread? Forests and drought. Science 368:261–266. http://dx.doi.org/10.1126/science.aat7631.

Brunner I, Herzog C, Dawes MA, Arend M, Sperisen C (2015) How tree roots respond to drought. Front Plant Sci 6:1–16. https://doi.org/10.3389/fpls.2015.00547.

Cardoso AA, Batz TA, McAdam SAM (2020) Xylem embolism resistance determines leaf mortality during drought in persea americana. Plant Physiol 182:547–554. http://dx.doi.org/10.1104/pp.19.00585.

Carrasco OL, Bucci SJ, Di Francescantonio D, Lezcano OA, Campanello PI, Scholz FG, Rodríguez S, Madanes N, Cristiano PM, Hao GY, Holbrook NM, Goldstein G (2014) Water storage dynamics in the main stem of subtropical tree species differing in wood density, growth rate and life history traits. Tree Physiol 35:354–365. http://dx.doi.org/10.1093/treephys/tpu087.

Chave J, Coomes D, Jansen S, Lewis SL, Swenson NG, Zanne AE (2009) Towards a worldwide wood economics spectrum. Ecol Lett 12:351–366. http://dx.doi.org/10.1111/j.1461-0248.2009.01285.x.

Choat B, Ball MC, Luly JG, Holtum JAM (2005) Hydraulic architecture of deciduous and evergreen dry rainforest tree species from north-eastern Australia. Trees - Struct Funct 19:305–311. http://dx.doi.org/10.1007/s00468-004-0392-1.

Corlett RT (2016) The Impacts of Droughts in Tropical Forests. Trends Plant Sci 21:584–593. http://dx.doi.org/10.1016/j.tplants.2016.02.003.

Danuser G (1999) Photogrammetric calibration of a stereo light microscope. J Microsc 193:62–83. https://doi.org/10.1046/j.1365-2818.1999.00425.x.

Eamus D (1999) Ecophysiological traits of deciduous and evergreen woody species in the seasonally dry tropics. Trends Ecol Evol 14:11–16. https://doi.org/10.1016/s0169-5347(98)01532-8.

Fournier LA (1974) Un método cuantitativo para la medición de características fenológicas en árboles. Turrialba 24:422–423.

Granier A (1985) Une nouvelle méthode pour la mesure du flux de sève brute dans le tronc des arbres. Ann des Sci For 42:193–200. https://doi.org/10.1051/forest:19850204.

Hacke UG, Sperry JS, Pockman WT, Davis SD, McCulloh KA (2001) Trends in wood density and structure are linked to prevention of xylem implosion by negative pressure. Oecologia 126:457–461. http://dx.doi.org/10.1007/s004420100628.

Hacke UG, Spicer R, Schreiber SG, Plavcová L (2017) An ecophysiological and developmental perspective on variation in vessel diameter. Plant Cell Environ 40:831–845. https://doi.org/10.1111/pce.12777.

Hajek P, Kurjak D, Von Wühlisch G, Delzon S, Schuldt B (2016) Intraspecific variation in wood anatomical, hydraulic, and foliar traits in ten European beech provenances differing in growth yield. Front Plant Sci 7:791. https://doi.org/10.3389/fpls.2016.00791.

Hajek P, Leuschner C, Hertel D, Delzon S, Schuldt B (2014) Trade-offs between xylem hydraulic properties, wood anatomy and yield in Populus. Mol Hum Reprod 34:744–756. https://doi.org/10.1093/treephys/tpu048.

Hoeber S, Leuschner C, Köhler L, Arias-Aguilar D, Schuldt B (2014) The importance of hydraulic conductivity and wood density to growth performance in eight tree species from a tropical semi-dry climate. For Ecol Manage 330:126–136. http://dx.doi.org/10.1016/j.foreco.2014.06.039.

Intergovernmental Panel on Climate Change (IPCC) (2023) Climate Change 2022 – Impacts, Adaptation and Vulnerability. Cambridge University Press.

Janssen TAJ, Hölttä T, Fleischer K, Naudts K, Dolman H (2020) Wood allocation trade-offs between fiber wall, fiber lumen, and axial parenchyma drive drought resistance in neotropical trees. Plant Cell Environ 43:965–980. https://doi.org/10.1111/pce.13687.

Johansen DA (1940) Plant microtechnique. Plant Microtech:523.

Johnson KM, Brodribb TJ (2023) Evidence for a trade-off between growth rate and xylem cavitation resistance in Callitris rhomboidea. Tree Physiol 43:1055–1065. https://doi.org/10.1093/treephys/tpad037.

Liang X, Ye Q, Liu H, Brodribb TJ (2021) Wood density predicts mortality threshold for diverse trees. New Phytol 229:3053–3057. https://doi.org/10.1111/nph.17117.

Lima TRA, Carvalho ECD, Martins FR, Oliveira RS, Miranda RS, Müller CS, Pereira L, Bittencourt PRL, Sobczak JCMSM, Gomes-Filho E, Costa RC, Araújo FS (2018) Lignin composition is related to xylem embolism resistance and leaf life span in trees in a tropical semiarid climate. New Phytol 219:1252–1262. http://doi.wiley.com/10.1111/nph.15211.

Lima ALA, Rodal MJN (2010) Phenology and wood density of plants growing in the semi-

arid region of northeastern Brazil. J Arid Environ 74:1363–1373. http://dx.doi.org/10.1016/j.jaridenv.2010.05.009.

Lima ALA de, Rodal MJN, Castro CC, Antonino ACD, Melo AL de, Gonçalves-Souza T, Sampaio EV de SB (2021) Phenology of high- and low-density wood deciduous species responds differently to water supply in tropical semiarid regions. J Arid Environ 193. http://dx.doi.org/10.1016/j.jaridenv.2021.104594.

Lima ALA de, Sá Barretto Sampaio EV de, Castro CC de, Rodal MJN, Antonino ACD, Melo AL de (2012) Do the phenology and functional stem attributes of woody species allow for the identification of functional groups in the semiarid region of Brazil? Trees - Struct Funct 26:1605–1616. http://dx.doi.org/10.1007/s00468-012-0735-2.

Markesteijn L, Poorter L, Bongers F, Paz H, Sack L (2011) Hydraulics and life history of tropical dry forest tree species: Coordination of species' drought and shade tolerance. New Phytol 191:480–495. https://doi.org/10.1111/j.1469-8137.2011.03708.x.

Markesteijn L, Poorter L, Paz H, Sack L, Bongers F (2011) Ecological differentiation in xylem cavitation resistance is associated with stem and leaf structural traits. Plant, Cell Environ 34:137–148. https://doi.org/10.1111/j.1365-3040.2010.02231.x.

Martin CMS-, Muscarella R, Hammond WM, Jansen S, Brodribb TJ, Choat B, Johnson DM, Uriarte GV-GM (2023) Hydraulic variability of tropical forests is largely independent of water availability. 00:1–11. https://doi/10.1111/ele.14314.

Mcdowell N, Pockman WT, Allen CD, Breshears DD, Cobb N, Kolb T, Plaut J, Sperry J, West A, Williams DG, Yepez EA (2008) Mechanisms of plant survival and mortality during drought: why do some plants survive while others succumb to drought? New Phytol 178:719-739. https://10.1111/j.1469-8137.2008.02436.x.

Medeiros M, Wright CL, de Lima ALA, da Silva Brito ND, Souza R, Silva JRI, Souza E (2024) Divergent hydraulic strategies of two deciduous tree species to deal with drought in the Brazilian semi-arid region. Trees - Struct Funct. 38:681–694. https://doi.org/10.1007/s00468-024-02506-9

Meinzer FC, Johnson DM, Lachenbruch B, McCulloh KA, Woodruff DR (2009) Xylem hydraulic safety margins in woody plants: Coordination of stomatal control of xylem tension with hydraulic capacitance. Funct Ecol 23:922–930.

https://doi.org/10.1111/j.1365-2435.2009.01577.x.

Mencuccini M, Rosas T, Rowland L, Choat B, Cornelissen H, Jansen S, Kramer K, Lapenis A, Manzoni S, Niinemets Ü, Reich P, Schrodt F, Soudzilovskaia N, Wright IJ, Martínez-Vilalta J (2019) Leaf economics and plant hydraulics drive leaf : wood area ratios. New Phytol 224:1544–1556. https://doi.org/10.1111/nph.15998.

Oliveira RS, Dawson TE, Burgess SSO, Nepstad DC (2005) Hydraulic redistribution in three Amazonian trees. Oecologia 145:354–363. https://doi.org/10.1007/s00442-005-0108-2.

Oliveira RS, Eller CB, Barros F de V., Hirota M, Brum M, Bittencourt P (2021) Linking plant hydraulics and the fast–slow continuum to understand resilience to drought in tropical ecosystems. New Phytol 230:904–923. https://doi.org/10.1111/nph.17266.

Parker AJ, Haskins EF, Deyrup-Olsen I (1982) Toluidine Blue: A Simple, Effective Stain for Plant Tissues. Am Biol Teach 44:487–489. https://doi.org/10.2307/4447575.

Pereira PDC, Da Silva TGF, Zolnier S, De Morais JEF, Dos Santos DC (2015) Morfogênese da palma forrageira irrigada por gotejamento. Rev Caatinga 28:184–195. https://doi.org/10.1590/1983-21252015v28n321rc.

Pérez-Harguindeguy N, Díaz S, Garnier E, Lavorel S, Poorter H, Jaureguiberry P, Bret-Harte MS, Cornwell WK, Craine JM, Gurvich DE, Urcelay C, Veneklaas EJ, Reich PB, Poorter L, Wright IJ, Ray P, Enrico L, Pausas JG, De Vos AC, Buchmann N, Funes G, Quétier F, Hodgson JG, Thompson K, Morgan HD, Ter Steege H, Van Der Heijden MGA, Sack L, Blonder B, Poschlod P, Vaieretti M V., Conti G, Staver AC, Aquino S, Cornelissen JHC (2013) New handbook for standardised measurement of plant functional traits worldwide. Aust J Bot 61:167–234. https://doi.org/10.1071/BT12225.

Phillips OL, Heijden G Van Der, Lewis SL, Lo G, Lloyd J, Malhi Y, Monteagudo A, Almeida S, Da EA, Andelman S, Andrade A, Arroyo L, Aymard G, Baker TR, Costa L, Feldpausch TR, Fisher JB, Fyllas NM, Freitas MA, Jime E, Keeling H, Tim J, Gloor E, Higuchi N, Lovett JC, Meir P, Mendoza C, Morel A, Nu P, Prieto A, Quesada CA, Peh KS, Pen A, Schwarz M, Silva J, Silveira M, Slik JWF, Sonké B, Sota Thomas A, Stropp J, Taplin JR, Vasquez R, Vilanova E (2010) Drought–mortality relationships for tropical forests Oliver. New Phytol 187:631–646. https://doi.org/10.1111/j.1469-8137.2010.03359.x.

Pineda-García F, Paz H, Meinzer FC (2012) Drought resistance in early and late secondary successional species from a tropical dry forest: The interplay between xylem resistance to embolism, sapwood water storage and leaf shedding. Plant, Cell Environ 36:405–418. https://doi.org/10.1111/j.1365-3040.2012.02582.x.

Pinho BX, Tabarelli M, Engelbrecht BMJ, Sfair J, Melo FPL (2019) Plant functional assembly is mediated by rainfall and soil conditions in a seasonally dry tropical forest. Basic Appl Ecol 40:1–11. https://doi.org/10.1016/j.baae.2019.08.002.

Poorter L, Castilho C V., Schietti J, Oliveira RS, Costa FRC (2018) Can traits predict individual growth performance? A test in a hyperdiverse tropical forest. New Phytol 219:109–121. https://doi.org/10.1111/nph.15206.

Poorter L, McDonald I, Alarcon A, Fichtler E, Licona J-C, Peña-Carlos M, Sterck F, Villegas Z, Sass-klaassen U (2010) The importance of wood traits and hydraulic conductance for the performance and life history strategies of 42 rainforest tree species. New Phytol 185:481–492. https://doi.org/10.1111/j.1469-8137.2009.03092.x.

Poorter L, Rozendaal DMA, Bongers F, de Almeida-Cortez JS, Almeyda Zambrano AM, Álvarez FS, Andrade JL, Villa LFA, Balvanera P, Becknell JM, Bentos T V., Bhaskar R, Boukili V, Brancalion PHS, Broadbent EN, César RG, Chave J, Chazdon RL, Colletta GD, Craven D, de Jong BHJ, Denslow JS, Dent DH, DeWalt SJ, García ED, Dupuy JM, Durán SM, Espírito Santo MM, Fandiño MC, Fernandes GW, Finegan B, Moser VG, Hall JS, Hernández-Stefanoni JL, Jakovac CC, Junqueira AB, Kennard D, Lebrija-Trejos E, Letcher SG, Lohbeck M, Lopez OR, Marín-Spiotta E, Martínez-Ramos M, Martins S V., Massoca PES, Meave JA, Mesquita R, Mora F, de Souza Moreno V, Müller SC, Muñoz R, Muscarella R, de Oliveira Neto SN, Nunes YRF, Ochoa-Gaona S, Paz H, Peña-Claros M, Piotto D, Ruíz J, Sanaphre-Villanueva L, Sanchez-Azofeifa A, Schwartz NB, Steininger MK, Thomas WW, Toledo M, Uriarte M, Utrera LP, van Breugel M, van der Sande MT, van der Wal H, Veloso MDM, Vester HFM, Vieira ICG, Villa PM, Williamson GB, Wright SJ, Zanini KJ, Zimmerman JK, Westoby M (2019) Wet and dry tropical forests show opposite successional pathways in wood density but converge over time. Nat Ecol Evol 3:928–934. https://doi.org/10.1038/s41559-019-0882-6.

Reich PB, Wright IJ, Cavender-Bares J, Craine JM, Oleksyn J, Westoby M, Walters MB (2003) The evolution of plant functional variation: Traits, spectra, and strategies. Int J

Plant Sci 164:S143-S164.

Ryan MG, Phillips N, Bond BJ (2006) The hydraulic limitation hypothesis revisited. Plant, Cell Environ 29:367–381. http://10.1111/j.1365-3040.2005.01478.x.

Schenk HJ, Steppe K, Jansen S (2015) Nanobubbles: A new paradigm for air-seeding in xylem. Trends Plant Sci 20:199–205. http://dx.doi.org/10.1016/j.tplants.2015.01.008.

da Silva E Teodoro ÉDM, da Silva APA, Brito ND da S, Rodal MJN, Shinozaki-Mendes RA, de Lima ALA (2022) Functional traits determine the vegetative phenology of woody species in riparian forest in semi-arid Brazil. Plant Ecol 223:1137–1153. https://doi.org/10.1007/s11258-022-01264-3.

Silva PF da, Lima JR de S, Antonino ACD, Souza R, de Souza ES, Silva JRI, Alves EM (2017) Seasonal patterns of carbon dioxide, water and energy fluxes over the Caatinga and grassland in the semi-arid region of Brazil. J Arid Environ 147:71–82. http://dx.doi.org/10.1016%2Fj.jaridenv.2017.09.003.

Smith-Martin CM, Muscarella R, Ankori-Karlinsky R, Delzon S, Farrar SL, Salva-Sauri M, Thompson J, Zimmerman JK, Uriarte M (2023) Hydraulic traits are not robust predictors of tree species stem growth during a severe drought in a wet tropical forest. Funct Ecol 37:447–460. https://doi.org/10.1111/1365-2435.14235.

Souza BC de, Carvalho ECD, Oliveira RS, de Araujo FS, de Lima ALA, Rodal MJN (2020) Drought response strategies of deciduous and evergreen woody species in a seasonally dry neotropical forest. Oecologia 1:221–236. https://doi.org/10.1007/s00442-020-04760-3.

Souza BC de, Oliveira RS, De Araújo FS, De Lima ALA, Rodal MJN (2015) Divergências funcionais e estratégias de resistência à seca entre espécies decíduas e sempre verdes tropicais. Rodriguesia 66:21–32. https://doi.org/10.1590/2175-7860202172077.

Sperry JS (2000) Hydraulic constraints on plant gas exchange. In: Agricultural and Forest Meteorology. pp 13–23.

Sperry JS, Stiller V, Hacke UG (2003) Xylem Hydraulics and the Soil–Plant–Atmosphere Continuum. Agron J 95:1362. https://doi.org/10.2134/agronj2003.1362

Tonet V, Brodribb T, Bourbia I (2024) Variation in xylem vulnerability to cavitation shapes the photosynthetic legacy of drought. Plant Cell Environ 47:1160–1170.

https://doi.org/10.1111/pce.14788.

Venturas MD, Sperry JS, Hacke UG (2017) Plant xylem hydraulics: What we understand, current research, and future challenges. J Integr Plant Biol 59:356–389. https://doi.org/10.1111/jipb.12534.

Vieira AJR, Lisi CS (2019) Caatinga tree wood anatomy: Perspectives on use and conservation. Floresta e Ambient 26:2–14. https://doi.org/10.1590/2179-8087.099717.

Wang L, Dai Y, Guo J, Gao R, Wan X (2016) Interaction of hydraulic failure and carbon starvation on Robinia pseudoacacia seedlings during drought. Linye Kexue/Scientia Silvae Sin 52:1–9. http://dx.doi.org/10.11707/j.1001-7488.20160601.

Wei Y, Chen Y-J, Siddiq Z, Zhang J-L, Zhang S-B, Jansen S, Cao K-F (2023) Hydraulic traits and photosynthesis are coordinated with trunk sapwood capacitance in tropical tree species. Tree Physiol 00:1–12. https://doi.org/10.1093/treephys/tpad107.

Wright CL, de Lima ALA, de Souza ES, West JB, Wilcox BP (2021) Plant functional types broadly describe water use strategies in the Caatinga, a seasonally dry tropical forest in northeast Brazil. Ecol Evol 11:11808–11825. https://doi.org/10.1002/ece3.7949.

Wright IJ, Reich PB, Westoby M, Ackerly DD, Baruch Z, Bongers F, Cavender-bares J, Chapin T, Cornelissen JHC, Diemer M, Flexas J, Garnier E, Groom PK, Gulias J (2004) Wrighe et.al.; 2004 The worldwide leaf economics spectrum.pdf. 12:821–827. https://doi.org/10.1038/nature02403.

Wright CL, West JB, de Lima ALA, Souza ES, Medeiros M, Wilcox BP (2023) Contrasting water-use strategies revealed by species-specific transpiration dynamics in the Caatinga dry forest. Tree Physiol:1–15. https://doi.org/10.1093/treephys/tpad137.

Xu H, Wang H, Prentice IC, Harrison SP, Wright IJ (2021) Coordination of plant hydraulic and photosynthetic traits: confronting optimality theory with field measurements. New Phytol 232:1286–1296. https://doi.org/10.1111/nph.17656.

Yu T, Feng Q, Si J, Pinkard EA (2019) Coordination of stomatal control and stem water storage on plant water use in desert riparian trees. Trees - Struct Funct 33:787–801. http://dx.doi.org/10.1007/s00468-019-01816-7.

Tables and Figures

Table 1. Characteristics for the selected species from the three plant functional types (PFT), deciduous low wood density (LWD), evergreen high wood density (EH), and deciduous high wood density (HWD). Species characteristics are stem-specific wood density (WD), diameter close to the ground (D), and tree height (HT), n=5. *Values obtained from (Lima et al. 2012).

PFT	Species	Family	WD (g cm^{-3})	D (cm)	HT (m)
LWD	*Commiphora leptophloeos* (Mart.) J.B.Gillett	Burseraceae	0.32±0.06	30.3±9.3	5.46±0.95
	Spondias tuberosa Arruda	Anacardiaceae	0.49±0.02*	78.9±37.8	5.63±0.95
	Amburana cearensis (Allemao) A.C.Sm.	Fabaceae	0.51±0.09	13.84±3.4	4.00±0.90
EH	*Sarcomphalus joazeiro* (Mart.) Hauenshild	Rhamnaceae	0.62±0.01*	21.0±6.4	5.45±0.44
HWD	*Cenostigma pyramidale* (Tul.) Gagnon & G. P. Lewis	Fabaceae	0.69±0.09	12.0±2.0	5.84±1.35

	Aspidosperma pyrifolium Mart. & Zucc.	Apocynaceae	0.74±0.04	9.3±2.1	2.90±0.15

Table 2. Abbreviations and units of the variables examined in the study.

Variables	**Abreviations**	**Unit**
Wood density	WD	g cm^{-3}
Vessel diameter	D	µm
Xylem wall thickness	XWT	µm
Vessel density	VD	mm^2
Vessel element length	VEL	µm
Sapwood area	As	cm^2
Stomatal condutance	gs	mmol m^{-2} s^{-1}
Xylem water potential in predawn	PD	MPa
Sap flow velocity	Js	cm h^{-1}
Theoretical hydraulic conductivity	K_h	cm^2 s^{-1} MPa^{-1}
Xylem hydraulic conductivity	K_s	cm^2 s^{-1} MPa^{-1}
Net Photosynthesis	*A*	µmol CO_2 m^{-2} s^{-1}

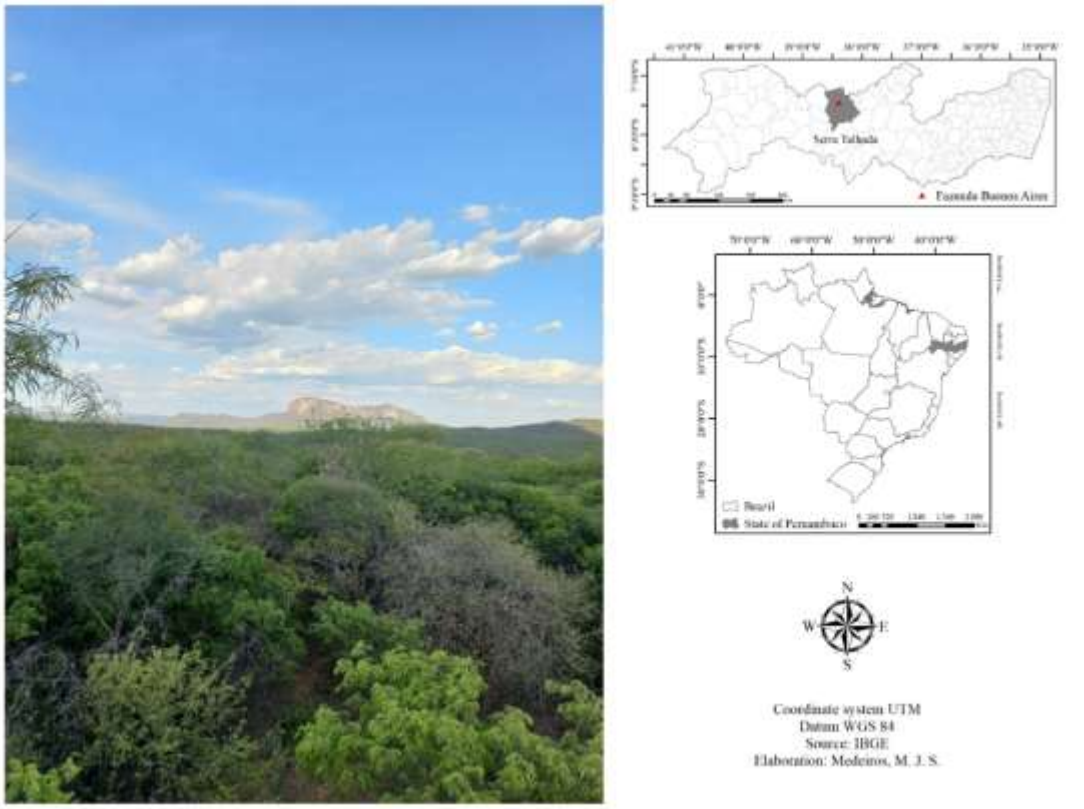

Figure 1. Map of the location of the experimental area. Fazenda Buenos Aires, municipality of Serra Talhada-Pernambuco, Brazil, and Photo of Fazenda Buenos Aires Farm, during the rainy season. Photo credit: M. Medeiros.

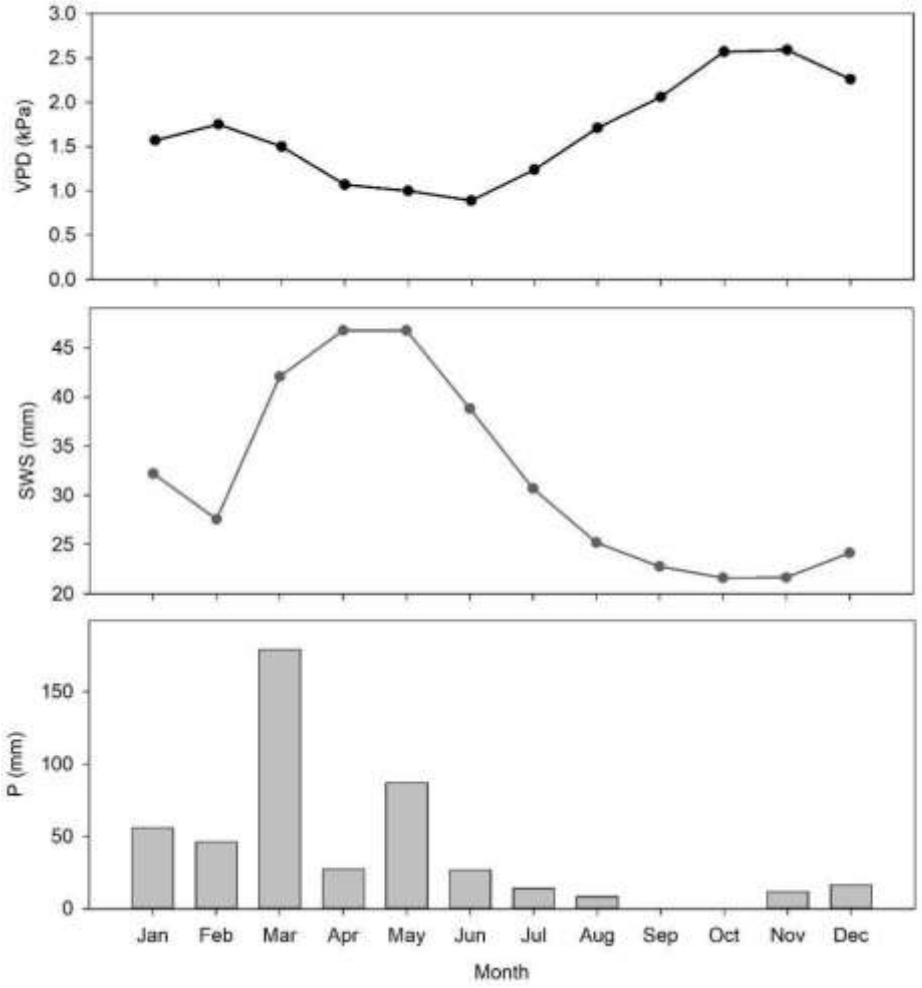

Figure 2. Monthly average vapor pressure deficit (VPD), average soil water storage (SWS) and total precipitation (P) from January to December 2023 at Fazenda Buenos Aires, Serra Talhada, PE, Brazil.

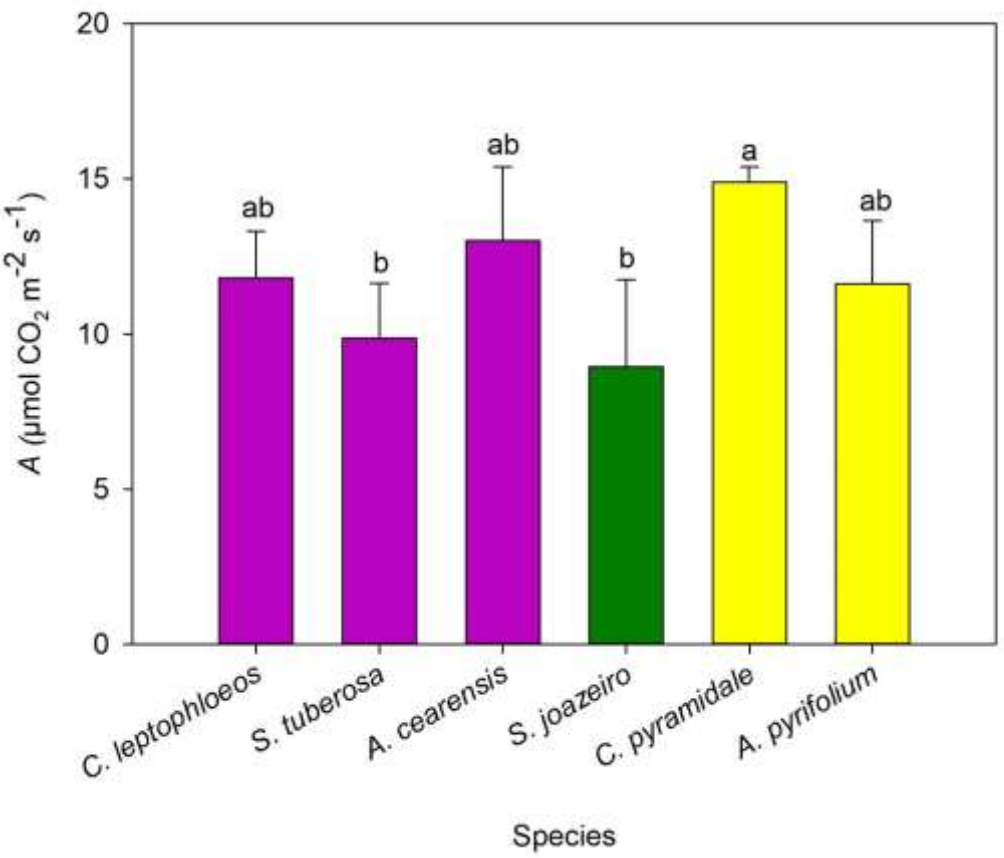

Figure 3. Net photosynthetic CO_2 assimilation (*A*) by species and plant function type (PFT: deciduous low wood density, LWD; deciduous high wood density HWD; and evergreen high wood density EH) during the rainy season (April 27, 2023). See Table 1 for plant functional groups color. Letters denote difference by the Student-Newman-Keuls Test between species.

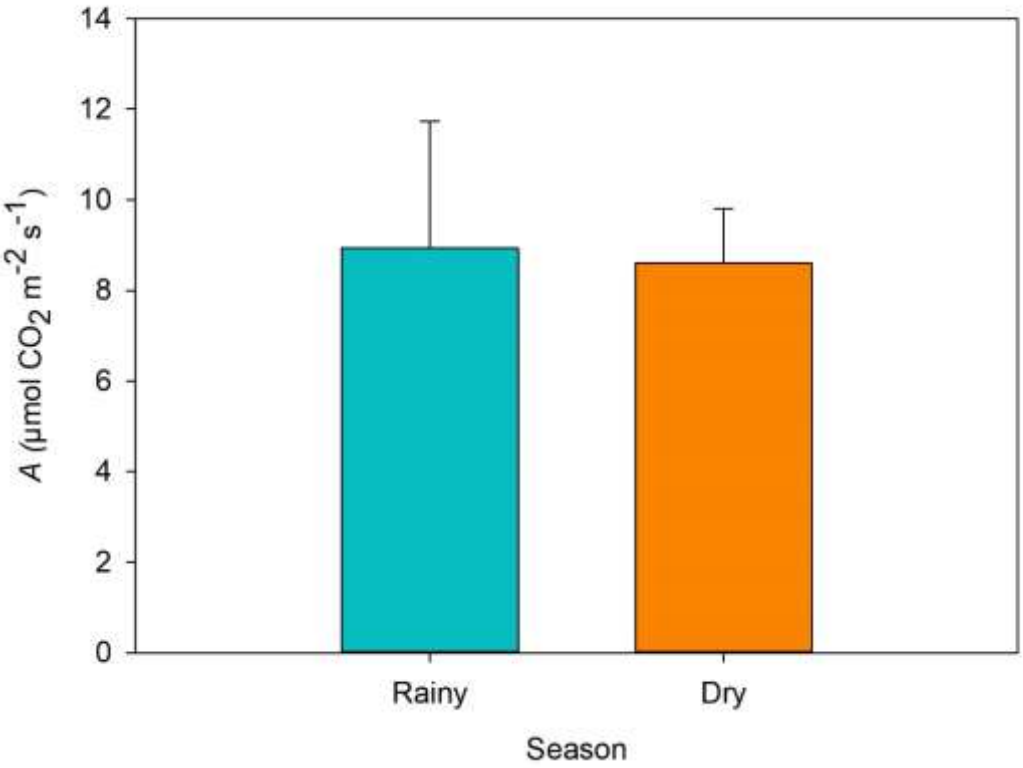

Figure 4. Net photosynthetic CO_2 assimilation (*A*) *Sarcomphalus joazeiro* (evergreen high wood density EH) during the rainy season (April 27, 2023) and dry season (September 26, 2023). ANOVA non-significant at 5% significance.

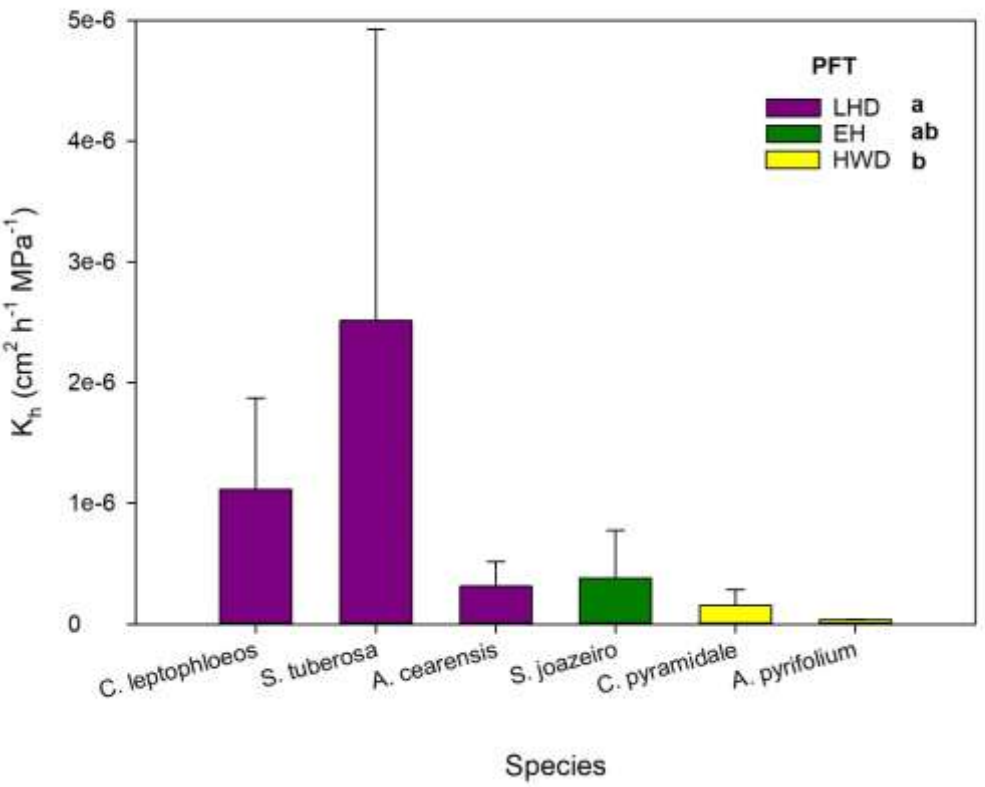

Figure 5. Hydraulic conductivity (K_h) by species and plant function type (PFT: deciduous low wood density, LWD; deciduous high wood density HWD; and evergreen high wood density EH) during the rainy season (April 27, 2023). See Table 1 for plant functional groups color. Letters denote difference by the Student-Newman-Keuls Test between plant functional groups. Average and standard deviation: LWD ($1.31E^{-06}$±$1.59E^{-06}$ cm^2 h^{-1} MPa^{-1}), EH ($3.81E^{-07}$±$3.96E^{-07}$cm^2 h^{-1} MPa^{-1}) and HWD ($9.37E^{-08}$±$1.07E^{-07}$ cm^2 h^{-1} MPa^{-1})

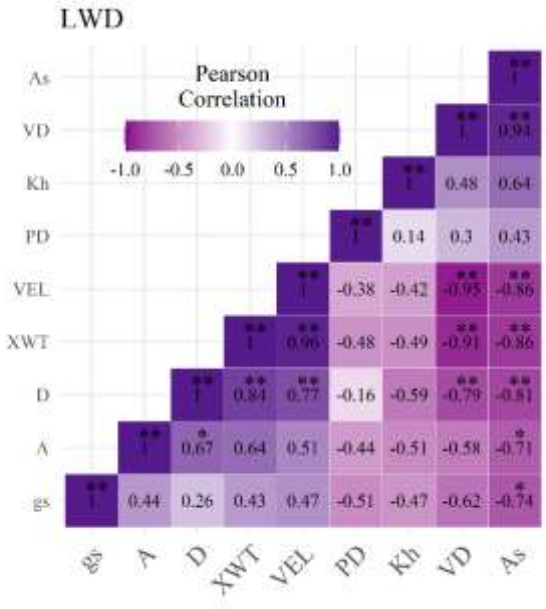

Figure 6. Pearson correlation matrix by plant function type (PFT: deciduous low wood density, LWD). WD= wood density; g_s = Stomatal Conductance; PD= xylem water potential in predawn; D= Vessel lumen diameter; XWT= Xylem wall thickness; VD= Vessel density; VEL= Vessel element length; As= Sapwood area; Kh= Theoretical hydraulic conductivity; A = Net Photosynthesis. *(p<0.05), **(p<0.01).

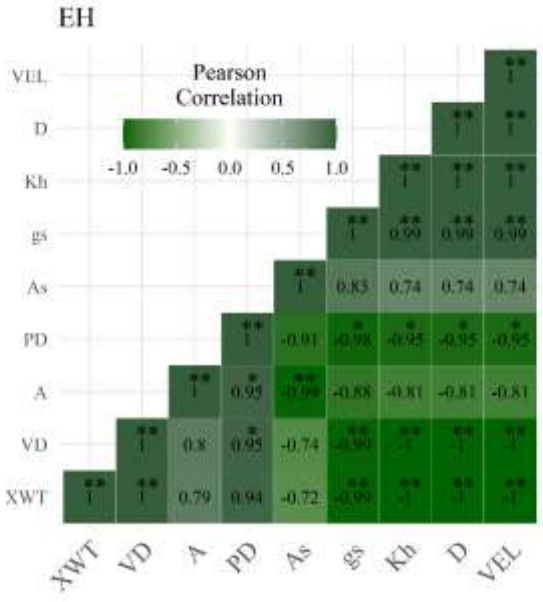

Figure 7. Pearson correlation matrix by plant function type (PFT: deciduous high wood density evergreen, EH). WD= wood density; gs= Stomatal Conductance; PD= xylem water potential in predawn; D= Vessel lumen diameter; XWT= Xylem wall thickness; VD= Vessel density; VEL= Vessel element length; As= Sapwood area; Kh= Theoretical hydraulic conductivity; A = Net Photosynthesis. *(p<0.05), **(p<0.01).

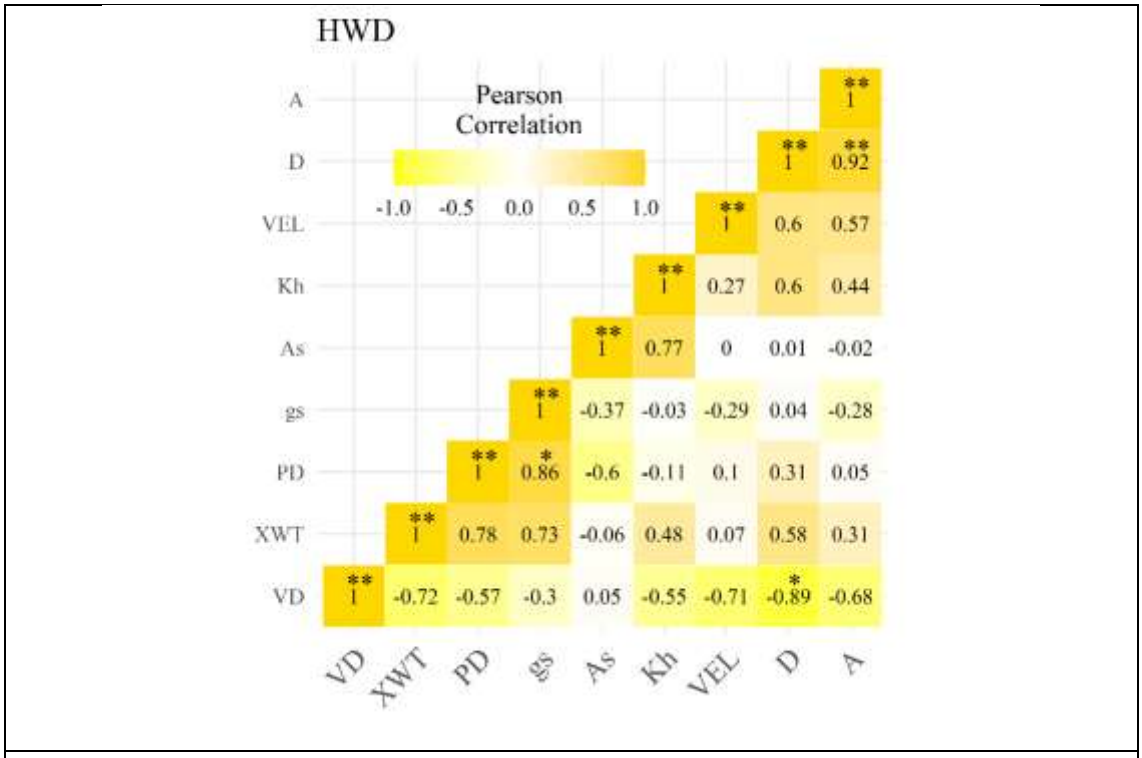

Figure 8. Pearson correlation matrix by plant function type (PFT: deciduous high wood density, HWD). WD= wood density; gs= Stomatal Conductance; PD= xylem water potential in predawn; D= Vessel lumen diameter; XWT= Xylem wall thickness; VD= Vessel density; VEL= Vessel element length; As= Sapwood area; Kh= Theoretical hydraulic conductivity; A = Net Photosynthesis. *(p<0.05), **(p<0.01).

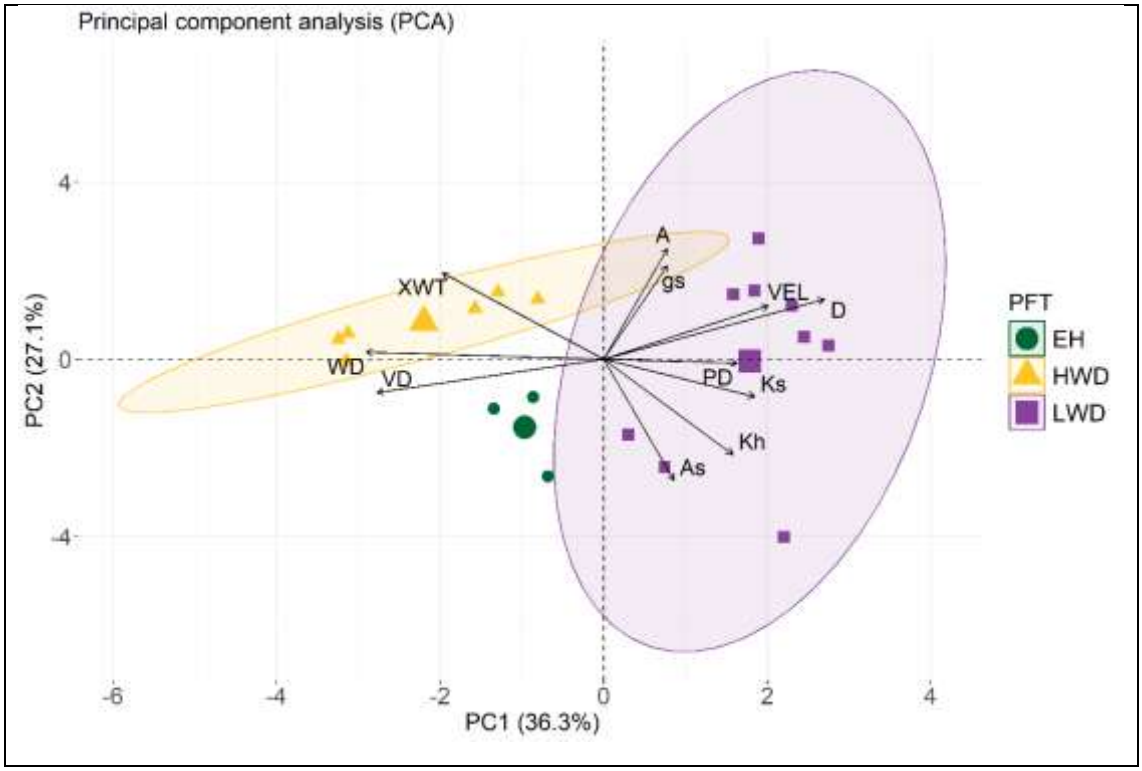

Figure 9. Principal Component Analysis - PCA by plant function type (PFT: deciduous low wood density, LWD; deciduous high wood density, HWD and evergreen high wood density, EH). WD= wood density; gs= Stomatal Conductance; PD= xylem water potential in predawn; D= Vessel lumen diameter; XWT= Xylem wall thickness; VD= Vessel density; VEL= Vessel element length; As= Sapwood area; Kh= Hydraulic conductivity; Ks= Xylem hydraulic conductivity; A = Net Photosynthesis;

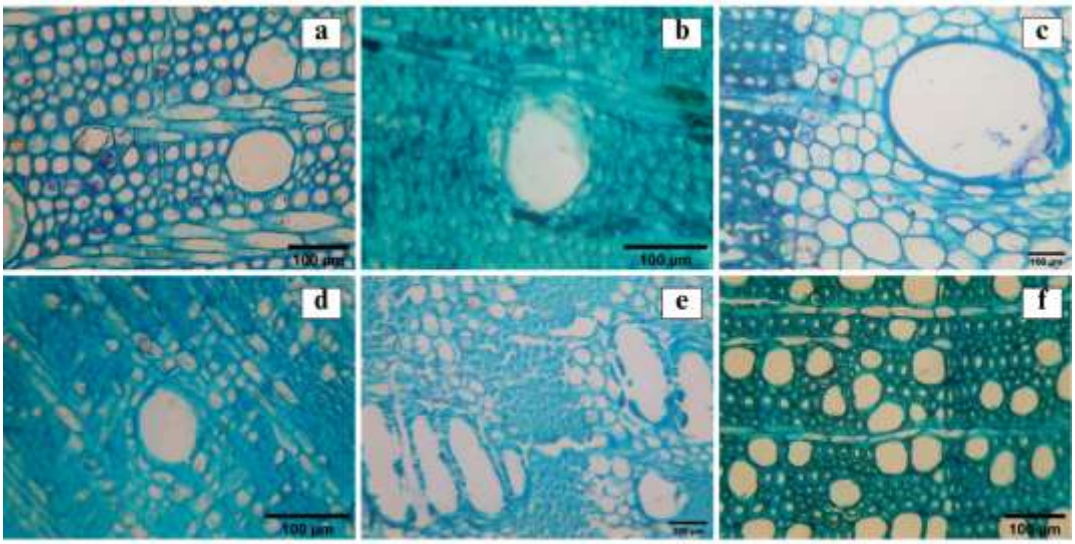

Figure 10. Cross-sectional histological sections by species deciduous low wood density: (a) *Commiphora leptophloeos*, (b) *Spondias tuberosa* and (c) *Amburana cearensis*; evergreen high wood density: (d) *Sarcomphalus joazeiro*; deciduous high wood density: (e) *Cenostigma pyramidale* and (f) *Aspidosperma pyrifolium*.

Supplemental Figs

S1. Photos of sample collection for active xylem with an increment auger.

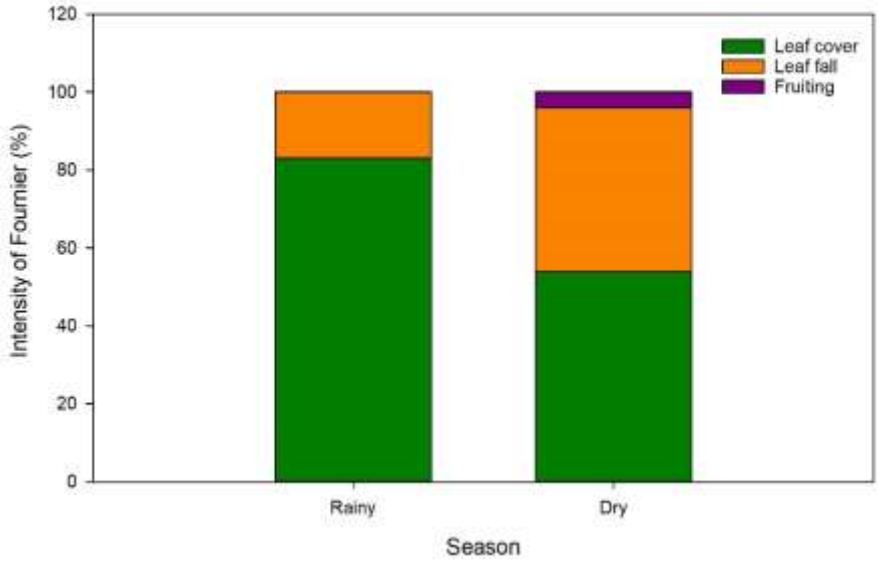

S2. Phenology of *Sarcomphalus joazeiro* in the rainy and dry seasons of 2023.

Artigo 2 - El Niño and La Niña events can modulate sap flow dynamics and non-structural carbohydrates in a tropical dry forest

Maria Medeiros[1]; Angela Lucena Nascimento de Jesus[2,3]; José Raliuson Inácio Silva [2]; André Luiz Alves de Lima[2]; Eduardo Soares de Souza[2]; Hervé Cochard[4]; Mauro Guida Santos[1]

[1]Department of Botany, Bioscience Center, Federal University of Pernambuco, Recife, PE, Brazil.

[2]Federal Rural University of Pernambuco, Serra Talhada Academic Unit, Serra Talhada, PE, Brazil.

[3]Department of Science, Biological Sciences Center, Federal University of Ceara, Fortaleza-CE, Brazil

[4]Université Clermont Auvergne, INRAE, PIAF, 63000 Clermont-Ferrand, France.

*Corresponding author: *Maria Jucicléa dos S. Medeiros*, maria.juciclea@ufpe.br

Abstract

Climate change has intensified the cyclical El Niño and La Niña phenomena, which impact ecosystems, increasing forest mortality rates. In northeastern Brazil, El Niño generated prolonged drought episodes resulting in significant implications for forest dynamics. The objective of our study was to understand how sap velocity and non-structural carbohydrates (NSC) storage of tree species in a Brazilian tropical dry forest respond to the La Niña and El Niño climatic phenomena that occur in 2022 and 2023, respectively. We measured monthly sap velocity (Js), xylem water potential (Ψ_x) in predawn and midday, and NSC. In addition to meteorological data: rainfall, real evapotranspiration (ET), vapor pressure deficit (VPD), and soil water variation (ΔS) through a flux tower installed in the study area. The regressions between Js and VPD, we found that the species *C. leptoplhoeos*, *A. cearensis* and *A. pyrifolium* showed negative relationships in 2023 ($p<0.001$): *C. leptoplhoeos* ($r = -0.89$), *A. cearensis* ($r = -0.72$) and *A. pyrifolium* ($r = -0.76$). In the 2022 rainy season, Ψ_x was higher in the species *C. leptophloeos* (-0.20 MPa) and *S. tuberosa* (-0.21 MPa) and more negative in *S. joazeiro* in

midday (-3.2 MPa). The results show that there was a significant reduction in NSC of the roots in the species *C. leptophloeos* (73%), *A. cearensis* (30%) and *S. tuberosa* (67%) in 2023 in the dry season. Our results indicate that the species do not have a specific control on sap speed with the intensification of drought due to the El Niño phenomenon (2023). *S. joazeiro* may be more tolerant to drought because it has higher Js than the other species. The species *C. leptophloeos*, *A. cearensis* and *S. tuberosa* could be more vulnerable to drought because they drastically reduce their NSC reserves in the roots under intense drought due to El Niño (2023).

Keywords: Caatinga, Drought, ENSO, Soluble sugar, Starch, Xylem water potential

Introduction

Extreme weather events have caused large-scale drought-induced forest mortality (Decarsin et al., 2024; Yang et al., 2018). El Niño and La Niña are climate cycles that normally occur. However, climate change has intensified the effects of these phenomena (Berenguer et al., 2021; Cai et al., 2015). National Oceanic and Atmospheric Administration (NOAA) describes and monitors El Niño-Southern Oscillation (ENSO) intensity from ocean temperature measurements. The period during which neither El Niño or La Niña occurs is called the neutral phase, characterized by intermediate periods (Silva et al., 2022). In Brazil, El Niño causes drought in the North and Northeast regions, while La Niña does the opposite, causing rain in the North and Northeast (de Medeiros and de Oliveira, 2021). In its last season in 2022, La Niña presented its extremes, causing greater intensity of rainfall in the semi-arid region of Northeast Brazil (INMET, 2024). In 2023, extreme drought was observed due to the 2023-2024 El Niño, which was classified as strong in intensity according to National Institute of Meteorology (INMET, 2024). Intensifying drought could cause tree death due to hydraulic failure or carbon starvation processes (Mantova et al., 2022; McDowell et al., 2008; Sala et al. 2012).

During water deficit, plants can suffer damage to their hydraulic system (Liang et al., 2021). Due to water shortages, bubbles enter the xylem, interrupting the flow of sap and causing cavitation of vessels (Sperry, 2000). Due to cavitation processes, the sap flow does not reach part of the tree and causes the death of branches or the entire tree if the water deficit is prolonged (Bréda et al., 2006; Cardoso et al., 2020). Another cause of tree death is carbon starvation, which occurs due to the reduction of carbon stocks, which are essential for the plant's vital

metabolism (Sevanto et al., 2014). The reduction in carbon stocks occurs due to the reduction in the rate of CO_2 assimilation, when there is a reduction in CO_2 input through stomatal closure or leaf senescence (Yu et al., 2019). Therefore, carbon demand is not met to maintain metabolism and carbohydrate synthesis (Zhang et al., 2015a).

Nonstructural carbohydrates (NSC) are made up of soluble sugar and starch (Rosell et al., 2021). Soluble sugar is synthesized during photosynthesis and transported to other parts of the plant, where it is used as an energy source or can be converted to starch, as a form of storage that can be used in the long term (Palacio et al., 2018b; Sala et al., 2010). NSC reflect the ecophysiological responses of plants, as they play a crucial role in osmotic adjustment, in the removal of reactive oxygen species and function as signaling molecules in response to stress (Piper, 2011; Rosell et al., 2021). Furthermore, the progression of drought can also influence the storage of NSC, promoting a reduction in carbohydrate reserves due to the limitation of photosynthesis, which reduces the level of photoassimilates, leading to carbon depletion (McDowell et al., 2022). Thus, if the drought persists, there will be a greater metabolic demand that will no longer be met by photosynthesis, which can lead to a carbon imbalance that can lead to the death of the tree (Piper, 2011). However, while carbon reduction persists, depletion does not always occur, as research indicates that species more adapted to drought have the ability to store carbon reserves in the form of starch (Hartmann and Trumbore, 2016).

Forest species from semi-arid environments have adaptive strategies for surviving drought (de Oliveira et al., 2015; Poorter et al., 2019; Santos et al., 2014). These strategies involve both morphological and physiological adaptations, such as leaf senescence and stomatal closure to reduce water loss (Yu et al., 2019), deep root systems, which allow access to underground water sources (Oliveira et al., 2021b) and, accumulation of carbon reserves, which provides energy for the plant during the dry season (Kawai et al., 2022; Resco de Dios and Gessler, 2021). However, understanding of the mechanisms involved in tree mortality is still limited. Although recent models have attempted to integrate factors such as hydraulic failure and carbon starvation (Mencuccini et al., 2019; Venturas et al., 2017; Yang et al., 2018), the exact and interdependent influence of each on woody plant mortality due to drought is still not completely clear, highlighting the complexity of the problem and the need for further research (Allen et al., 2017; McDowell et al., 2008b).

Studies have linked tree mortality to hydraulic failure and carbon starvation in temperate forests (Bréda et al., 2006; Furze et al., 2019), tropical forests (O'Brien et al., 2014; Oliveira et

al., 2019) and tropical dry forest (Medeiros et al., 2024; Santos et al., 2021). However, considering the scenarios of temperature anomalies in dry tropical forests, studies are needed to assess the influence of climate phenomena on dry forests, such as the Caatinga (Santos et al. 2024). Several previous studies showed influence of El Niño in the Amazon (Barros et al., 2019; Gimenez et al., 2019; Meng et al., 2022; Santos et al., 2018). However, it is necessary for studies like these to be carried out in other biomes, since climate change intensifies the El Niño and La Niña phenomena throughout the world. In addition, other forests, besides the Amazon, are considered large carbon sinks, such as the Caatinga, a Brazilian dry tropical forest (Silva et al., 2017). Therefore, it is necessary to understand how sap flow and NSC storage of trees respond to climatic events.

In view of the above, we asked in our study: 1) How do the sap flow and NSC storage of Caatinga species respond to the La Niña and El Niño climate phenomena? 2) Was the sap flow of the species greater in the rainiest year? 3) Does the intensification of drought cause a reduction in the NSC reserves of the species? To answer these questions, we investigated the speed of sap flow and NSC storage during the rainy and dry seasons between the years 2022 and 2023, in which La Niña and El Niño events occurred, respectively.

Material and Methods

Study area

We conducted the experiment at Fazenda Buenos Aires (07° 56' 50" S, 38° 23' 29" W), located in the municipality of Serra Talhada, PE, Brazil (Figure 1). The Köppen classification is BSh', which is a climate characterized by being semi-arid and hot with a rainy season and a dry season. The average annual precipitation is estimated at 632 mm. Average monthly air temperatures range between 23.6 and 27.7 °C, and maximum temperatures exceed 32 °C (Pereira et al., 2015).

Species

We selected six species widely distributed in the Caatinga dry forest: *Amburana cearensis* (Allemao) A.C.Sm. (Fabaceae), *Spondias tuberosa* Arruda (Anacardiaceae), *Commiphora leptophloeos* (Mart.) J.B.Gillett (Burseraceae), *Cenostigma pyramidale* (Tul.) Gagnon & G. P. Lewis (Fabaceae), *Aspidosperma pyrifolium* Mart. & Zucc. (Apocynaceae), *Sarcomphalus*

joazeiro (Rhamnaceae). We selected five trees of each species to install sap flow sensors for monitoring for 19 consecutive months (March 2022 to September 2023).

Water balance

We collected precipitation data, which was measured with a rain gauge (model TE 525 WS-L, Texas Electronics, Dallas, TX, USA), vapor pressure deficit (VPD) and actual evapotranspiration (ET) from an 11 m high flux tower (3 m above the tree canopy), which has equipment that constitutes the Eddy Covariance method. Data were recorded by a data logger (model CR1000, Campbell Scientific Inc., Logan, UT, USA) every 60 s. We calculated VPD and ET according to Silva et al. (2017). Soil water storage was calculated according to the number of layers (five layers) and the thickness of each soil layer in which the sensors were installed.

$$(S=\sum q_n \Delta Z_n) \quad (1)$$

Where S is the sum of soil moisture of all layers, q_n is the number of soil layers (up to 5) and ΔZ is the soil depth interval. Thun, we calculate the variation of water in the soil per month., ΔS.

$$\Delta S = \theta_f - \theta_i \quad (2)$$

Where θ_f is the soil moisture profile at the end of the month, and θ_i is the soil moisture at the beginning of the month.

Sap flow velocity *(Js)*

Based on the methodology of Granier (1985) and adaptation by Wright et al. (2023), we installed a sensor on the main stem of each tree (at a height of 50 cm above the ground), penetrating 10 mm into the xylem. The sensor consisted of two probes, both installed 10 cm apart. The upper probe was the heat probe, while the lower probe (the reference probe) read the temperature absorbed by the sap. The temperature difference between the probes was considered the heat transfer rate. When the temperature reading of the upper probe was equal to the reading of the lower probe, we considered that the sap was being transported rapidly to the tree canopy. Based on Granier (1985), the sap flow velocity can be calculated with the following equations:

From the sensor data, the (dimensionless) heat transfer rate was calculated as:

$$K = (\Delta T_{Max} - \Delta T) / \Delta T \quad (3)$$

where ΔT_{Max} is the temperature difference between the two probes at zero sap flow (at night), and ΔT is the difference between the probes when the tree is transpiring and the sap is flowing. Then the mean flow velocity, Js (cm h^{-1}) was calculated as:

$$Js = 119 * 10^{-6} * K^{1,23} \quad (4)$$

To compare sap velocity between the rainy and dry seasons, we selected two months from each season that had sufficient data from all species for analysis: March and April (rainy season) and June and July (dry season). This representation was selected because deciduous species lose almost all of their leaves from August onwards.

Xylem water potential

We performed xylem water potential (Ψx) measurements once in each rainy and dry season of 2022 and 2023, before dawn (predawn) between 4 and 5 am, and at noon (midday) between 12 and 13 pm, using a Scholander-type pressure chamber.

Stomatal conductance

We measured once in each rainy and dry season of 2022 and 2023 the stomatal conductance (gs) on two fully expanded leaves of each tree in the morning (9–10 am) using a porometer (Decagon Devices, Inc. 2365 NE Hopkins Court Pullman WA 99163).

Non-structural carbohydrates (NSC)

We collected samples from different parts of the trees during the rainy season: leaves, stems and roots, and during the dry season, due to deciduousness, we collected only stem and root samples. We collected completely healthy and expanded leaves; stem samples were collected from branches with ~5 mm in diameter and root samples were collected from thin roots ~2 mm thick. We collected samples at around 3 pm. Immediately after collection, to stop enzymatic activity, the samples were placed in a microwave oven at 700w for 3 minutes (Audrey G. Quentin et al., 2015).

Before performing the analysis, we performed a preliminary test to establish the dry weight (mg) to be used in the extraction process. In this process, we measured the SS content of 10 mg, 20 mg, and 40 mg of dry matter from two randomly selected individuals in each organ of the

species. With this, we aimed to verify whether the SS concentration increased in proportion to the dry matter mass. This procedure allowed us to evaluate the saturation level of the extracts. Therefore, we determined the dry weight of 20 mg as appropriate for all organs to proceed with the analysis.

We performed the quantification of soluble sugars (SS) using 80% ethanolic suspension according to (Farrar, 1993). The samples were ground in a mortar and suspended in 1,200 µl of 80% ethanol. After shaking, the samples were incubated for 90 minutes in a water bath at 70°C. Then, the material was centrifuged at 15,000 g-force and the supernatant was collected. This process was repeated using 600 µl of 80% ethanol for another 30 minutes. We determined the concentration of soluble sugars using the phenol-sulfuric acid method by adding 0.5 ml of 5% phenol and 2.5 ml of sulfuric acid to the aliquot of the extract. Finally, we determined the SS concentration using a double-beam spectrophotometer at 487 nm (Genesis 10S UV-Vis, Thermo Scientific) (Dubois et al., 1956).

After SS determination, we quantified the starch in the samples, in which we resuspended the pellets in 800 µl of 0.2 M KOH solution and vortexed. Then, we placed the supernatant in a water bath at 95 °C for 2 hours. After this time, the samples were adjusted to pH 5.5 with 200 µl of acetic acid and centrifuged at 15,000 g-force and the supernatant was then collected. The samples were hydrolyzed with 10 units of amyloglucosidase (A1602, Sigma-Aldrich) for 1 hour in a thermal bath at 55 °C to digest the gelatinized starch into glucose. Starch concentrations (measured as glucose equivalents) were measured at 487 nm using a double-beam spectrophotometer (Dubois et al., 1956).

Statistical analysis

To answer how the sap flow of species responds to the La Niña and El Niño climate phenomena, we performed regressions ($p < 0.001$) between vapor pressure deficit (VPD) vs sap velocity (Js) and tested the means between the rainy and dry months between 2022 and 2023 using the SNK (Student-Newman-Keuls) test. We also performed analysis of variance (ANOVA) to compare Ψx and gs between years and between species; NSC, SS and starch, between species and between 2022 and 2023 for each organ (leaf, stem and root) in the rainy and dry seasons. When there was a significant difference between years or species, the data were analyzed using the SNK (Student-Newman-Keuls) test ($p < 0.05$). The analyses and graphs were performed using the R programming language v.4.2.0 (R Core Team 2022) and SigmaPlot version 14.0.**Results**

Environmental variables

The total annual rainfall was 772 mm in 2022 (La Niña) and 472 mm in 2023 (El Niño). The rainiest month of 2022 and 2023 was March with 165 mm and 179 mm, respectively (Figure 2). While the driest months were from July to November, with September having no rain recorded in 2022 and July only 14 mm recorded in 2023, August 8 mm, September and October having no rain recorded and November only 12 mm (Figure 2). The ET in 2022 was highest in January (82 mm), March (80 mm) and April (81 mm). In 2023, the highest ET was 63 mm in January and 69 mm in June (Figure 2). From August to November 2023, the ET was zero. The VPD in 2022 was highest in October with 2.13 kPa and lowest in June with 0.76 kPa. The VPD in 2023 was highest in October and November with 2.57 and 2.59, respectively (Figure 2). The soil water balance showed that in 2022 it was lowest in March (-24 mm) and October (-22 mm) and highest in April (30 mm) and November (33 mm). While in 2023 it was highest in March (45 mm) and lowest in April (-32 mm) (Figure 2).

Interannual variability in sap velocity (Js) vs VPD

The Js of *S. joazeiro* was higher than the other species (Figures 3 and 4). However, the species did not show significant differences between the years 2022 and 2023 in Js (Figures 3 and 4). When we analyzed the correlations between Js and VPD, we found that the species *C. leptoplhoeos, A. cearensis* and *A. pyrifolium* showed negative relationship in 2023 ($p<0.001$): *C. leptoplhoeos* ($r = -0.89$), *A. cearensis* ($r = -0.72$) and *A. pyrifolium* ($r = -0.76$) (Figure 5).

Xylem water potential (Ψ_x)

In the 2022 rainy season, Ψ_x was higher in the species *C. leptophloeos* (-0.20 MPa) and *S. tuberosa* (-0.21 MPa) and more negative in *S. joazeiro* in *midday* (-3.2 MPa) (Figure 6a). There were differences between the years 2022 and 2023 in the measurements taken in midday, with Ψ_x being more negative for all species in the year 2022, except for *A. pyrifolium* (Figure 6a). In the dry season, the species *C. leptophloeos*, *A. cearensis* and *S. tuberosa* presented higher Ψ_x (Figure 6b). There were differences between the years 2022 and 2023 in the measurements taken at *midday*, with Ψ_x being more negative for all species in the year 2023 Figure 6 b). *C. pyramidale* showed Ψ_x more negative than the other species (-6.48 MPa) (Figure 6 b).

Stomatal conductance (gs)

In the rainy season in 2022, there were significant differences between species. C. leptophloeos showed the highest averages, while *S. joazeiro* showed the lowest averages of gs (Figure 7 a).

There were differences between the years 2022 and 2023 in the afternoon (am) for all species, except in *S. joazeiro*, which did not show significant differences between gs throughout the periods of the day (Figure 7 a).

In the dry season, the species *C. leptophloeos*, *A. cearensis* and *S. tuberosa* lost their leaves, and no gs measurements were recorded for these species (Figure 7 b). There were no differences between species, however, there were differences in gs between years within each period of the day (Figure 7 b). The highest gs was measured in *S. joazeiro* during the rainy season of 2022, reaching 381.72 mmol m^2 s^{-1}.

Concentration of non-structural carbohydrates

During the rainy season, the species presented a higher concentration of NSC in 2022 in the leaves, being higher in the species *C. leptophloeos*, *A. cearensis* and *S. tuberosa* (Figure 8 a), except for the species *C. pyramidale*, *A. pyrifolium* and *S. joazeiro*, which did not present a significant difference between 2022 and 2023 in the leaves (Figure 8 a).

In the stem, the species *C. leptophloeos* and *S. tuberosa* presented a higher concentration of NSC in 2022, while *A. cearensis* presented a higher concentration in 2023 (Figure 8 a). The species *C. pyramidale*, *A. pyrifolium* and *S. joazeiro* presented a lower concentration of NSC than the other species (Figure 8 a).

When we analyzed the roots in rainy season, the results show that the species *C. leptophloeos*, *A. cearensis* and *S. tuberosa* presented a higher NSC in 2023 (Figure 8 a). The lowest NSC concentration was recorded in *C. pyramidale* in 2023 (Figure 8 a).

In the dry season, *S. joazeiro* presented higher NSC in 2022 in the leaves (Figure 8 b). In the stem, only *A. pyrifolium* presented a significant difference between 2022 and 2023, being higher in 2022 (Figure 8 b). However, when we evaluated the roots, the results show that there was a significant reduction in NSC in the species *C. leptophloeos*, *A. cearensis* and *S. tuberosa* in 2023 (Figure 8 b). Only the species *A. pyrifolium* presented higher NSC in 2023 in the roots than in 2022 (Figure 8 b).

Discussion

Our results show that species exhibited different seasonal behavior during La Niña (2022) and El Niño (2023) events. The El Niño phenomenon caused different responses to drought-induced

water limitations, with clear differences between the years 2022 and 2023. Among species-specific differences in sap velocity, *S. joazeiro* stood out by presenting high Js compared to the other species. However, the species did not show significant differences between years in Js, suggesting that species do not have a specific control on sap velocity with the intensification of drought, indicating that under intense drought the probability of more cavitation events occurring in species due to hydraulic failure. When we evaluated NSC storage under intense drought in 2023, we found that the species *C. leptophloeos*, *A. cearensis* and S. *tuberosa* drastically reduced their reserves in the roots. These species have low wood density, which is more vulnerable to xylem cavitation and depends on stored resources to flower and/or sprout new leaves in the dry season.

Influence of VPD on sap velocity and NSC storage

The 2023-2024 El Niño was one of the strongest on record, causing successive record high temperatures in Brazil (National Institute of Meteorology, INMET, 2024). Due to climate change, La Niña and El Niño events may become more frequent and intense (Cai et al., 2015). The La Niña phenomenon lasted approximately two and a half years, ending in early 2023, according to the United States National Oceanic and Atmospheric Administration (NOAA).

The El Niño phenomenon caused increased atmospheric demand, leading to high vapor pressure deficit (VPD) (Grossiord et al., 2020), causing a reduction in Js in some species, such as *C. leptoplhoeos, A. cearensis* and *A. pyrifolium*. VPD is the driving force for transpiration in plants and generally leads to reduced plant transpiration (Burkhardt and Pariyar, 2016; Will et al., 2013). A 3°C increase in temperature can increase VPD by 45% (Will et al., 2013).

Higher VPD is likely to intensify physiological stress in plants during drought periods by increasing plant water loss or reducing carbon uptake through stomatal closure (McDowell et al., 2008b; Will et al., 2013). The results found by Will et al. 2013 support the hypothesis that increased VPD increases transpiration and causes rapid mortality in plants subjected to drought.

Plant responses to VPD depend on the water strategy of each species (Burkhardt and Pariyar, 2016). Some plants respond quickly to water deficit through stomatal closure, maintaining a considerable leaf water potential, although there is a reduction in stomatal conductance and reduced CO_2 absorption (McDowell et al., 2022). While other species continue to transpire as leaf water potential decreases, or as the risk of hydraulic failure increases (Liang et al., 2021; McDowell et al., 2008b; Sevanto et al., 2014).

Some studies have shown that the 2015–2016 El Niño drought caused changes in the water relations of Amazonian plants, such as decreased sap velocity due to xylem embolism processes (Fontes et al., 2018) and stomatal closure that caused reduction photosynthesis in plant leaves from a Central Amazon forest (Santos et al., 2018).

The availability of water in the soil is also a limiting factor for tree transpiration, because when the soil dries out drastically, plant roots find it difficult to uptake enough water for transpiration, causing tension in the xylem vessels and resulting in xylem embolism (Oliveira et al., 2021a; Tonet et al., 2024). Hydraulic failure occurs when there is an interruption in the transport of sap flow in the xylem, which is caused by embolism (formation of air bubbles, which prevent adequate flow, blocking the xylem) (Venturas et al., 2017).

Trees that have a deeper root system may be more drought tolerant (Oliveira et al., 2005). The presence of deep roots in the species *S. joazeiro* possibly favored high sap velocity throughout 2022 and 2023, despite the more pronounced drought in 2023 due to the occurrence of El Niño. The study by Meng et al. (2022) showed that sap velocity was largely limited by reduced soil moisture during the drought in Central Amazonia during the 2015–16 El Niño drought.

Impact of El Niño on NSC reserves

The 73% reduction in NSC in the roots of *C. leptophloeos*, 30% in *A. cearensis* and 67% in *S. tuberosa*, under the intensification of the 2023 drought, possibly occurred because there was a reduction in NSC synthesis, resulting from the low photosynthetic rate (Piper, 2011; Sala et al., 2010). Some studies have already found that El Niño affects the physiology of trees, for example, it was found that the carbon sink of the tropical forest decreases during El Niño due to the reduction in photosynthesis and the increase in respiration rates (Cavaleri et al., 2017).

C. leptophloeos, *A. cearensis* e *S. tuberosa* are deciduous species with low wood density that store large amounts of starch in their roots (Medeiros et al., 2025). These species were the most affected by the 2023 drought, as the reduction in NSC was more pronounced in their storage organs, stem and roots than in the other species. *C. leptophloeos*, *A. cearensis* e *S. tuberosa* maximize NSC synthesis during the rainy season and store large amounts of NSC as starch for long-term use. This is a strategy used by many deciduous species for drought tolerance (Palacio et al., 2018a; Sala et al., 2010). The species *C. leptophloeos*, *A. cearensis* and *S. tuberosa* use during the dry season part of the stored NSC for leaf sprouting and

flowering (Lima et al., 2012; Medeiros et al., 2025). However, high demand for carbohydrates leads to carbon depletion (McDowell et al., 2008b). Furthermore, the reduction of NSC can also significantly impact the reproduction of Caatinga species, since these compounds are essential for sustaining phenological processes, such as flowering, fruiting and seed development (Lima et al., 2012). Therefore, the reduction of these reserves can compromise the reproductive success and natural regeneration capacity of populations, harming the resilience of Caatinga ecosystems in the face of climate change.

Recent studies as in Bretfeld et al. (2018) and Berenguer et al. (2021) revealed robust changes in the characteristics of El Niño in response to simulated future greenhouse warming. This indicates that the intensification of drought by the El Niño phenomenon in dry forests such as the Caatinga, may cause greater losses, since many species have the strategy of losing leaves at the beginning of the dry season and using their reserves for sprouting at the peak of the dry season (Lima et al., 2012), and consequently in the long term, the depletion of reserves eventually leads to carbon starvation and tree death (McDowell et al., 2008b).

Tropical ecosystems, including semiarid regions, are key to interannual variation in global carbon storage (Zuidema et al., 2022). These regions, exhibit greater climate variability and make a significant contribution to interannual fluctuations in the carbon sink (Zuidema et al., 2022).

Implications in the face of climate change

Our results indicate that the intense drought caused by El Niño does not alter the sap velocity of the species, suggesting that the species studied do not have a specific control over the sap velocity, leading to the inference that more cavitation events will possibly occur in Caatinga species due to hydraulic failure under severe drought. Deciduous species with low wood density were most affected by the NSC reduction, causing a reduction of up to 73% in *C. leptophloeos* in the 2023 dry season. The evergreen species *S. joazeiro* may be more tolerant because it is able to fully exploit soil water uptake to maintain its transpiration even under extreme drought (Wright et al., 2023).

Evergreen species such as *S. joazeiro* in the Caatinga have lower abundance compared to deciduous species (Souza et al., 2020). However, the greater implantation of evergreen species (more drought tolerant) in the Caatinga may cause greater exploitation of soil water and an imbalance between the rainy and dry seasons. As a result, the seasonal pattern may change.

Therefore, species diversity is essential to maintain the ecohydrological balance of forests. Furthermore, as the climate becomes hotter and drier, soil moisture tends to be the primary regulatory factor for transpiration, rather than light availability. Transpiration in tropical forests plays a crucial role in modulating the global hydrological cycle and regulating climate patterns, influencing the redistribution of water in the atmosphere (Meng et al., 2022; Poyatos et al., 2021).

Variations in forest transpiration have significant implications for biosphere-atmosphere interactions at local, regional, and global scales, impacting water and carbon balances (Meng et al., 2022). Therefore, forest diversification should be implemented together with management strategies that aim to implement drought-resistant species (Decarsin et al., 2024). It is important to note that it is still unclear to what extent species can resist drought or what the mortality rate of trees in dry Caatinga forests is, so how forest patterns will change in response to future warming, due to El Niño and La Niña phenomena, remains uncertain.

Conclusion

We conclude that the species do not have a specific control on sap speed with the intensification of drought due to the El Niño phenomenon (2023). *S. joazeiro* may be more tolerant to drought because it has higher Js than the other species. We also found that the species *C. leptophloeos*, *A. cearensis* and *S. tuberosa* are more vulnerable to drought because they drastically reduce their NSC reserves in the roots under intense drought due to El Niño (2023).

Conflict of Interest

None declared

Funding

This work had financial support from FACEPE (Facepe-Pronem-APQ-0336-2.03/14). MM is funded by (FACEPE Fellow-IBPG-0330-2.07/21) and Sandwich PhD Scholarship Program by the French Embassy in Brazil, Campus France Brazil (BGF- 160421Y-TerrEE Scholarship, 2024). The work was also supported by INCT: National Observatory of Water and Carbon Dynamics in the Caatinga Biome – ONDACBC, contributing with meteorological data from the flow tower installed in the study area.

Acknowledgements

We would like to thank the scientific initiation students from the Plant Physiology laboratory (LFV), Department of Botany at UFPE, for their assistance with laboratory analyses, the Study Group on Semiarid Ecohydrology and the Center for Functional Ecology of Plants (NEFPlan), Universidade Federal Rural de Pernambuco, Serra Talhada Academic Unit (UFRPE/UAST) for assistance in fieldwork. We also thank the Postgraduate Program in Plant Production at UFRPE/UAST for the availability of equipment and laboratories. The first author would like to thank the members of Laboratoire de Physique et Physiologie intégratives de l'Arbre en environnement Fluctuant (PIAF, INRAE) for their support during the sandwich doctoral stay.

Data Availability Statement

The data that support the findings of this study are available from the corresponding author upon reasonable request.

Authors' Contributions

MM, HC and MGS conceived the study with input from all authors. MM, ALAL, JRIS and ALJ and collected data. MM analyzed the data and wrote the manuscript. MGS, ALAL and ES provided supervision and resources. All authors approved the manuscript for publication.

Conflict of Interest

None declared.

Tables and figures

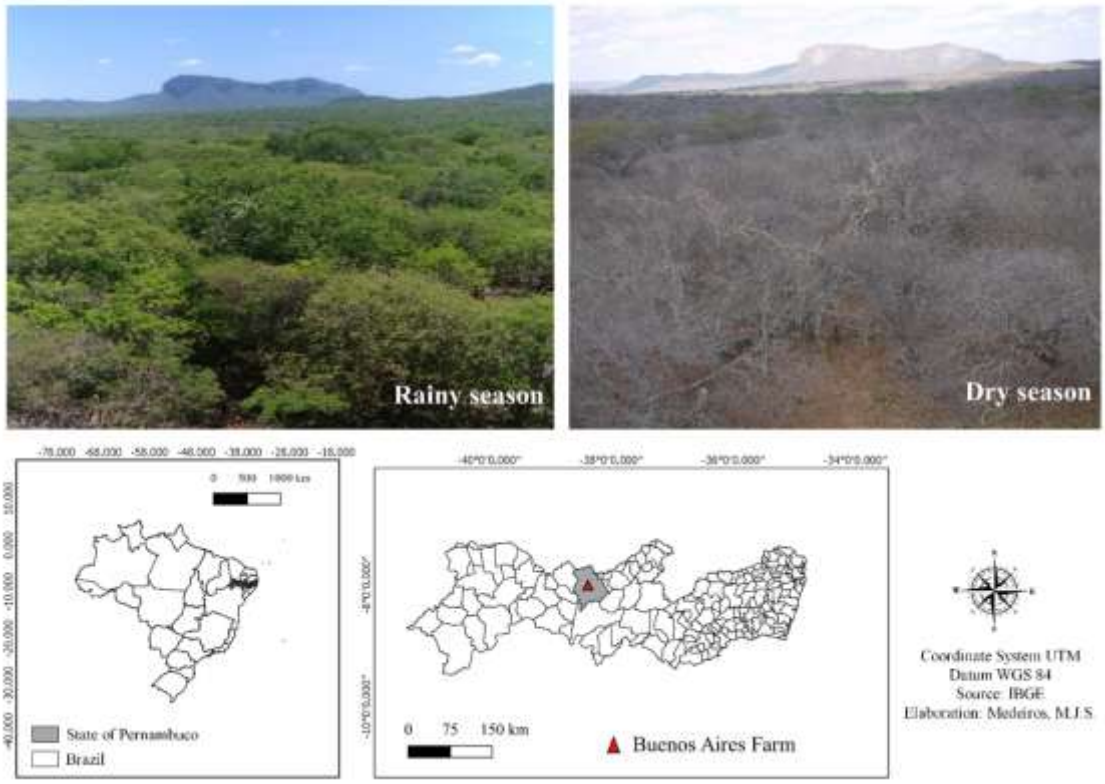

Figure 1. Map and photos of vegetation in the rainy and dry season of the study area, Fazenda Buenos Aires, Serra Talhada, PE-Brazil. Photo credits: Maria Medeiros (rainy season) and Cynthia Wright (dry season).

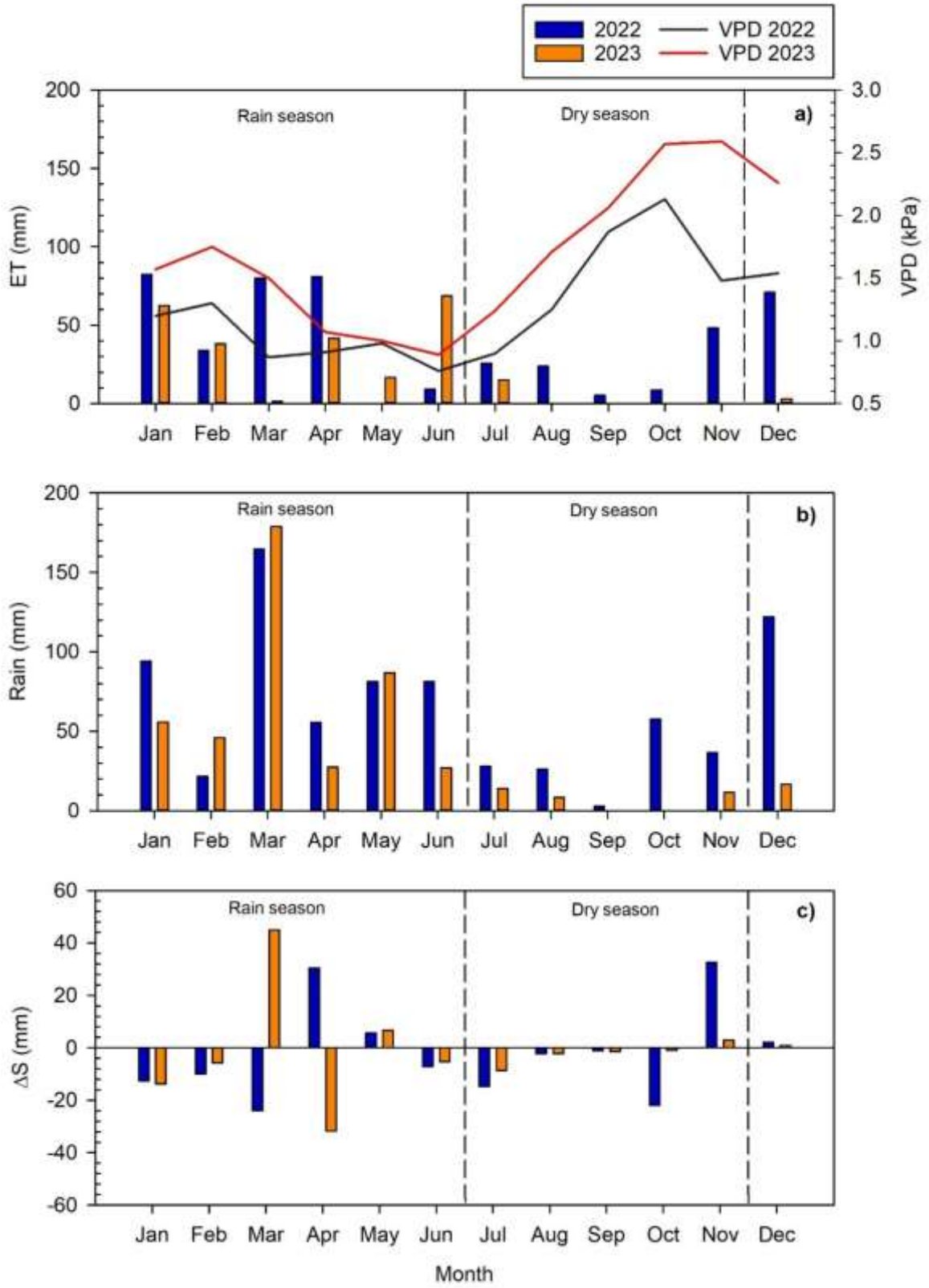

Figure 2. Water balance for the years 2022 and 2023 in the study area, Serra Talhada-Pernambuco, Brazil. a) Evapotranspiration (ET, mm) and Vapor pressure deficit (VPD, kPa), b) Rainfall (Rain, mm), c) Soil water variation (ΔS, mm). Dashed lines separate the months corresponding to the rainy (December to June) and dry (July to November) seasons.

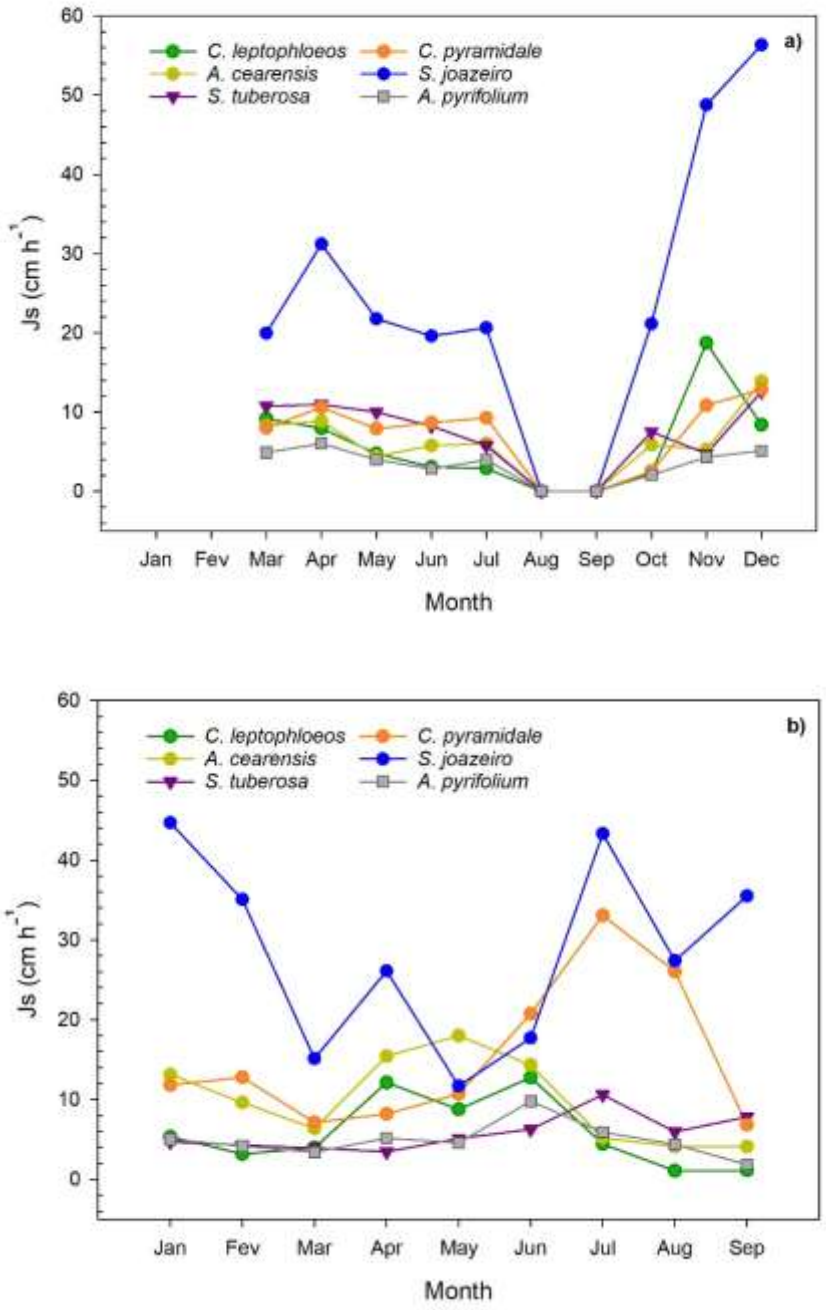

Figure 3. Monthly sap flow velocity of six species of a Brazilian dry forest, Caatinga. a) Average monthly sap flow velocity in 2022. b) Average monthly sap flow velocity in 2023.

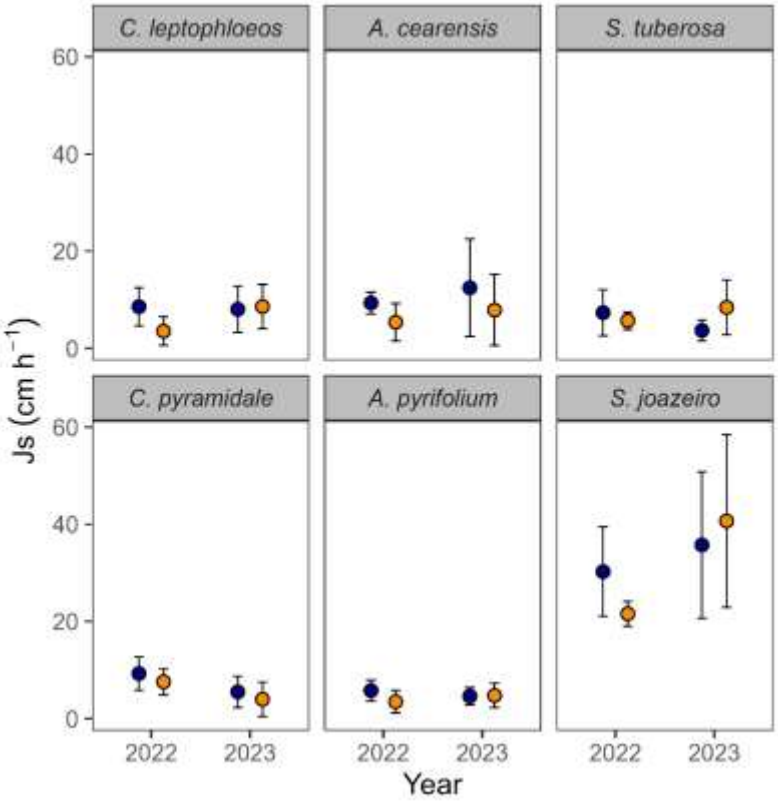

Figure 4. Sap velocity (Js) in Caatinga species in the months of March to April (rainy season) and June to July (dry season), municipality of Serra Talhada-PE. Blue dots represent the rainy season and orange dots represent the dry season in the years 2022 and 2023.

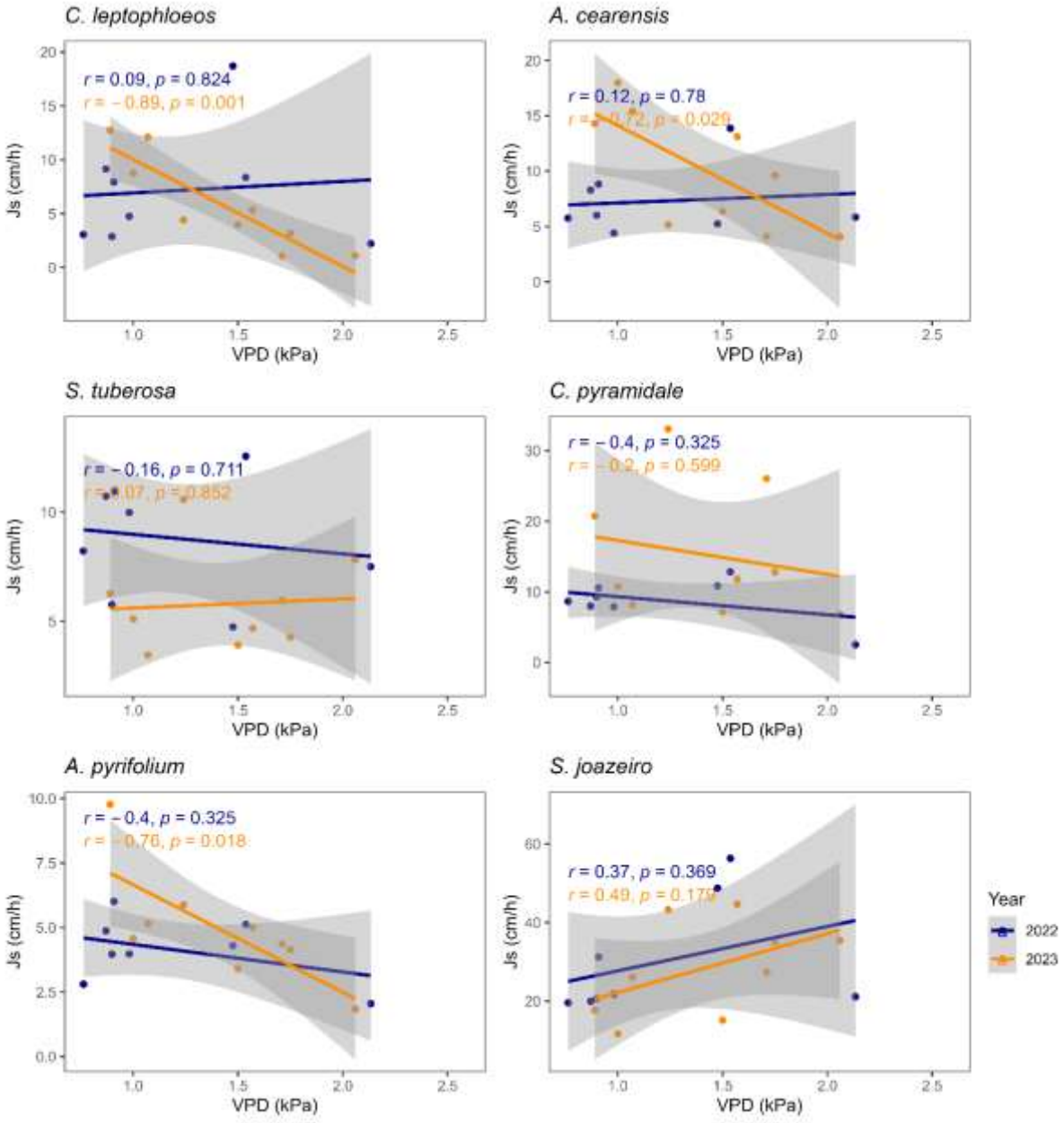

Figure 5. Relationships between vapor pressure deficit (VPD) and sap velocity (Js) in Caatinga tree species in 2022 and 2023, in the municipality of Serra Talhada, Pernambuco, Brazil. ($p<0.001$).

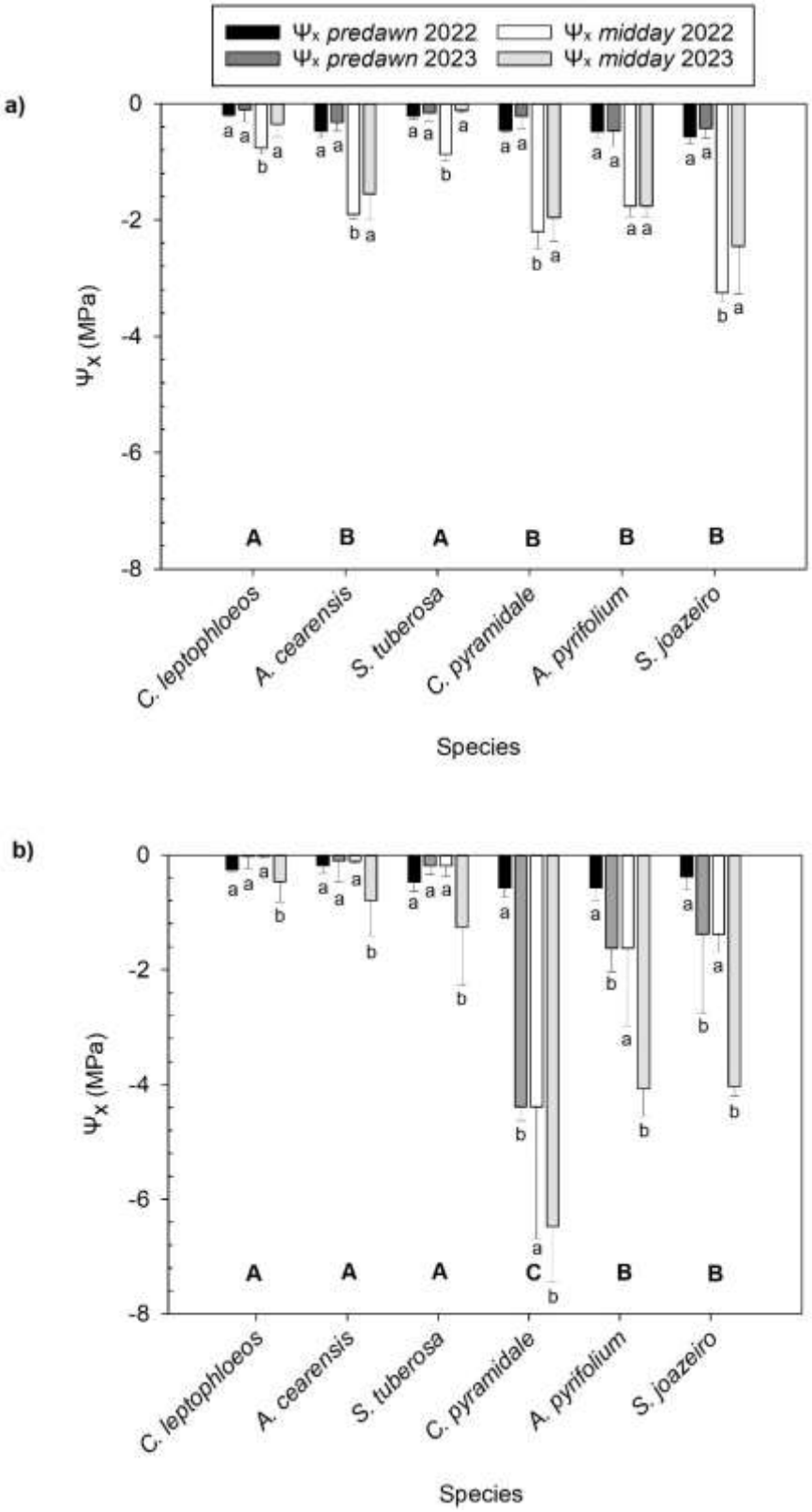

Figure 6. Xylem water potential (Ψx) in the rainy and dry seasons of 2022 and 2023 in six woody species of a Brazilian dry forest, Caatinga. a) Ψ_x in the rainy season of 2022 and 2023. b) Ψ_x in the dry season of 2022. Uppercase letters compare species independently of year; Lowercase letters compare years within each day period (*predawn* or *midday*) in each specie.

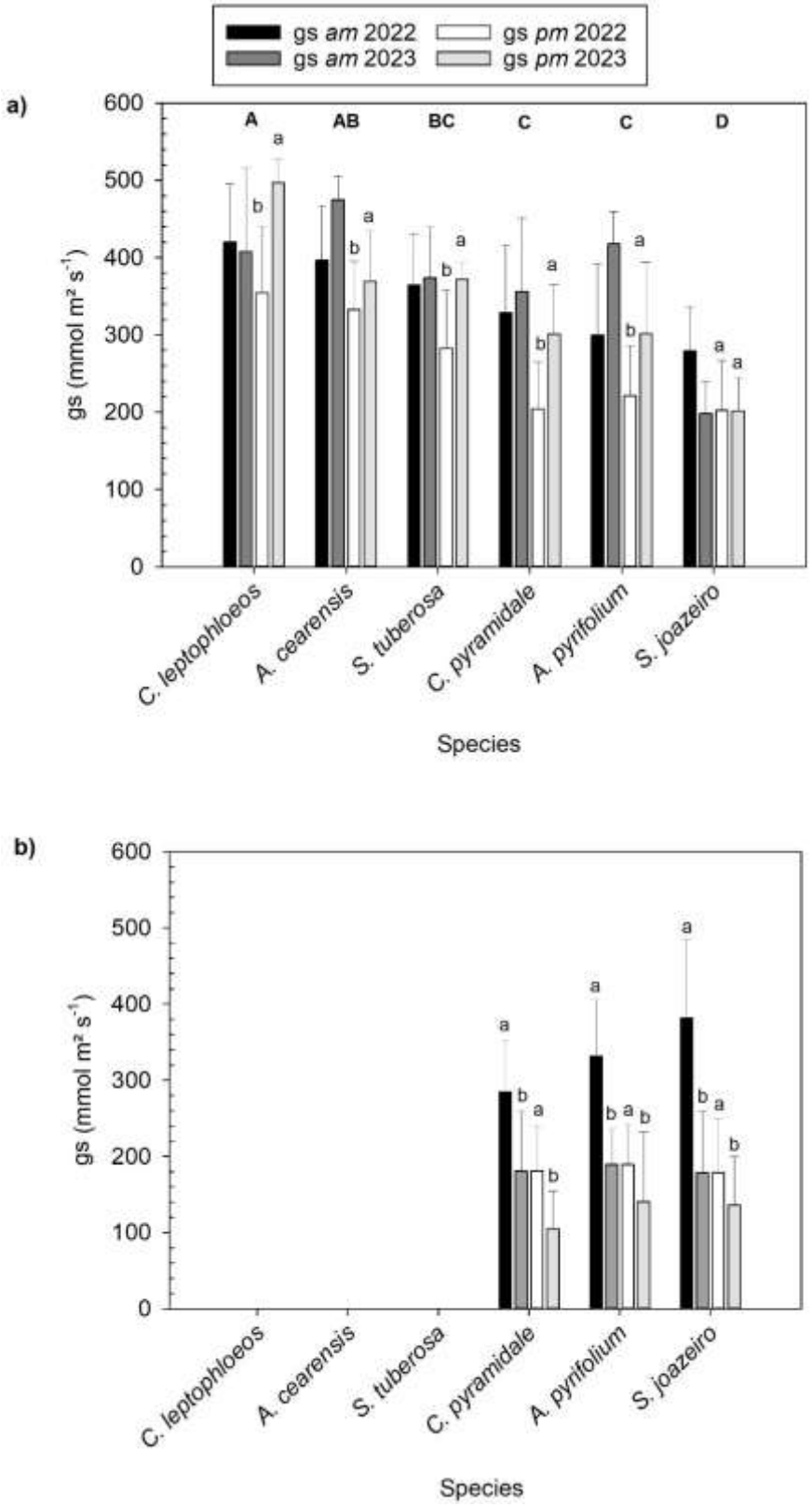

Figure 7. Stomatal conductance (gs) in the rainy and dry seasons of 2022 and 2023 in six woody species of a Brazilian dry forest, Caatinga. a) gs in the rainy season of 2022 and 2023. b) gs in the dry season of 2022. Uppercase letters compare species independently of year; Lowercase letters compare years within each day period (*am: ante meridiem and pm: post meridiem*) in each specie.

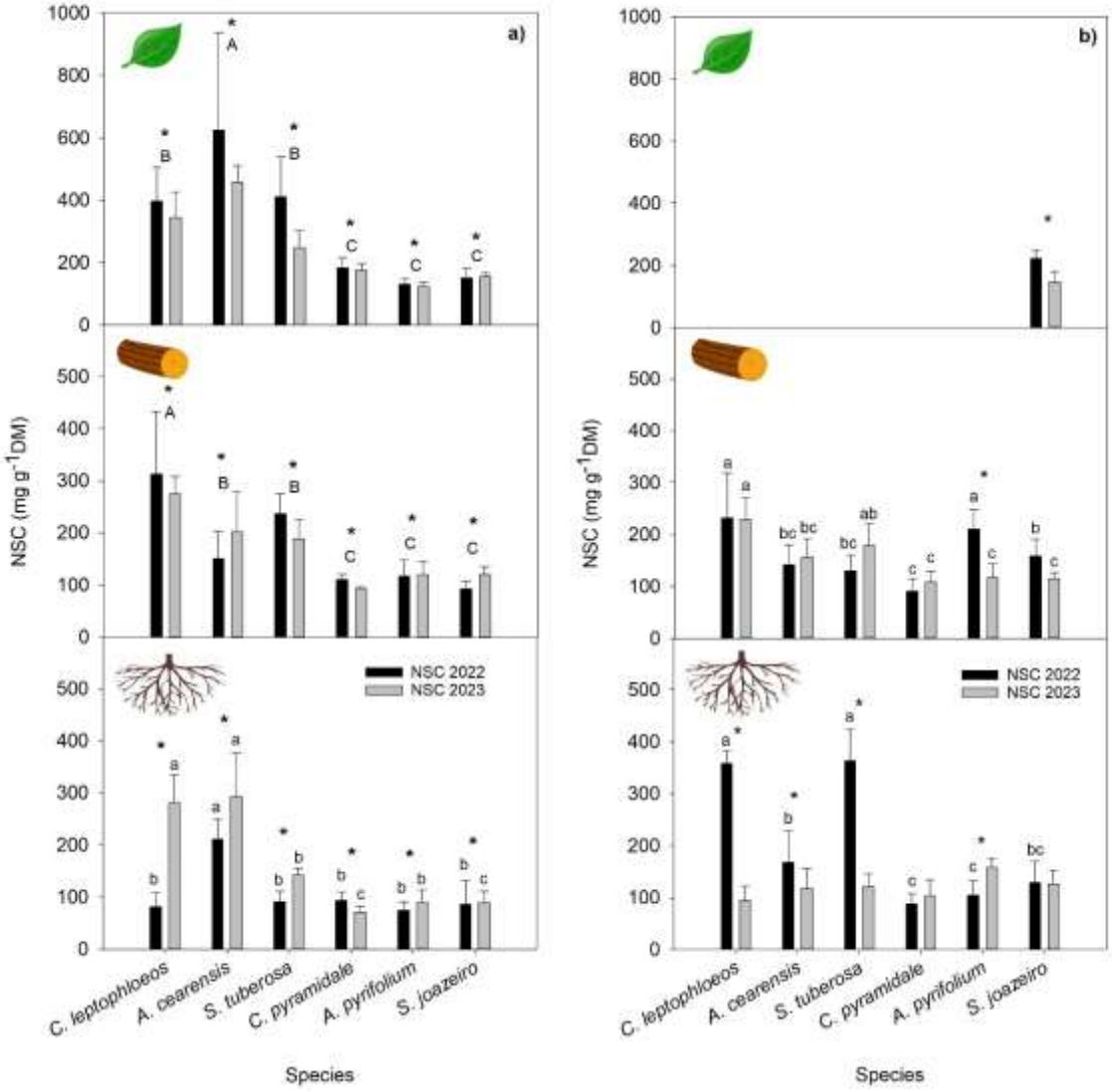

Figure 8. Nonstructural carbohydrates (NSC) in the rainy and dry seasons of 2022 and 2023 in six woody species from a Brazilian dry forest, Caatinga. a) NSC in the rainy season of 2022 and 2023 in different organs: leaf, stem and root. b) NSC in the dry season of 2022 and 2023 in different organs: leaf, stem and root. Uppercase letters compare species regardless of year; Lowercase letters compare species within each year (significant interaction); * indicates difference between years for each species.

Table 1. Summary of the means of the species variables: *C. leptophloeos, A. cearensis, S. tuberosa, C. pyramidale, A. pyrifolium* and *S. joazeiro* in the rainy and dry seasons of 2022 and 2023. Ψx (Xylem water potential at predawn); gs (Stomatal conductance measured between 9 and 10 a.m.); Js (Mean sap flow velocity); NSC (Non-structural carbohydrates in leaf, stem and root). The measurements were carried out in an area of the Caatinga dry forest in the municipality of Serra Talhada – PE, Brazil. empty space means that the measurement was not performed due to the absence of leaves.

2022							**2023**					
Rainy season							**Rainy season**					
Variables							**Variables**					
Species	Ψ_x (MPa)	gs (mmol m^2 s^{-1})	Js (cm h^{-1})	NSC (mg g^{-1} DM) Leaf	Stem	Root	Ψ_x (MPa)	gs (mmol m^2 s^{-1})	Js (cm h^{-1})	NSC (mg g^{-1} DM) Leaf	Stem	Root
C. leptophloeos	-0.20±0.02	420.5±75.1	7.55±1.93	397.0±107.9	312.7±120.6	81.9±26.8	-0.10±0.21	408.0±107.8	6.66±3.72	345.5±80.3	275.4±32.7	281.3±52.0
A. cearensis	-0.47±0.10	396.6±70.3	8.85±3.88	625.0±313.5	151.2±50.5	211.1±38.3	-0.32±0.16	474.9±30.9	12.5±4.60	458.8±52.2	202.3±76.7	292.3±84.1
S. tuberosa	-0.21±0.06	364.4±66.8	11.05±1.06	411.7±126.0	236.6±38.3	91.9±19.2	-0.16±0.13	373.7±66.8	4.28±0.64	248.9±53.0	189.2±37.1	141.8±14.2
C. pyramidale	-0.46±0.04	329.0±88.0	9.81±2.37	183.7±33.0	110.3±10.0	93.7±16.6	-0.22±0.21	356.3±95.0	10.11±2.39	175.8±21.1	92.4±4.6	71.2±11.4
A. pyrifolium	-0.48±0.11	300.0±92.1	4.99±0.84	130.5±19.0	116.4±31.5	74.4±17.1	-0.47±0.27	417.7±42.1	4.45±0.71	124.8±11.9	119.4±25.9	89.9±24.2
S. joazeiro	-0.57±0.12	279.2±57.5	33.31±16.75	151.52±30.2	92.9±14.4	86.2±46.7	-0.43±0.16	198.5±41.6	34.19±12.9	155.6±11.7	120.1±15.2	90.1±20.5
Dry season							**Dry season**					
Variables							**Variables**					
Species	Ψ_x (MPa)	gs (mmol m^2 s^{-1})	Js (cm h^{-1})	NSC (mg g^{-1} DM) Leaf	Stem	Root	Ψ_x (MPa)	gs (mmol m^2 s^{-1})	Js (cm h^{-1})	NSC (mg g^{-1} DM) Leaf	Stem	Root
C. leptophloeos	-0.26±0.04		6.72±8.00		231.0±86.8	358.4±24.1	-0.02±0.03		4.85±5.50		228.8±42.9	94.5±27.8
A. cearensis	-0.18±0.13		5.72±0.33		142.2±38.4	167.5±61.3	-0.10±0.03		6.92±4.95		156.8±35.0	117.8±38.9
S. tuberosa	-0.47±0.16		6.55±1.59		130.7±30.8	363.7±60.7	-0.19±0.17		7.65±2.11		179.3±41.9	121.5±25.0
C. pyramidale	-0.57±0.16	284.8±67.5	7.81±3.65		91.6±23.1	87.6±19.8	-4.39±2.29	181.0±59.3	21.66±11.10		108.0±22.5	103.3±30.6
A. pyrifolium	-0.57±0.23	331.9±73.2	3.28±1.04		210.8±38.4	104.4±28.7	-1.62±1.37	189.3±52.6	5.47±3.32		117.1±26.1	158.8±16.9
S. joazeiro	-0.38±0.23	381.7±103.1	27.52±14.17	223.4±27.5	159.1±32.7	129.0±41.3	-1.38±0.30	178.4±71.8	36.52±7.59	146.0±33.8	115.7±11.0	126.0±26.5

References

Allen, K., Dupuy, J.M., Gei, M.G., Hulshof, C., Medvigy, D., Pizano, C., Salgado-Negret, B., Smith, C.M., Trierweiler, A., Van Bloem, S.J., Waring, B.G., Xu, X., Powers, J.S., 2017. Will seasonally dry tropical forests be sensitive or resistant to future changes in rainfall regimes? Environ. Res. Lett. 12. https://doi.org/10.1088/1748-9326/aa5968

Arnan, X., Leal, I.R., Tabarelli, M., Andrade, J.F., Barros, M.F., Câmara, T., Jamelli, D., Knoechelmann, C.M., Menezes, T.G.C., Menezes, A.G.S., Oliveira, F.M.P., de Paula, A.S., Pereira, S.C., Rito, K.F., Sfair, J.C., Siqueira, F.F.S., Souza, D.G., Specht, M.J., Vieira, L.A., Arcoverde, G.B., Andersen, A.N., 2018. A framework for deriving measures of chronic anthropogenic disturbance: Surrogate, direct, single and multi-metric indices in Brazilian Caatinga. Ecol. Indic. 94, 274–282. https://doi.org/10.1016/j.ecolind.2018.07.001

Barros, F. de V., Bittencourt, P.R.L., Brum, M., Restrepo-Coupe, N., Pereira, L., Teodoro, G.S., Saleska, S.R., Borma, L.S., Christoffersen, B.O., Penha, D., Alves, L.F., Lima, A.J.N., Carneiro, V.M.C., Gentine, P., Lee, J.E., Aragão, L.E.O.C., Ivanov, V., Leal, L.S.M., Araujo, A.C., Oliveira, R.S., 2019. Hydraulic traits explain differential responses of Amazonian forests to the 2015 El Niño-induced drought. New Phytol. 223, 1253–1266. https://doi.org/10.1111/nph.15909

Berenguer, E., Lennox, G.D., Ferreira, J., Malhi, Y., Aragão, L.E.O.C., Barreto, J.R., Del Bon Espírito-Santo, F., Figueiredo, A.E.S., França, F., Gardner, T.A., Joly, C.A., Palmeira, A.F., Quesada, C.A., Rossi, L.C., de Seixas, M.M.M., Smith, C.C., Withey, K., Barlow, J., 2021. Tracking the impacts of El Niño drought and fire in human-modified Amazonian forests. Proc. Natl. Acad. Sci. U. S. A. 118. https://doi.org/10.1073/pnas.2019377118

Bhusal, N., Han, S.G., Yoon, T.M., 2019. Impact of drought stress on photosynthetic response, leaf water potential, and stem sap flow in two cultivars of bi-leader apple trees (Malus × domestica Borkh.). Sci. Hortic. (Amsterdam). 246, 535–543. https://doi.org/10.1016/j.scienta.2018.11.021

Blanco-Sánchez, M., Ramos-Muñoz, M., Pías, B., Ramírez-Valiente, J.A., Díaz-Guerra, L., Escudero, A., Matesanz, S., 2022. Natural selection favours drought escape and an acquisitive resource-use strategy in semi-arid Mediterranean shrubs. Funct. Ecol. 36, 2289–2302. https://doi.org/10.1111/1365-2435.14121

Borchert, R., 1994. Soil and stem water storage determine phenology and distribution of tropical dry forest trees. Ecology 75, 1437–1449. https://doi.org/10.2307/1937467

Borchert, R., Pockman, W.T., 2005. Water storage capacitance and xylem tension in isolated branches of temperate and tropical trees. Tree Physiol. 25, 457–466. https://doi.org/10.1093/treephys/25.4.457

Bosch, D.D., Marshall, L.K., Teskey, R., 2014. Forest transpiration from sap flux density measurements in a Southeastern Coastal Plain riparian buffer system. Agric. For. Meteorol. 187, 72–82. https://doi.org/10.1016/j.agrformet.2013.12.002

Bréda, N., Huc, R., Granier, A., Dreyer, E., 2006. Temperate forest trees and stands under severe drought: a review of ecophysiological responses, adaptation processes and long-term consequences. Ann. For. Sci. 63, 625–644.

Bretfeld, M., Ewers, B.E., Hall, J.S., 2018. Plant water use responses along secondary forest succession during the 2015–2016 El Niño drought in Panama. New Phytol. 219, 885–899. https://doi.org/10.1111/nph.15071

Brito, N.D. da S., Medeiros, M.J. dos S., Souza, E.S. de, Lima, A.L.A. de, 2022a. Drought response strategies for deciduous species in the semiarid Caatinga derived from the interdependence of anatomical, phenological and bio-hydraulic attributes. Flora Morphol. Distrib. Funct. Ecol. Plants 288. https://doi.org/10.1016/j.flora.2022.152009

Brito, N.D. da S., Medeiros, M.J. dos S., Souza, E.S. de, Lima, A.L.A. de, 2022b. Drought response strategies for deciduous species in the semiarid Caatinga derived from the interdependence of anatomical, phenological and bio-hydraulic attributes. Flora Morphol. Distrib. Funct. Ecol. Plants 288. https://doi.org/10.1016/j.flora.2022.152009

Brodribb, T.J., Cochard, H., 2009. Hydraulic failure defines the recovery and point of death in water-stressed conifers. Plant Physiol. 149, 575–584. https://doi.org/10.1104/pp.108.129783

Brodribb, T.J., Holbrook, N.M., Gutiérrez, M. V., 2002. Hydraulic and photosynthetic co-ordination in seasonally dry tropical forest trees. Plant, Cell Environ. 25, 1435–1444. https://doi.org/10.1046/j.1365-3040.2002.00919.x

Burkhardt, J., Pariyar, S., 2016. How does the VPD response of isohydric and anisohydric plants depend on leaf surface particles? Plant Biol. 18, 91–100. https://doi.org/10.1111/plb.12402

Cai, W., Wang, G., Santoso, A., Mcphaden, M.J., Wu, L., Jin, F.F., Timmermann, A., Collins, M., Vecchi, G., Lengaigne, M., England, M.H., Dommenget, D., Takahashi, K., Guilyardi, E., 2015. Increased frequency of extreme La Niña events under greenhouse warming. Nat. Clim. Chang. 5, 132–137. https://doi.org/10.1038/nclimate2492

Calbi, M., Boenisch, G., Boulangeat, I., Bunker, D., Catford, J.A., Changenet, A., Culshaw, V., Dias, A.S., Hauck, T., Joschinski, J., Kattge, J., Mimet, A., Pianta, M., Poschlod, P., Weisser, W.W., Roccotiello, E., 2024. A novel framework to generate plant functional groups for ecological modelling. Ecol. Indic. 166, 112370. https://doi.org/10.1016/j.ecolind.2024.112370

Cardoso, A.A., Batz, T.A., McAdam, S.A.M., 2020. Xylem embolism resistance determines leaf mortality during drought in persea americana. Plant Physiol. 182, 547–554. https://doi.org/10.1104/pp.19.00585

Carrasco, O.L., Bucci, S.J., Di Francescantonio, D., Lezcano, O.A., Campanello, P.I., Scholz, F.G., Rodríguez, S., Madanes, N., Cristiano, P.M., Hao, G.Y., Holbrook, N.M., Goldstein, G., 2014. Water storage dynamics in the main stem of subtropical tree species differing in wood density, growth rate and life history traits. Tree Physiol. 35, 354–365. https://doi.org/10.1093/treephys/tpu087

Cavaleri, M.A., Coble, A.P., Ryan, M.G., Bauerle, W.L., Loescher, H.W., Oberbauer, S.F., 2017. Tropical rainforest carbon sink declines during El Niño as a result of reduced photosynthesis and increased respiration rates. New Phytol. 216, 136–149. https://doi.org/10.1111/NPH.14724

Chave, J., Coomes, D., Jansen, S., Lewis, S.L., Swenson, N.G., Zanne, A.E., 2009. Towards a worldwide wood economics spectrum. Ecol. Lett. 12, 351–366.

https://doi.org/10.1111/j.1461-0248.2009.01285.x

Chuste, P.A., Maillard, P., Bréda, N., Levillain, J., Thirion, E., Wortemann, R., Massonnet, C., 2020. Sacrificing growth and maintaining a dynamic carbohydrate storage are key processes for promoting beech survival under prolonged drought conditions. Trees - Struct. Funct. 34, 381–394. https://doi.org/10.1007/s00468-019-01923-5

da Silva E Teodoro, É.D.M., da Silva, A.P.A., Brito, N.D. da S., Rodal, M.J.N., Shinozaki-Mendes, R.A., de Lima, A.L.A., 2022. Functional traits determine the vegetative phenology of woody species in riparian forest in semi-arid Brazil. Plant Ecol. 223, 1137–1153. https://doi.org/10.1007/s11258-022-01264-3

Dalmolin, Â.C., de Almeida Lobo, F., Vourlitis, G., Silva, P.R., Dalmagro, H.J., Antunes, M.Z., Ortíz, C.E.R., 2015. Is the dry season an important driver of phenology and growth for two Brazilian savanna tree species with contrasting leaf habits? Plant Ecol. 216, 407–417. https://doi.org/10.1007/s11258-014-0445-5

de Alcântara, L.R.P., Coutinho, A.P., Neto, S.M.D.S., de Gusmão da Cunha Rabelo, A.E.C., Antonino, A.C.D., 2021. Computational modeling of the hydrological processes in caatinga and pasture areas in the brazilian semi-arid. Water (Switzerland) 13. https://doi.org/10.3390/w13131877

De Guzman, M.E., Santiago, L.S., Schnitzer, S.A., Álvarez-Cansino, L., 2017. Trade-offs between water transport capacity and drought resistance in neotropical canopy liana and tree species. Tree Physiol. 37, 1404–1414. https://doi.org/10.1093/treephys/tpw086

de Medeiros, F.J., de Oliveira, C.P., 2021. Dynamical Aspects of the Recent Strong El Niño Events and Its Climate Impacts in Northeast Brazil. Pure Appl. Geophys. 178, 2315–2332. https://doi.org/10.1007/s00024-021-02758-3

de Oliveira, C.C., Zandavalli, R.B., de Lima, A.L.A., Rodal, M.J.N., 2015. Functional groups of woody species in semi-arid regions at low latitudes. Austral Ecol. 40, 40–49. https://doi.org/10.1111/aec.12165

Decarsin, R., Guillemot, J., le Maire, G., Blondeel, H., Meredieu, C., Achard, E., Bonal, D., Cochard, H., Corso, D., Delzon, S., Doucet, Z., Druel, A., Grossiord, C., Torres-Ruiz, J.M., Bauhus, J., Godbold, D.L., Hajek, P., Jactel, H., Jensen, J., Mereu, S., Ponette, Q., Rewald, B., Ruffault, J., Sandén, H., Scherer-Lorenzen, M., Serrano-León, H., Simioni, G., Verheyen, K., Werner, R., Martin-StPaul, N., 2024. Tree drought–mortality risk depends more on intrinsic species resistance than on stand species diversity. Glob. Chang. Biol. 30. https://doi.org/10.1111/gcb.17503

Dubois, M., Gilles, K.A., Hamilton, J.K., Rebers, P.A., Smith, F., 1956. Colorimetric Method for Determination of Sugars and Related Substances. Anal. Chem. 28, 350–356. https://doi.org/10.1021/ac60111a017

Farrar, J.F., 1993. Carbon partitioning, in: Photosynthesis and Production in a Changing Environment. Springer Netherlands, Dordrecht, pp. 232–246. https://doi.org/10.1007/978-94-011-1566-7_15

Fletcher, L.R., Scoffoni, C., Farrell, C., Buckley, T.N., Pellegrini, M., Sack, L., 2022. Testing the association of relative growth rate and adaptation to climate across natural ecotypes of Arabidopsis. New Phytol. 236, 413–432. https://doi.org/10.1111/nph.18369

Fontes, C.G., Dawson, T.E., Jardine, K., McDowell, N., Gimenez, B.O., Anderegg, L.,

Negrón-Juárez, R., Higuchi, N., Fine, P.V.A., Araújo, A.C., Chambers, J.Q., 2018. Dry and hot: The hydraulic consequences of a climate change–type drought for Amazonian trees. Philos. Trans. R. Soc. B Biol. Sci. 373. https://doi.org/10.1098/rstb.2018.0209

Fournier, L.A., 1974. Un método cuantitativo para la medición de características fenológicas en árboles. Turrialba 24, 422–423.

Frappart, F., Biancamaria, S., Normandin, C., Blarel, F., Bourrel, L., Aumont, M., Azemar, P., Vu, P.L., Le Toan, T., Lubac, B., Darrozes, J., 2018. Influence of recent climatic events on the surface water storage of the Tonle Sap Lake. Sci. Total Environ. 636, 1520–1533. https://doi.org/10.1016/j.scitotenv.2018.04.326

Furze, M.E., Huggett, B.A., Aubrecht, D.M., Stolz, C.D., Carbone, M.S., Richardson, A.D., 2019. Whole-tree nonstructural carbohydrate storage and seasonal dynamics in five temperate species. New Phytol. 221, 1466–1477. https://doi.org/10.1111/nph.15462

Gimenez, B.O., Jardine, K.J., Higuchi, N., Negrón-Juárez, R.I., Sampaio-Filho, I. de J., Cobello, L.O., Fontes, C.G., Dawson, T.E., Varadharajan, C., Christianson, D.S., Spanner, G.C., Araújo, A.C., Warren, J.M., Newman, B.D., Holm, J.A., Koven, C.D., McDowell, N.G., Chambers, J.Q., 2019. Species-specific shifts in diurnal sap velocity dynamics and hysteretic behavior of ecophysiological variables during the 2015–2016 el niño event in the amazon forest. Front. Plant Sci. 10, 1–16. https://doi.org/10.3389/fpls.2019.00830

Granier, A., 1985. Une nouvelle méthode pour la mesure du flux de sève brute dans le tronc des arbres. Ann. des Sci. For. 42, 193–200. https://doi.org/10.1051/forest:19850204

Grossiord, C., Buckley, T.N., Cernusak, L.A., Novick, K.A., Poulter, B., Siegwolf, R.T.W., Sperry, J.S., McDowell, N.G., 2020. Plant responses to rising vapor pressure deficit. New Phytol. 226, 1550–1566. https://doi.org/10.1111/nph.16485

Grossiord, C., Sevanto, S., Borrego, I., Chan, A.M., Collins, A.D., Dickman, L.T., Hudson, P.J., McBranch, N., Michaletz, S.T., Pockman, W.T., Ryan, M., Vilagrosa, A., McDowell, N.G., 2017. Tree water dynamics in a drying and warming world. Plant Cell Environ. 40, 1861–1873. https://doi.org/10.1111/pce.12991

Hartmann, H., Trumbore, S., 2016. Understanding the roles of nonstructural carbohydrates in forest trees - from what we can measure to what we want to know. New Phytol. 211, 386–403. https://doi.org/10.1111/nph.13955

Intergovernmental Panel on Climate Change (IPCC), 2023. Climate Change 2022 – Impacts, Adaptation and Vulnerability, Climate Change 2022 – Impacts, Adaptation and Vulnerability. Cambridge University Press. https://doi.org/10.1017/9781009325844

IPCC (Intergovernmental Panel on Climate Change), n.d.

Janssen, T.A.J., Hölttä, T., Fleischer, K., Naudts, K., Dolman, H., 2020. Wood allocation trade-offs between fiber wall, fiber lumen, and axial parenchyma drive drought resistance in neotropical trees. Plant Cell Environ. 43, 965–980. https://doi.org/10.1111/pce.13687

Jiao, L., Lu, N., Fu, B., Wang, J., Li, Z., Fang, W., Liu, J., Wang, C., Zhang, L., 2018. Evapotranspiration partitioning and its implications for plant water use strategy: Evidence from a black locust plantation in the semi-arid Loess Plateau, China. For. Ecol. Manage. 424, 428–438. https://doi.org/10.1016/j.foreco.2018.05.011

Kannenberg, S.A., Phillips, R.P., 2020. Non-structural carbohydrate pools not linked to hydraulic strategies or carbon supply in tree saplings during severe drought and subsequent recovery. Tree Physiol. 40, 259–271. https://doi.org/10.1093/treephys/tpz132

Kawai, K., Waengsothorn, S., Ishida, A., 2022. Sapwood density underlies xylem hydraulics and stored carbohydrates across 13 deciduous tree species in a seasonally dry tropical forest in Thailand. Trees - Struct. Funct. 37, 485–495. https://doi.org/10.1007/s00468-022-02364-3

Liang, X., Ye, Q., Liu, H., Brodribb, T.J., 2021. Wood density predicts mortality threshold for diverse trees. New Phytol. 229, 3053–3057. https://doi.org/10.1111/nph.17117

Lima, A.L.A., Rodal, M.J.N., 2010. Phenology and wood density of plants growing in the semi-arid region of northeastern Brazil. J. Arid Environ. 74, 1363–1373. https://doi.org/10.1016/j.jaridenv.2010.05.009

Lima, A.L.A. de, Rodal, M.J.N., Castro, C.C., Antonino, A.C.D., Melo, A.L. de, Gonçalves-Souza, T., Sampaio, E.V. de S.B., 2021. Phenology of high- and low-density wood deciduous species responds differently to water supply in tropical semiarid regions. J. Arid Environ. 193. https://doi.org/10.1016/j.jaridenv.2021.104594

Lima, A.L.A. de, Sá Barretto Sampaio, E.V. de, Castro, C.C. de, Rodal, M.J.N., Antonino, A.C.D., Melo, A.L. de, 2012. Do the phenology and functional stem attributes of woody species allow for the identification of functional groups in the semiarid region of Brazil? Trees - Struct. Funct. 26, 1605–1616. https://doi.org/10.1007/s00468-012-0735-2

Lima Filho, P.J.M., Santos, F., Antônio, C., 2009. Avaliações fenotípicas e fisiológicas de espécies de Spondias tendo como porta enxerto o umbuzeiro (Spondias tuberosa Cam.). Rev. Caatinga 22, 59–63.

Lima, T.R.A., Carvalho, E.C.D., Martins, F.R., Oliveira, R.S., Miranda, R.S., Müller, C.S., Pereira, L., Bittencourt, P.R.L., Sobczak, J.C.M.S.M., Gomes-Filho, E., Costa, R.C., Araújo, F.S., 2018. Lignin composition is related to xylem embolism resistance and leaf life span in trees in a tropical semiarid climate. New Phytol. 219, 1252–1262. https://doi.org/10.1111/nph.15211

Mantova, M., Herbette, S., Cochard, H., Torres-Ruiz, J.M., 2022. Hydraulic failure and tree mortality: from correlation to causation. Trends Plant Sci. 27, 335–345. https://doi.org/10.1016/j.tplants.2021.10.003

Markesteijn, L., Poorter, L., Bongers, F., Paz, H., Sack, L., 2011a. Hydraulics and life history of tropical dry forest tree species: Coordination of species' drought and shade tolerance. New Phytol. 191, 480–495. https://doi.org/10.1111/j.1469-8137.2011.03708.x

Markesteijn, L., Poorter, L., Paz, H., Sack, L., Bongers, F., 2011b. Ecological differentiation in xylem cavitation resistance is associated with stem and leaf structural traits. Plant, Cell Environ. 34, 137–148. https://doi.org/10.1111/j.1365-3040.2010.02231.x

McDowell, N., Pockman, W.T., Allen, C.D., Breshears, D.D., Cobb, N., Kolb, T., Plaut, J., Sperry, J., West, A., Williams, D.G., Yepez, E.A., 2008a. Mechanisms of plant survival and mortality during drought: why do some plants survive while others succumb to drought? New Phytol. 178, 719–739. https://doi.org/10.1111/j.1469-8137.2008.02436.x

McDowell, N., Pockman, W.T., Allen, C.D., Breshears, D.D., Cobb, N., Kolb, T., Plaut, J., Sperry, J., West, A., Williams, D.G., Yepez, E.A., 2008b. Mechanisms of plant survival

and mortality during drought: Why do some plants survive while others succumb to drought? New Phytol. 178, 719–739. https://doi.org/10.1111/j.1469-8137.2008.02436.x

McDowell, N.G., Sapes, G., Pivovaroff, A., Adams, H.D., Allen, C.D., Anderegg, W.R.L., Arend, M., Breshears, D.D., Brodribb, T., Choat, B., Cochard, H., De Cáceres, M., De Kauwe, M.G., Grossiord, C., Hammond, W.M., Hartmann, H., Hoch, G., Kahmen, A., Klein, T., Mackay, D.S., Mantova, M., Martínez-Vilalta, J., Medlyn, B.E., Mencuccini, M., Nardini, A., Oliveira, R.S., Sala, A., Tissue, D.T., Torres-Ruiz, J.M., Trowbridge, A.M., Trugman, A.T., Wiley, E., Xu, C., 2022. Mechanisms of woody-plant mortality under rising drought, CO2 and vapour pressure deficit. Nat. Rev. Earth Environ. 3, 294–308. https://doi.org/10.1038/s43017-022-00272-1

Medeiros, M., Lima, A.L.A. de, Silva, J.R.I., Jesus, A.L.N. de, Wright, C.L., Souza, E.S. De, Santos, M.G., 2025. Seasonal Shifts in Tree Water Use and Non - Structural Carbohydrate Storage in a Tropical Dry Forest. Plant Cell Environ. 48, 1–15. https://doi.org/10.1111/pce.15449

Medeiros, M., Wright, C.L., de Lima, A.L.A., da Silva Brito, N.D., Souza, R., Silva, J.R.I., Souza, E., 2024. Divergent hydraulic strategies of two deciduous tree species to deal with drought in the Brazilian semi-arid region. Trees 38, 681–694. https://doi.org/10.1007/s00468-024-02506-9

Meinzer, F.C., Johnson, D.M., Lachenbruch, B., McCulloh, K.A., Woodruff, D.R., 2009. Xylem hydraulic safety margins in woody plants: Coordination of stomatal control of xylem tension with hydraulic capacitance. Funct. Ecol. 23, 922–930. https://doi.org/10.1111/j.1365-2435.2009.01577.x

Mencuccini, M., Manzoni, S., Christoffersen, B., 2019. Modelling water fluxes in plants: from tissues to biosphere. New Phytol. 222, 1207–1222. https://doi.org/10.1111/nph.15681

Mendes, K.R., Campos, S., da Silva, L.L., Mutti, P.R., Ferreira, R.R., Medeiros, S.S., Perez-Marin, A.M., Marques, T. V., Ramos, T.M., de Lima Vieira, M.M., Oliveira, C.P., Gonçalves, W.A., Costa, G.B., Antonino, A.C.D., Menezes, R.S.C., Bezerra, B.G., Santos e Silva, C.M., 2020. Seasonal variation in net ecosystem CO2 exchange of a Brazilian seasonally dry tropical forest. Sci. Rep. 10, 1–16. https://doi.org/10.1038/s41598-020-66415-w

Meng, L., Chambers, J., Koven, C., Pastorello, G., Gimenez, B., Jardine, K., Tang, Y., McDowell, N., Negron-Juarez, R., Longo, M., Araujo, A., Tomasella, J., Fontes, C., Mohan, M., Higuchi, N., 2022. Soil moisture thresholds explain a shift from light-limited to water-limited sap velocity in the Central Amazon during the 2015-16 El Niño drought. Environ. Res. Lett. 17. https://doi.org/10.1088/1748-9326/ac6f6d

Nardini, A., Salleo, S., Jansen, S., 2011. More than just a vulnerable pipeline: xylem physiology in the light of ion-mediated regulation of plant water transport. J. Exp. Bot. 62, 4701–4718. https://doi.org/10.1093/jxb/err208

O'Brien, M.J., Leuzinger, S., Philipson, C.D., Tay, J., Hector, A., 2014. Drought survival of tropical tree seedlings enhanced by non-structural carbohydrate levels. Nat. Clim. Chang. 4, 710–714. https://doi.org/10.1038/nclimate2281

Oliveira, C.C., Zandavalli, R.B., de Lima, A.L.A., Rodal, M.J.N., 2015. Functional groups of woody species in semi-arid regions at low latitudes. Austral Ecol. 40, 40–49.

https://doi.org/10.1111/aec.12165

Oliveira, C.C. de, Zandavalli, R.B., de Lima, A.L.A., Rodal, M.J.N., 2015. Functional groups of woody species in semi-arid regions at low latitudes. Austral Ecol. 40, 40–49. https://doi.org/10.1111/aec.12165

Oliveira, R.S., Costa, F.R.C., van Baalen, E., de Jonge, A., Bittencourt, P.R., Almanza, Y., Barros, F. de V., Cordoba, E.C., Fagundes, M. V., Garcia, S., Guimaraes, Z.T.M., Hertel, M., Schietti, J., Rodrigues-Souza, J., Poorter, L., 2019. Embolism resistance drives the distribution of Amazonian rainforest tree species along hydro-topographic gradients. New Phytol. 221, 1457–1465. https://doi.org/10.1111/nph.15463

Oliveira, R.S., Dawson, T.E., Burgess, S.S.O., Nepstad, D.C., 2005. Hydraulic redistribution in three Amazonian trees. Oecologia 145, 354–363. https://doi.org/10.1007/s00442-005-0108-2

Oliveira, R.S., Eller, C.B., Barros, F. de V., Hirota, M., Brum, M., Bittencourt, P., 2021a. Linking plant hydraulics and the fast–slow continuum to understand resilience to drought in tropical ecosystems. New Phytol. 230, 904–923. https://doi.org/10.1111/nph.17266

Oliveira, R.S., Eller, C.B., Barros, F. de V., Hirota, M., Brum, M., Bittencourt, P., 2021b. Linking plant hydraulics and the fast–slow continuum to understand resilience to drought in tropical ecosystems. New Phytol. https://doi.org/10.1111/nph.17266

Palacio, S., Camarero, J.J., Maestro, M., Alla, A.Q., Lahoz, E., Montserrat-Martí, G., 2018a. Are storage and tree growth related? Seasonal nutrient and carbohydrate dynamics in evergreen and deciduous Mediterranean oaks. Trees - Struct. Funct. 32, 777–790. https://doi.org/10.1007/s00468-018-1671-6

Palacio, S., Jesús, ·, Camarero, J., Melchor, ·, Alla, A.Q., Lahoz, E., Montserrat-Martí, G., 2018b. Are storage and tree growth related? Seasonal nutrient and carbohydrate dynamics in evergreen and deciduous Mediterranean oaks 32, 777–790. https://doi.org/10.1007/s00468-018-1671-6

Paloschi, R.A., Ramos, D.M., Ventura, D.J., Souza, R., Souza, E., Morellato, L.P.C., Nóbrega, R.L.B., Coutinho, Í.A.C., Verhoef, A., Körting, T.S., Borma, L.D.S., 2021. Environmental drivers of water use for caatinga woody plant species: Combining remote sensing phenology and sap flow measurements. Remote Sens. 13, 1–18. https://doi.org/10.3390/rs13010075

Pereira, P.D.C., Da Silva, T.G.F., Zolnier, S., De Morais, J.E.F., Dos Santos, D.C., 2015. Morfogênese da palma forrageira irrigada por gotejamento. Rev. Caatinga 28, 184–195.

Pérez-Harguindeguy, N., Díaz, S., Garnier, E., Lavorel, S., Poorter, H., Jaureguiberry, P., Bret-Harte, M.S., Cornwell, W.K., Craine, J.M., Gurvich, D.E., Urcelay, C., Veneklaas, E.J., Reich, P.B., Poorter, L., Wright, I.J., Ray, P., Enrico, L., Pausas, J.G., De Vos, A.C., Buchmann, N., Funes, G., Quétier, F., Hodgson, J.G., Thompson, K., Morgan, H.D., Ter Steege, H., Van Der Heijden, M.G.A., Sack, L., Blonder, B., Poschlod, P., Vaieretti, M. V., Conti, G., Staver, A.C., Aquino, S., Cornelissen, J.H.C., 2013. New handbook for standardised measurement of plant functional traits worldwide. Aust. J. Bot. 61, 167–234. https://doi.org/10.1071/BT12225

Pineda-García, F., Paz, H., Meinzer, F.C., 2012. Drought resistance in early and late secondary successional species from a tropical dry forest: The interplay between xylem

resistance to embolism, sapwood water storage and leaf shedding. Plant, Cell Environ. 36, 405–418. https://doi.org/10.1111/j.1365-3040.2012.02582.x

Piper, F.I., 2011. Drought induces opposite changes in the concentration of non-structural carbohydrates of two evergreen Nothofagus species of differential drought resistance. Ann. For. Sci. 68, 415–424. https://doi.org/10.1007/s13595-011-0030-1

Poorter, L., Castilho, C. V., Schietti, J., Oliveira, R.S., Costa, F.R.C., 2018. Can traits predict individual growth performance? A test in a hyperdiverse tropical forest. New Phytol. 219, 109–121. https://doi.org/10.1111/nph.15206

Poorter, L., McDonald, I., Alarcon, A., Fichtler, E., Licona, J.-C., Peña-Carlos, M., Sterck, F., Villegas, Z., Sass-klaassen, U., 2010. The importance of wood traits and hydraulic conductance for the performance and life history strategies of 42 rainforest tree species - Poorter - 2009 - New Phytologist - Wiley Online Library. New Phytol. 481–492.

Poorter, L., Rozendaal, D.M.A., Bongers, F., de Almeida-Cortez, J.S., Almeyda Zambrano, A.M., Álvarez, F.S., Andrade, J.L., Villa, L.F.A., Balvanera, P., Becknell, J.M., Bentos, T. V., Bhaskar, R., Boukili, V., Brancalion, P.H.S., Broadbent, E.N., César, R.G., Chave, J., Chazdon, R.L., Colletta, G.D., Craven, D., de Jong, B.H.J., Denslow, J.S., Dent, D.H., DeWalt, S.J., García, E.D., Dupuy, J.M., Durán, S.M., Espírito Santo, M.M., Fandiño, M.C., Fernandes, G.W., Finegan, B., Moser, V.G., Hall, J.S., Hernández-Stefanoni, J.L., Jakovac, C.C., Junqueira, A.B., Kennard, D., Lebrija-Trejos, E., Letcher, S.G., Lohbeck, M., Lopez, O.R., Marín-Spiotta, E., Martínez-Ramos, M., Martins, S. V., Massoca, P.E.S., Meave, J.A., Mesquita, R., Mora, F., de Souza Moreno, V., Müller, S.C., Muñoz, R., Muscarella, R., de Oliveira Neto, S.N., Nunes, Y.R.F., Ochoa-Gaona, S., Paz, H., Peña-Claros, M., Piotto, D., Ruíz, J., Sanaphre-Villanueva, L., Sanchez-Azofeifa, A., Schwartz, N.B., Steininger, M.K., Thomas, W.W., Toledo, M., Uriarte, M., Utrera, L.P., van Breugel, M., van der Sande, M.T., van der Wal, H., Veloso, M.D.M., Vester, H.F.M., Vieira, I.C.G., Villa, P.M., Williamson, G.B., Wright, S.J., Zanini, K.J., Zimmerman, J.K., Westoby, M., 2019. Wet and dry tropical forests show opposite successional pathways in wood density but converge over time. Nat. Ecol. Evol. 3, 928–934. https://doi.org/10.1038/s41559-019-0882-6

Poyatos, R., Granda, V., Flo, V., Adams, M.A., Adorján, B., Aguadé, D., Aidar, M.P.M., Allen, S., Alvarado-Barrientos, M.S., Anderson-Teixeira, K.J., Aparecido, L.M., Altaf Arain, M., Aranda, I., Asbjornsen, H., Baxter, R., Beamesderfer, E., Berry, Z.C., Berveiller, D., Blakely, B., Boggs, J., Bohrer, G., Bolstad, P. V., Bonal, D., Bracho, R., Brito, P., Brodeur, J., Casanoves, F., Chave, J., Chen, H., Cisneros, C., Clark, K., Cremonese, E., Dang, H., David, J.S., David, T.S., Delpierre, N., Desai, A.R., Do, F.C., Dohnal, M., Domec, J.C., Dzikiti, S., Edgar, C., Eichstaedt, R., El-Madany, T.S., Elbers, J., Eller, C.B., Euskirchen, E.S., Ewers, B., Fonti, P., Forner, A., Forrester, D.I., Freitas, H.C., Galvagno, M., Garcia-Tejera, O., Ghimire, C.P., Gimeno, T.E., Grace, J., Granier, A., Griebel, A., Guangyu, Y., Gush, M.B., Hanson, P.J., Hasselquist, N.J., Heinrich, I., Hernandez-Santana, V., Herrmann, V., Hölttä, T., Holwerda, F., Irvine, J., Na Ayutthaya, S.I., Jarvis, P.G., Jochheim, H., Joly, C.A., Kaplick, J., Kim, H.S., Klemedtsson, L., Kropp, H., Lagergren, F., Lane, P., Lang, P., Lapenas, A., Lechuga, V., Lee, M., Leuschner, C., Limousin, J.M., Linares, J.C., Linderson, M.L., Lindroth, A., Llorens, P., López-Bernal, Á., Loranty, M.M., Lüttschwager, D., MacInnis-Ng, C., Maréchaux, I., Martin, T.A., Matheny, A., McDowell, N., McMahon, S., Meir, P., Mészáros, I., Migliavacca, M., Mitchell, P., Mölder, M., Montagnani, L., Moore, G.W., Nakada, R., Niu, F., Nolan, R.H., Norby, R., Novick, K., Oberhuber, W., Obojes, N., Oishi, A.C.,

Oliveira, R.S., Oren, R., Ourcival, J.M., Paljakka, T., Perez-Priego, O., Peri, P.L., Peters, R.L., Pfautsch, S., Pockman, W.T., Preisler, Y., Rascher, K., Robinson, G., Rocha, H., Rocheteau, A., Röll, A., Rosado, B.H.P., Rowland, L., Rubtsov, A. V., Sabaté, S., Salmon, Y., Salomón, R.L., Sánchez-Costa, E., Schäfer, K.V.R., Schuldt, B., Shashkin, A., Stahl, C., Stojanović, M., Suárez, J.C., Sun, G., Szatniewska, J., Tatarinov, F., TesaÅ™, M., Thomas, F.M., Tor-Ngern, P., Urban, J., Valladares, F., Van Der Tol, C., Van Meerveld, I., Varlagin, A., Voigt, H., Warren, J., Werner, C., Werner, W., Wieser, G., Wingate, L., Wullschleger, S., Yi, K., Zweifel, R., Steppe, K., Mencuccini, M., Martínez-Vilalta, J., 2021. Global transpiration data from sap flow measurements: The SAPFLUXNET database, Earth System Science Data. https://doi.org/10.5194/essd-13-2607-2021

Quentin, Audrey G., Pinkard, E.A., Ryan, M.G., Tissue, D.T., Baggett, L.S., Adams, H.D., Maillard, P., Marchand, J., Landhäusser, S.M., Lacointe, A., Gibon, Y., Anderegg, W.R.L., Asao, S., Atkin, O.K., Bonhomme, M., Claye, C., Chow, P.S., Clément-Vidal, A., Davies, N.W., Dickman, L.T., Dumbur, R., Ellsworth, D.S., Falk, K., Galiano, L., Grünzweig, J.M., Hartmann, H., Hoch, G., Hood, S., Jones, J.E., Koike, T., Kuhlmann, I., Lloret, F., Maestro, M., Mansfield, S.D., Martínez-Vilalta, J., Maucourt, M., McDowell, N.G., Moing, A., Muller, B., Nebauer, S.G., Niinemets, Ü., Palacio, S., Piper, F., Raveh, E., Richter, A., Rolland, G., Rosas, T., Joanis, B. Saint, Sala, A., Smith, R.A., Sterck, F., Stinziano, J.R., Tobias, M., Unda, F., Watanabe, M., Way, D.A., Weerasinghe, L.K., Wild, B., Wiley, E., Woodruff, D.R., 2015. Non-structural carbohydrates in woody plants compared among laboratories. Tree Physiol. 35, 1146–1165. https://doi.org/10.1093/treephys/tpv073

Quentin, Audrey G, Pinkard, E.A., Ryan, M.G., Tissue, D.T., Scott Baggett, L., Adams, H.D., Maillard, P., Marchand, J., Landhäusser, S.M., Muller, B., Nebauer, S.G., Niinemets, Ü., Palacio, S., Piper, F., Raveh, E., Richter, A., Rolland, G., Rosas, T., Saint Joanis, B., Sala, A., Smith, R.A., Sterck, F., Stinziano, J.R., Tobias, M., Unda, F., Watanabe, M., Way, D.A., Weerasinghe, L.K., Wild, B., Wiley, E., Woodruff, D.R., 2015. Shinichi Asao 3,4 , Owen K. Atkin 15, 16 , Marc Bonhomme 10, 11 , Caroline Claye 17 , Pak S. Jordi Martínez-Vilalta 35, 13. https://doi.org/10.1093/treephys/tpv073

Reich, P.B., Wright, I.J., Cavender-Bares, J., Craine, J.M., Oleksyn, J., Westoby, M., Walters, M.B., 2003. The evolution of plant functional variation: Traits, spectra, and strategies. Int. J. Plant Sci. 164.

Resco de Dios, V., Gessler, A., 2021. Sink and source co-limitation in the response of stored non-structural carbohydrates to an intense but short drought. Trees - Struct. Funct. 1–4. https://doi.org/10.1007/s00468-021-02116-9

Rito, K.F., Arroyo-Rodríguez, V., Queiroz, R.T., Leal, I.R., Tabarelli, M., 2017. Precipitation mediates the effect of human disturbance on the Brazilian Caatinga vegetation. J. Ecol. 105, 828–838. https://doi.org/10.1111/1365-2745.12712

Rosell, J.A., Piper, F.I., Jiménez-Vera, C., Vergílio, P.C.B., Marcati, C.R., Castorena, M., Olson, M.E., 2021. Inner bark as a crucial tissue for non-structural carbohydrate storage across three tropical woody plant communities. Plant Cell Environ. 44, 156–170. https://doi.org/10.1111/pce.13903

Rosner, S., Heinze, B., Savi, T., Dalla-Salda, G., 2019. Prediction of hydraulic conductivity loss from relative water loss: new insights into water storage of tree stems and branches. Physiol. Plant. 165, 843–854. https://doi.org/10.1111/ppl.12790

Sala, A., Piper, F., Hoch, G., 2010. Physiological mechanisms of drought-induced tree mortality are far from being resolved. New Phytol. 186, 274–281. https://doi.org/10.1111/j.1469-8137.2009.03167.x

Santana-Vieira, D.D.S., Freschi, L., Da Hora Almeida, L.A., Moraes, D.H.S. De, Neves, D.M., Dos Santos, L.M., Bertolde, F.Z., Soares Filho, W.D.S., Coelho Filho, M.A., Gesteira, A.D.S., 2016. Survival strategies of citrus rootstocks subjected to drought. Sci. Rep. 6, 1–12. https://doi.org/10.1038/srep38775

Santos, V.A.H.F. dos, Ferreira, M.J., Rodrigues, J.V.F.C., Garcia, M.N., Ceron, J.V.B., Nelson, B.W., Saleska, S.R., 2018. Causes of reduced leaf-level photosynthesis during strong El Niño drought in a Central Amazon forest, Global Change Biology. https://doi.org/10.1111/gcb.14293

Santos, W.R. dos, Jardim, A.M. da R.F., Souza, L.S.B. de, Souza, C.A.A. de, Morais, J.E.F. de, Alves, C.P., Araujo Júnior, G. do N., Silva, M.J. da, Salvador, K.R. da S., Silva, M.V. da, Morellato, L.P.C., Silva, T.G.F. da, 2024. Can changes in land use in a semi-arid region of Brazil cause seasonal variation in energy partitioning and evapotranspiration? J. Environ. Manage. 367. https://doi.org/10.1016/j.jenvman.2024.121959

Santos, M., Barros, V., Lima, L., Frosi, G., Santos, M.G., 2021. Whole plant water status and non-structural carbohydrates under progressive drought in a Caatinga deciduous woody species. Trees. https://doi.org/10.1007/s00468-021-02113-y

Santos, M.G., Oliveira, M.T., Figueiredo, K. V., Falcão, H.M., Arruda, E.C.P., Almeida-Cortez, J., Sampaio, E.V.S.B., Ometto, J.P.H.B., Menezes, R.S.C., Oliveira, A.F.M., Pompelli, M.F., Antonino, A.C.D., 2014. Caatinga, the Brazilian dry tropical forest: Can it tolerate climate changes? Theor. Exp. Plant Physiol. 26, 83–99. https://doi.org/10.1007/s40626-014-0008-0

Schenk, H.J., Steppe, K., Jansen, S., 2015. Nanobubbles: A new paradigm for air-seeding in xylem. Trends Plant Sci. 20, 199–205. https://doi.org/10.1016/j.tplants.2015.01.008

Scoffoni, C., Albuquerque, C., Brodersen, C.R., Townes, S. V., John, G.P., Cochard, H., Buckley, T.N., McElrone, A.J., Sack, L., 2017. Leaf vein xylem conduit diameter influences susceptibility to embolism and hydraulic decline. New Phytol. 213, 1076–1092. https://doi.org/10.1111/nph.14256

Sevanto, S., Mcdowell, N.G., Dickman, L.T., Pangle, R., Pockman, W.T., 2014. How do trees die? A test of the hydraulic failure and carbon starvation hypotheses. Plant, Cell Environ. 37, 153–161. https://doi.org/10.1111/pce.12141

Silva, P.F. da, Lima, J.R. de S., Antonino, A.C.D., Souza, R., de Souza, E.S., Silva, J.R.I., Alves, E.M., 2017. Seasonal patterns of carbon dioxide, water and energy fluxes over the Caatinga and grassland in the semi-arid region of Brazil. J. Arid Environ. 147, 71–82. https://doi.org/10.1016/j.jaridenv.2017.09.003

Silva, K.A., de Souza Rolim, G., de Oliveira Aparecido, L.E., 2022. Forecasting El Niño and La Niña events using decision tree classifier. Theor. Appl. Climatol. 148, 1279–1288. https://doi.org/10.1007/s00704-022-03999-5

Smith, M.G., Miller, R.E., Arndt, S.K., Kasel, S., Bennett, L.T., 2018. Whole-tree distribution and temporal variation of non-structural carbohydrates in broadleaf evergreen trees. Tree

Physiol. 38, 570–581. https://doi.org/10.1093/treephys/tpx141

Souza, B.C. de, Carvalho, E.C.D., Oliveira, R.S., de Araujo, F.S., de Lima, A.L.A., Rodal, M.J.N., 2020. Drought response strategies of deciduous and evergreen woody species in a seasonally dry neotropical forest. Oecologia 1, 221–236. https://doi.org/10.1007/s00442-020-04760-3

Souza, B.C. de, Oliveira, R.S., De Araújo, F.S., De Lima, A.L.A., Rodal, M.J.N., 2015. Divergências funcionais e estratégias de resistência à seca entre espécies decíduas e sempre verdes tropicais. Rodriguesia 66, 21–32. https://doi.org/10.1590/2175-7860201566102

Sperry, J.S., 2000. Hydraulic constraints on plant gas exchange. Agric. For. Meteorol. 104, 13–23. https://doi.org/10.1016/S0168-1923(00)00144-1

Steppe, K., Vandegehuchte, M.W., Tognetti, R., Mencuccini, M., 2015. Sap flow as a key trait in the understanding of plant hydraulic functioning. Tree Physiol. 35, 341–345. https://doi.org/10.1093/treephys/tpv033

Tomasella, M., Petrussa, E., Petruzzellis, F., Nardini, A., Casolo, V., 2020. The possible role of non-structural carbohydrates in the regulation of tree hydraulics. Int. J. Mol. Sci. 21. https://doi.org/10.3390/ijms21010144

Tonet, V., Brodribb, T., Bourbia, I., 2024. Variation in xylem vulnerability to cavitation shapes the photosynthetic legacy of drought. Plant Cell Environ. 47, 1160–1170. https://doi.org/10.1111/pce.14788

Venturas, M.D., Sperry, J.S., Hacke, U.G., 2017. Plant xylem hydraulics: What we understand, current research, and future challenges. J. Integr. Plant Biol. 59, 356–389. https://doi.org/10.1111/jipb.12534

Vico, G., Thompson, S.E., Manzoni, S., Molini, A., Albertson, J.D., Almeida-Cortez, J.S., Fay, P.A., Feng, X., Guswa, A.J., Liu, H., Wilson, T.G., Porporato, A., 2014. Climatic, ecophysiological, and phenological controls on plant ecohydrological strategies in seasonally dry ecosystems. Ecohydrology 8, 660–681. https://doi.org/10.1002/eco.1533

Wang, L., Dai, Y., Guo, J., Gao, R., Wan, X., 2016. Interaction of hydraulic failure and carbon starvation on Robinia pseudoacacia seedlings during drought. Linye Kexue/Scientia Silvae Sin. 52, 1–9. https://doi.org/10.11707/j.1001-7488.20160601

Westoby, M., Falster, D.S., Moles, A.T., Vesk, P.A., Wright, I.J., 2002. Plant ecological strategies: Some leading dimensions of variation between species. Annu. Rev. Ecol. Syst. 33, 125–159. https://doi.org/10.1146/annurev.ecolsys.33.010802.150452

Will, R.E., Wilson, S.M., Zou, C.B., Hennessey, T.C., 2013. Increased vapor pressure deficit due to higher temperature leads to greater transpiration and faster mortality during drought for tree seedlings common to the forest-grassland ecotone. New Phytol. 200, 366–374. https://doi.org/10.1111/nph.12321

Wright, C.L., de Lima, A.L.A., de Souza, E.S., West, J.B., Wilcox, B.P., 2021. Plant functional types broadly describe water use strategies in the Caatinga, a seasonally dry tropical forest in northeast Brazil. Ecol. Evol. 11, 11808–11825. https://doi.org/10.1002/ece3.7949

Wright, C.L., West, J.B., de Lima, A.L.A., Souza, E.S., Medeiros, M., Wilcox, B.P., 2023.

Contrasting water-use strategies revealed by species-specific transpiration dynamics in the Caatinga dry forest. Tree Physiol. 1–15. https://doi.org/10.1093/treephys/tpad137

Würth, M.K.R., Peláez-Riedl, S., Wright, S.J., Körner, C., 2005. Non-structural carbohydrate pools in a tropical forest. Oecologia 143, 11–24. https://doi.org/10.1007/s00442-004-1773-2

Yang, B., Peng, C., Harrison, S.P., Wei, H., Wang, H., Zhu, Q., Wang, M., 2018. Allocation mechanisms of non-structural carbohydrates of Robinia pseudoacacia L. Seedlings in response to drought and waterlogging. Forests 9, 1–16. https://doi.org/10.3390/f9120754

Yu, T., Feng, Q., Si, J., Pinkard, E.A., 2019. Coordination of stomatal control and stem water storage on plant water use in desert riparian trees. Trees - Struct. Funct. 33, 787–801. https://doi.org/10.1007/s00468-019-01816-7

Zhang, T., Cao, Y., Chen, Y., Liu, G., 2015a. Non-structural carbohydrate dynamics in Robinia pseudoacacia saplings under three levels of continuous drought stress. Trees - Struct. Funct. 29, 1837–1849. https://doi.org/10.1007/s00468-015-1265-5

Zhang, T., Cao, Y., Chen, Y., Liu, G., 2015b. Non-structural carbohydrate dynamics in Robinia pseudoacacia saplings under three levels of continuous drought stress. Trees - Struct. Funct. 29, 1837–1849. https://doi.org/10.1007/s00468-015-1265-5

Zuidema, P.A., Babst, F., Groenendijk, P., Trouet, V., Abiyu, A., Acuña-Soto, R., Adenesky-Filho, E., Alfaro-Sánchez, R., Aragão, J.R.V., Assis-Pereira, G., Bai, X., Barbosa, A.C., Battipaglia, G., Beeckman, H., Botosso, P.C., Bradley, T., Bräuning, A., Brienen, R., Buckley, B.M., Camarero, J.J., Carvalho, A., Ceccantini, G., Centeno-Erguera, L.R., Cerano-Paredes, J., Chávez-Durán, Á.A., Cintra, B.B.L., Cleaveland, M.K., Couralet, C., D'Arrigo, R., del Valle, J.I., Dünisch, O., Enquist, B.J., Esemann-Quadros, K., Eshetu, Z., Fan, Z.X., Ferrero, M.E., Fichtler, E., Fontana, C., Francisco, K.S., Gebrekirstos, A., Gloor, E., Granato-Souza, D., Haneca, K., Harley, G.L., Heinrich, I., Helle, G., Inga, J.G., Islam, M., Jiang, Y. mei, Kaib, M., Khamisi, Z.H., Koprowski, M., Kruijt, B., Layme, E., Leemans, R., Leffler, A.J., Lisi, C.S., Loader, N.J., Locosselli, G.M., Lopez, L., López-Hernández, M.I., Lousada, J.L.P.C., Mendivelso, H.A., Mokria, M., Montóia, V.R., Moors, E., Nabais, C., Ngoma, J., Nogueira Júnior, F. de C., Oliveira, J.M., Olmedo, G.M., Pagotto, M.A., Panthi, S., Pérez-De-Lis, G., Pucha-Cofrep, D., Pumijumnong, N., Rahman, M., Ramirez, J.A., Requena-Rojas, E.J., Ribeiro, A. de S., Robertson, I., Roig, F.A., Rubio-Camacho, E.A., Sass-Klaassen, U., Schöngart, J., Sheppard, P.R., Slotta, F., Speer, J.H., Therrell, M.D., Toirambe, B., Tomazello-Filho, M., Torbenson, M.C.A., Touchan, R., Venegas-González, A., Villalba, R., Villanueva-Diaz, J., Vinya, R., Vlam, M., Wils, T., Zhou, Z.K., 2022. Tropical tree growth driven by dry-season climate variability. Nat. Geosci. 15, 269–276. https://doi.org/10.1038/s41561-022-00911-8

Supplementary information

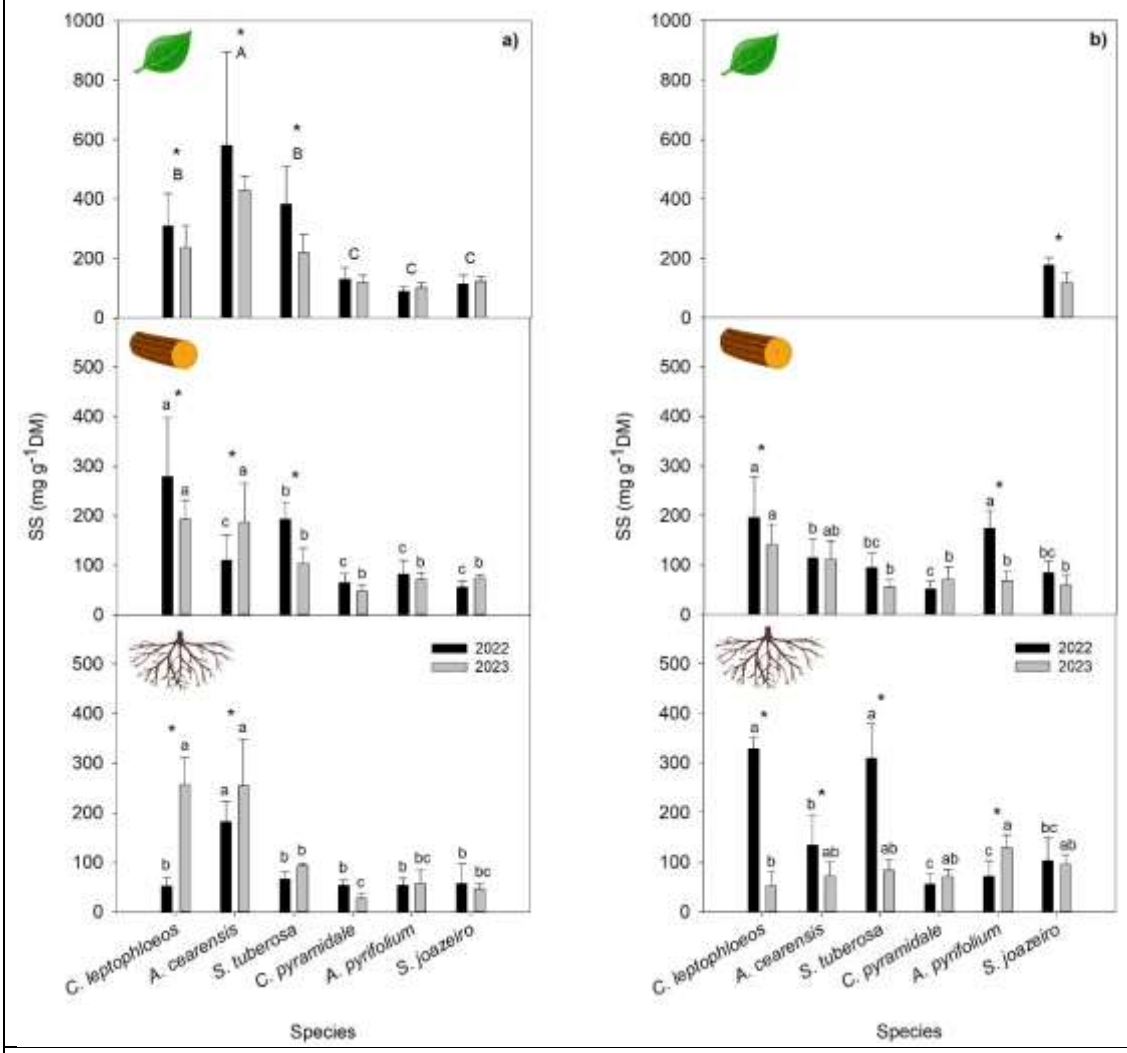

Figure S1. Soluble sugar (SS) in the rainy and dry seasons of 2022 and 2023 in six woody species from a Brazilian dry forest, Caatinga. a) SS in the rainy season of 2022 and 2023 in different organs: leaf, stem and root. b) SS in the dry season of 2022 and 2023 in different organs: leaf, stem and root. Uppercase letters compare species regardless of year; Lowercase letters compare species within each year (significant interaction); * indicates difference between years for each species.

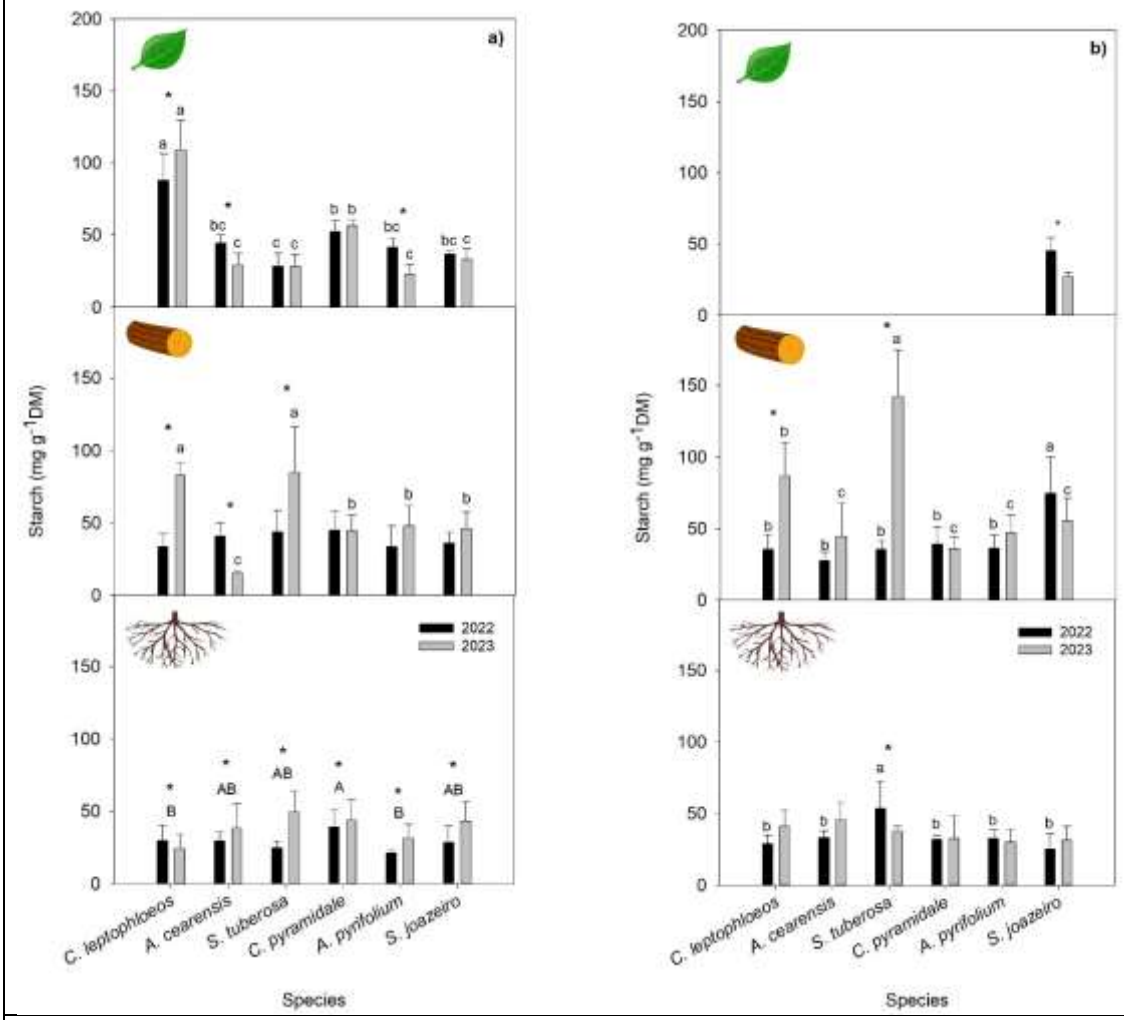

Figure S2. Starch in the rainy and dry seasons of 2022 and 2023 in six woody species from a Brazilian dry forest, Caatinga. a) Starch in the rainy season of 2022 and 2023 in different organs: leaf, stem and root. b) Starch in the dry season of 2022 and 2023 in different organs: leaf, stem and root. Uppercase letters compare species regardless of year; Lowercase letters compare species within each year (significant interaction); * indicates difference between years for each species.

Apêndice A - Seasonal shifts in tree water use and non-structural carbohydrate storage in a tropical dry forest

Plant, Cell & Environment

DOI: http://doi.org/10.1111/pce.15449

Maria Medeiros[1]; André Luiz Alves de Lima[2]; José Raliuson Inácio Silva [2]; Angela Lucena Nascimento de Jesus[2]; Cynthia L. Wright[3]; Eduardo Soares de Souza[2]; Mauro Guida Santos[1]

[1]Department of Botany, Bioscience Center, Federal University of Pernambuco, Recife-PE, Brazil.

[2]Federal Rural University of Pernambuco, Serra Talhada Academic Unit, Serra Talhada, PE, Brazil.

[3]Southern Research Station, USDA Forest Service, Knoxville, TN, USA

* Corresponding author: *Maria Jucicléa dos S. Medeiros*, maria.juciclea@ufpe.br

Abstract

Predictions of increased drought frequency and intensity have the potential to threaten to forest globally. The key to trees response to drought is an understanding of tree water use and carbohydrate storage. Our objective was to evaluate sap velocity and dynamics of non-structural carbohydrates (NSC) in native trees of a dry tropical forest, during rainy and drought periods. We evaluated six key species of the Caatinga: three deciduous species with low wood density (WD), two deciduous species with high WD and one evergreen species during the rainy and dry periods. We measured sap velocity, xylem water potential, stomatal conductance, phenology and NSC. We found that the evergreen specie had higher sap velocity and frequent NSC production. While the low deciduous WD species showed low sap velocity, store water and NSC mainly in the stem and roots, and have leaf sprouting and flowering at the end of the dry period. The deciduous high WD also showed low sap velocity, however, with low stored NSC. These results suggest that under longer dry seasons and an irregular rainy seasons, species with low WD that use part of the stored NSC to resprout still during dry season may be the most affected.

Keywords: Caatinga, deciduous, evergreen, NSC, semiarid, stomatal conductance, wood density, water potential

Introduction

Increased drought frequency and intensity have emerged as a novel threat to forests globally (Allen *et al.* 2017; IPCC 2023). In Seasonally Dry Tropical Forests (SDTF), drought conditions arise due to irregular rainfall and high evaporative demand. However, prolonged drought conditions are expected under climate change scenarios which alter rainfall regimes or reduced total annual rainfall. These changes, could fundamentally affect vegetation responses and lead to SDTF which are sensitive and vulnerable (Allen et al., 2017). In this context, a broad understanding of plant response and function under drought conditions is needed.

Drought can cause tree hydraulic failure through embolism and cavitation (i.e. interruption of sap velocity in the xylem), and if strong enough, can lead to the death of organs or the entire plant (Scoffoni et al., 2017). In addition to hydraulic failure, drought can also lead to tree mortality due to carbon starvation, in which the tree suffers carbon depletion due to stomatal closure (McDowell et al., 2022). This can occur because, under water limitations, plants tend to close their stomata to avoid excessive water loss. In some case, species which are more sensitive to water deficit may close their stomata earlier, thus reducing the assimilation of CO_2, and consequently affecting carbohydrate reserves (McDowell et al., 2008b). Therefore, the effects of long-term drought can shift the dynamics of non-structural carbohydrates (NSC) storage and allocation, functions which are fundamental to maintaining metabolic, defense or osmoregulation functions (McDowell et al., 2022; Sevanto et al., 2014). Thus, an effective way to assess the impacts of drought stress is by tracking the dynamics of sap velocity together with non-structural carbohydrate storage (Granier, 1985; Zhang et al., 2015a).

The dynamics of sap velocity are related to tree water use, and hence essential to understanding the variation in responses between coexisting tree species in seasonally dry tropical forest (Bosch et al., 2014; Wright et al., 2023). Other measures such as water potential,

and stomatal conductance form a set of coordinated functional traits that, analyzed with the plant's morphological characteristics, help answer questions about water transport control (Vico et al., 2014).

Similarly, NSC, reflects on plants' ecophysiological responses, since drought progression can influence storage (Zhang et al., 2015a). NSC consists of soluble sugar (sucrose, fructose and glucose), which is responsible for growth, osmoprotection, transport and signaling, and starch that is stored long-term (Hartmann and Trumbore, 2016). Drought can influence variation of NSC indifferent organs of the trees; by changing it's allocation and partitioning in thick roots, stems and leaves (Hartmann & Trumbor 2016; Santos, Barros, Lima, Frosi & Santos 2021). Some studies have shown that seasonal carbohydrate dynamics may differ between coexisting evergreen and deciduous species. For example, according to the findings of Palacio *et al.* (2018), carbohydrate storage in branches was crucial in evergreen Mediterranean oaks, while it played a minor role in deciduous oaks. However, this relationship in SDTF species is still unclear, and analyzing sap velocity and NSC together can help explain species' different strategies to tolerate drought. In SDTF, tree functional groups can be classified based on morphological, physiological, and phenological traits (Lima & Rodal 2010). In the Caatinga SDTF of northeast Brazil specifically, functional groups have been defined based on phenology and wood density (WD) (Lima and Rodal, 2010; C. C. Oliveira et al., 2015). These function groups tend to align with hydraulic strategies and drought tolerances (Brito et al., 2022b; Wright et al., 2021). Generally, high WD species have greater mechanical stability, which promotes a high resistance to cavitation (Markesteijn et al., 2011b). Further, high WD species which are evergreen are characterized by thick-walled xylem which further promotes cavitation resistance (Janssen et al., 2020; Markesteijn et al., 2011b) and spend the entire year with leaves, allowing for continued rates of CO_2 assimilation and resource acquisition (Souza et al., 2015; Tonet et al., 2024). Moreover, metabolic and xylem hydraulics responses may be associated with WD

and leaf phenology, particularly considering that species with high WD have higher leaf life span (Lima et al., 2018; Poorter et al., 2019). In contrast, deciduous low WD species are characterized by wide vessels with thin walls and have a comparatively greater maximum xylem capacitance (Pineda-García et al., 2012; Poorter et al., 2010). Therefore, traits related to WD and stomatal control may indicate the presence of a trade-off, in which some species may invest more in hydraulic safety (more resistant xylem vessels, with greater vessel wall thickness and greater lignification), but have lower carbon assimilation, due to greater stomatal control, consequently, have lower NSC synthesis while other species maximize carbon assimilation and NSC synthesis, however, have lower hydraulic safety due to lower investment in their xylem vessels (Janssen et al., 2020; Oliveira et al., 2021a; Tomasella et al., 2020).

Previous work in SDTF found that the relationship between WD and seasonal changes in tree water status can be largely predicted by functional group (Borchert, 1994; Lima and Rodal, 2010; C. C. Oliveira et al., 2015; Souza et al., 2015). More recently, other studies found that drought tolerance, hydraulic architecture, water use and conductance also generally align with functional type (Wright et al. 2021; Brito *et al.* 2022; Wright *et al.* 2024; Medeiros *et al.* 2024). However, few studies have explored hydraulic and carbon trade-offs in SDTF, and the linkages between other physiological measures, such as sap flow velocity and NSC are needed (Santos et al., 2021; Wright et al., 2023).

Given this context, we ask: (1) How does sap velocity and NSC change between different periods of the year among coexisting species in a seasonally dry tropical forest? (2) Is there a water-carbon trade-off revealed by a relationship between hydraulic and carbohydrate storage functional traits? We studied six species that play essential ecological roles in the Caatinga to answer the questions: *Commiphora leptophloeos* (Mart.) J.B.Gillett, *Spondias tuberosa* Arruda, *Amburana cearensis* (Allemao) A.C.Sm. (deciduous with low WD); *Cenostigma pyramidale* (Tul.) Gagnon & G. P. Lewis and *Aspidosperma pyrifolium* Mart. & Zucc (deciduous with high

WD); and *Sarcomphalus joazeiro* (Mart.) Hauenshild (evergreen). Although we focus on species-level difference, we used the functional groups framework to hypothesize the following: deciduous species low-wood-density show seasonal differences in sap flow velocity rather than deciduous species high-wood-density, and species evergreen high-wood-density have the highest sap velocity. In addition, deciduous species accumulate more NSC in stems and roots during the dry period, while evergreen species have highest NSC concentration across leaf, stem and root organs, regardless of period of the year.

The Caatinga is a Brazilian biome that is often overshadowed by the global recognition of the Amazon Rainforest. While the general public associates Brazil or South America with the Amazon, there are other biomes, such as the Caatinga, that offer a completely different but equally important ecological environment. This biome plays a crucial role in maintaining biodiversity and ecosystem services, highlighting the need to understand the strategies of the species that live in it (Santos et al., 2014). This includes trees that can function as important "carbon sinks", mitigating the effects of climate change (Mendes et al., 2020).

Materials and methods

Study Site

The study site was located at the Fazenda Buenos Aires (07° 56'50" S, 38° 23' 29" W), outside of the Serra Talhada, PE, Brazil (Figure 1). The Köppen classification BSh which is characterized by the hot semi-arid climate. The average annual rainfall is estimated to be 632 mm. The rainy season, which generally occurs from January to April, accounts for 65% of this average. Monthly average air temperatures range between 23.6 and 27.7 °C, and maximum temperatures exceed 32 °C (Pereira et al., 2015). The soil texture class of the study area was homogeneous and classified as sandy loam (Alcântara *et al.* 2021)

In this study we performed measurements of sap velocity (Js) in three periods of 2022: Rainy period (March to May), transition period (June to July), and the period of the first rains (November to December); and measurements of Xylem water potential (Ψ_{xylem}), Stomatal conductance (g_s), and Concentration of Non-Structural Carbohydrates (NSC): Soluble sugar (SS), and Starch in March and November 2022.

Meteorological variables

Meteorological data was obtained from a flux tower located on site, and which is part of the AmeriFlux network (BR-CST). It is 11 m high, and 3 m above the forest canopy. Specifically, we obtained rainfall, relative humidity, air temperature, and volumetric soil water content. Data from all sensors were measured every 1 minute, and mean/sum data were recorded by a data logger (model CR1000, Campbell Scientific Inc., Logan, UT, USA) every 30 minutes (Silva et al., 2017). Rainfall was measured by a tipping-bucket style rain gauge (model TE 525 WS-L, Texas Electronics, Dallas, TX, USA). Relative humidity and air temperature were measured by (EE181-L, Cambpell Scientific) and the volumetric soil water content was measured by TDR type sensor (CS616, Campbell Scientific) at soil depths of 5, 10, 20, 30 and 40 cm. Temperature and relative humidity were used to calculate the vapor pressure deficit (Santos et al., 2024). Volumetric soil water content was used to calculate the change in soil water storage (ΔSWS, in mm) in the top 40 cm.

$$\Delta SWS = \Sigma [(\theta_{t+1} - \theta_{\_t}) * \Delta z_n] \quad (1)$$

where θ is the volumetric water content of the soil at time t, and the subsequent timestamp, t+1, ΔZ is the soil depth interval, and n is the soil depth interval, aggregated across the five layers. The ΔSWS was then averaged by day and summed by month.

Species selection

We studied six widely distributed tree species from the Caatinga dry forest that varied in their wood density from 0.32 to 0.74 g cm^3: *Commiphora leptophloeos* (Mart.) J.B.Gillett, *Spondias tuberosa* Arruda, *Amburana cearensis* (Allemao) A.C.Sm., *Cenostigma pyramidale* (Tul.) Gagnon & G. P. Lewis, and *Aspidosperma pyrifolium* Mart. & Zucc. Which also included an evergreen species: *Sarcomphalus joazeiro* (Mart.) Hauenshild (formerly *Ziziphus joazeiro* Mart.) (Lima and Rodal, 2010) (Table 1). These species have great ecological and economic importance, such as timber and medicinal uses for the Caatinga, in addition to providing ecosystem services (Arnan et al., 2018; Rito et al., 2017). For each species, we select three to five individuals to measure the functional traits detailed below.

Tree characteristics

Because tree size and WD may be related to water use and hydraulic strategy (Meinzer et al., 2009; Wright et al., 2021), we measured tree diameter, height, and stem-specific WD. Tree diameter was obtained with a measuring tape wrapped around the tree base just above the ground. Tree height was measured with a hypsometer (SNDWAY, SW-1000A). WD was either measured in the field or obtained from Lima et al. 2012 (i.e., *S. tuberosa* and. *S.joazeiro;* Table 1). To measure WD in the field, we collected samples of wood from branches that were approximately 2 mm thick and 2 cm long. Samples were collected from terminal branches approximately 2 m above the ground. After removing the bark, the wood sample was immersed in distilled water for 24 hours, until saturated, to determine sample volume (v) according to Archimedes' principle. Afterward, the samples were dried in an oven at a temperature of 70 °C for 72 hours to obtain the dry mass (m). Wood density was calculated as WD = m/v (Pérez-Harguindeguy et al., 2013).

Sap velocity

To measure tree water use dynamics, i.e. sap velocity, Granier-style thermal dissipation sensors were constructed and installed similar to the modifications in Wright *et al.*, (2024). For each individual, one sensor was installed in the main stem of the tree (at approximately 50 cm height). As in the Granier (1987) original design, the sensor consists of two probes: the upper probe is heated, while the lower probe is not. Thus, the temperature difference between the two probes equates to the heat transfer rate, which is a proxy of the water transfer rate. That is, when the upper probe temperature is close to the lower probe temperature (ΔT is small), sap velocity at the point of measurement is fast, and vice versa. We highlight that the installation of sap flow sensors provided measurements of unidirectional sap velocity and from a single point where the sensor was installed on each tree. Sap velocity was calculated using Grainer's original equations and the average sap velocity, Js (cm h^{-1}), is calculated as:

$$Js = 119 * 10^{-6} * K^{1.23} \quad ; \qquad (2)$$

where

$$K = (\Delta T_{Max} - \Delta T) / \Delta T \quad ; \qquad (3)$$

Here, ΔT_{Max} is the maximum temperature difference between the two probes at zero sap velocity, and ΔT is the difference between the probes when the tree is transpiring. We used the AquaFlux (Speckman et al., 2008) package in R to determine ΔT_{Max}, defined to occur during night-time hours when VPD approaches zero (below 0.3 kPa for at least 1 hour). As noted, some species are multi-stemmed individuals, such as *S. joazeiro* and *S. tuberosa*. For these, we considered the main stem to be the central stem with the largest diameter. Because we are more interested in the rates of water use, and due to a limited number of sensors, we made no attempt to upscale transpiration to the individual tree level.

To compare changes in Js between species, we summarize both the diurnal pattern as well as daily values averaged from the 11:00 to 15:00 time window to capture maximum

velocities during three periods: the peak rainy season (March 19 to May 31, 2022), the transition to the dry season (June 1 to July 19, 2022) and the first rains of the next rainy season (November 9 to December 31, 2022). We selected these three periods because sap velocity was perceptible, data gaps and sensor malfunctions were limited, and to relate to other traits as described in the next sections.

Phenology

We carried out phenological observations once in the rainy period (March 25, 2022) and dry period (November 3, 2022), of five phenophases of the species, defined as: 1) Canopy - total number of mature leaves; 2) Leaf fall – yellowing leaves or leafless branches; 3) Budding – leaf shoots; 4) Flowering – presence of flowers; 5) Fruiting – presence of fruit. Based on these observations, Fournier's Percentage of Intensity (1974) was applied, which estimates the intensity of each phenophase. For field observations, a scale from 0 to 100% was established, based on the intensity of each phenophase. From these observations, Fournier's Percentage of Intensity (Fournier, 1974), was applied to evaluate the phenology, in which the intensity of each phenophase is estimated through a semi-quantitative interval scale of five categories (0-4), with intervals of 25% between each of them: zero – absence of phenophase; 1 – presence of the phenophase with a magnitude between 1 and 25%; 2 – presence of phenophase with magnitude reaching between 26 to 50%; 3 - presence of phenophase with magnitude reaching between 51 to 75%; 4 - presence of phenophase with magnitude reaching between 76 and 100%.

Xylem water potential and stomatal conductance

We measured xylem water potential (Ψ_{xylem}) in terminal branches once during the rainy period (March 25, 2022) and once dry period (November 3, 2022), before dawn (4:00 to 5:00) and at noon (12:00 to 13:00) using a Scholander-type pressure chamber. We also measured the stomatal conductance (g_s) of fully exposed and sunlight-receiving leaves of terminal branches

in the lower stratum of the canopy. To do so, we used a porometer (Decagon Devices, Inc. 2365 NE Hopkins Court Pullman WA 99163) on the same days, but during different time intervals: am at 9:00 to 10:00 and pm at 14:00 to 15:00.

Concentration of non-structural carbohydrates in leaves, stems and roots

To measure NSC, we collected samples from each biological replicate from three organs: several fully expanded leaves (~800 mg), terminal branches (~5000 mg), and fine roots (~600 mg) (<2 mm) from the soil sub-surface (<10cm depth), which were sorted and stored (Audrey G Quentin et al., 2015). These samples were collected once in each period: rainy period (April 9, 2022), and dry period (October 19, 2022). First, we placed the samples in a microwave oven at 700W for 30 seconds to stop all enzymatic activity as per Quentin et al. (2015). After this procedure, samples were stored in paper bags at room temperature for a maximum of one month to analysis. To quantify total soluble sugars (SS) and starch for these samples, we used the methodology of Santana-Vieira *et al.* (2016), as described below.

We extracted SS from the dry material using 80% ethanolic suspension according to the methodology of Farrar (1995). The samples were ground in a mortar and suspended in 1,200 µl of 80% ethanol. After vortexed, the samples were incubated for 90 minutes in a water bath at 70°C. Subsequently, the material was centrifuged at 15,000 g-force and the supernatant was collected. This process was repeated using 600 µl of 80% ethanol for another 30 minutes. We determined the concentration of soluble sugars using the phenol-sulfuric acid method by adding 0.5 ml of 5% phenol and 2.5 ml of sulfuric acid to the extract aliquot. We measured the SS concentration using a dual-beam spectrophotometer at 487 nm (Genesis 10S UV-Vis, Thermo Scientific) (Dubois et al., 1956).

For starch quantification, the pellets were resuspended in 800 µl of 0.2 M KOH solution and vortexed. The supernatant was placed in a water bath at 95°C for 2 hours. Then, the samples

were adjusted to pH 5.5 with 200 µl of acetic acid and centrifuged at 15,000 g-force and the supernatant was then collected. Finally, the samples were hydrolyzed with 10 units of amyloglucosidase (A1602, Sigma-Aldrich) for 1 hour in a thermal bath at 55°C to digest the gelatinized starch into glucose. Starch concentrations (measured as glucose equivalents) were measured at 487 nm using a dual-beam spectrophotometer (Dubois et al., 1956). Before conducting the analysis, we conducted a preliminary test to establish the dry weight (mg) for use in the extraction process. This involved measuring the SS content of 10 mg, 20 mg, and 40 mg of dry matter from two randomly selected individuals in each organ of the species. Our objective was to verify if the concentration of SS increased in proportion to the mass of dry matter. This procedure enabled us to assess the saturation level of the extracts. Based on this evaluation, we determined that a dry weight of 20 mg would be appropriate for all organs.

Statistical analysis

To test how sap velocity differs by species and period, we tested several mixed effects models for repeated measures. First, we modeled sap velocity with species as a fixed effects factor, and species replicate as a random effects factor within each period. For this, we created three different models: one for the rainy period, one for the transition period, and one for the period with the first rains of the upcoming rainy season. Second, we modeled sap velocity with period as the fixed effects factors, and species as a random effects factor. For all mixed effects models, we confirmed homogeneity in the variance of the residuals and used Tukey's post hoc to denote differences between species or period. For NSC, SS, and starch, we compared between periods and species using an analysis of variance (ANOVA) since these variables were collected after longer time intervals and temporal auto correlation can be assumed as null. When there was a significant difference between period or species, the NSC, SS and starch data were compared between periods and species, using Tukey test, at 5%probability. We also performed ANOVA and Tukey test ($p<0.05$) to verify if there were differences in the means of xylem water potential

and stomatal conductance between species. In addition, we also performed a Principal Component Analysis (PCA) for possible grouping of variables between species. All analyses and graphing were performed using the R v.4.2.0 programming language (R Core Team, 2022).

Results

Environmental variables

The total annual rainfall recorded for 2022 was 772 mm (Figure 2), which is higher than the historical average. The rainiest months were March (165 mm), which we considered to be the peak of the rainy season (March to May), and December (122 mm), which we considered to be the start of the next rainy season (November to December). We recorded 56 mm of rainfall in April. However, due to the rain gauge's logger failure from March 23 to April 9, 2022 (39 days), this amount is likely underestimated. The driest month was September, during which no significant rainfall was recorded. A notable dry season rain event occurred on October 26 (53 mm). In November, it rained 37 mm. However, sizeable rain occurred from November 28 to December 2, 2022 (total of 88 mm over 5 days), marking the first events of the next rainy season. The ΔSWS was highest in March, corresponding to the month with the highest rainfall (Figure 2). The VPD was low from January to June, increasing from July to October. Despite the recorded dry season rain, the highest VPD peak occurred in October (2.23 kPa). From November onwards, there was a reduction in VPD (Figure 2).

Seasonality of sap velocity between species

Sap velocity (J_s) differed by species for each period, and between the peak rainy season vs. first rains (Figure 3; Supporting Information S1: Table S1). Most species showed greater sap velocity during the first rains season (months November to December) especially when compared to the transition period (Figure 3). The evergreen species, *S. joazeiro*, had the highest J_s compared to the species of the other functional groups, regardless of season, reaching an

average of 135 g s^{-1} m^{-2} during the first rains (Figure 3). All species showed an increase in sap velocity after 7:00 am and a decrease after 15:00 pm regardless of periods (Figure 4; Supporting Information S1: Figure S1).

The timing of peak J_s varied by species and period, ranging from 12:30 to 13:30. Specifically, during the rainy period, J_s peaks in *A. cearensis*, *S. joazeiro* and *C. pyramidale* occurred at 12:30 pm; in *A. pyrifolium* it occurred at 13:00 pm; and in *C. leptophloeos* and *S. tuberosa,* occurred later, at 13:30 pm (Figure 4; Supporting Information S1: Table S2). While in the transition period, only *C. leptophloeos* and *S. tuberosa* showed changes in their Js peak times. Both species had earlier peaks: *C. leptophloeos* peaked half an hour earlier and *S. tuberosa* peaked an hour earlier. During the first rains, the species exhibited later peaks, from half an hour to an hour later, except *S. joazeiro* which showed an earlier sap velocity peak (-0.5 h) (Figure 4; Supporting Information S1: Table S2).

Phenology

The phenology revealed different intensities in the proportion of phenophases among species (Supporting Information S1: Figure S2). Specifically, observations made on March 25, 2022 show that the intensity of crown coverage was 100% in *A. cearensis*. In contrast, the lowest crown coverage was registered in *C. leptophloeos*, corresponding to 27% of the proportion of its phenophases, However, *C. leptophloeos* presented a higher intensity of sprouting (20%) and fruiting (30%) when compared to the other species (Supporting Information S1: Figure S2a). Flowering was observed only in *C. pyramidale*, corresponding to 38% of its phenophases. As for *A. pyrifolium*, high leaf fall was recorded (33% of the proportion), and the flowering and fruiting phenophases were not observed on the evaluation date (Supporting Information S1: Figure S2a). For observations made on November 3, 2022, the month corresponding to the dry period, *C. leptophloeos* (31%), *S. tuberosa* (33%), and *S. joazeiro* (3%) flowered (Supporting

Information S1: Figure S2b). The deciduous species with low wood density started to sprout, while the deciduous species with high wood density had a higher proportion of sprouting, mainly *C. pyramidale* (45%). The *A. cearensis*, still showed a high proportion of leaf fall (51%) (Supporting Information S1: Figure S2b).

Changes in xylem water potential and stomatal conductance

During the peak rainy period (March), the xylem water potential (Ψ_{xylem}) was higher in the deciduous with low wood density, especially in the predawn, and in *S. tuberosa* (predawn: -0.21 MPa; midday: -0.87 MPa) (Figure 5a). *S. joazeiro* had lower Ψ_{xylem} in the midday (-3.25 MPa) differing significantly from the Ψ_{xylem} of the other species. In the dry period, Ψ_{xylem} did not differ among species during predawn (Figure 5a). However, midday Ψ_{xylem} was significantly higher in *C. leptophloeos* and *A. cearensis*, and significantly lower in *A. pyrifolium* (Figure 5a).

As for stomatal conductance (g_s), there was no statistically significant difference between species or between measurement intervals during the peak rainy period measurement (March 25, 2022) (Figure 5b). For the dry period measurement (November 3, 2022) g_s was not recorded for *C. leptophloeos*, *A. cearensis* and *S. tuberosa* due to leaf loss (Figure 5b). However, for this measurement, there was a significant difference between the deciduous species with high WD. The g_s was higher in *S. joazeiro*, followed by *A. pyrifolium*, and lower in *C. pyramidale*. Still, there was no difference between the pre-dawn and mid-day intervals of the day for each species (Figure 5b).

NSC concentration in different organs

The soluble sugars (SS) showed significant differences between the rainy and dry periods in some organs for the species, except for *S. joazeiro* (Figure 6a). The deciduous species with low WD showed higher SS concentrations in the leaves in the rainy season: *C. leptophloeos* (309.0±109.7 mg g^{-1} DM), *A. cearensis* (580.5±313.0 mg g^{-1} DM), *S. tuberosa* (383.0±127.7

mg g^{-1} DM) (Figure 6a). The highest concentration of SS was recorded in the leaves of *A. cearensis* (580.4±313.0 mg g^{-1} DM) and the lowest in *A. pyrifolium* (88.8±15.0 mg g^{-1} DM) (Figure 6a). Root SS concentration was higher in the dry period for *C. leptophloeos* (329.1 ± 22.7 mg g^{-1} DM) and *S. tuberosa* (310.0 ± 68.6 mg g^{-1} DM) (Figure 6a).

Starch differed in the leaf and/or root between the seasons for each deciduous species (Figure 6b), while for the evergreen species, the starch only difference in the stem between the periods (Figure 6b). *C. leptophloeos* presented a higher concentration of starch in the leaves than the other species (88.1±18.4 mg g^{-1} DM) (Figure 6b). The lowest concentration of starch in leaves was recorded in *S. tuberosa* in the rainy period (28.7±9.0 mg g^{-1} DM). However, this species had higher concentration of starch in the root during the dry period (53.7±19.4 mg g^{-1} DM) (Figure 7). In the dry period, only *S. joazeiro* differed in stem starch, being higher than the other species (74.8±25.3 mg g^{-1} DM) (Figure 7).

When we evaluated the total concentration of NSC in each organ, we found that the species *C. leptophloeos*, *A. cearensis* and *S. tuberosa* presented higher concentration in the leaves during the rainy period than the other species (Supporting Information S1: Figure S3). During the dry period, only *S. joazeiro* presented leaves for quantification of the NSC concentration, which did not differ between the rainy and dry periods (Supporting Information S1: Figure S3).

Principal component analysis (PCA)

The PCA indicates the separation of species by the concentration of NSC in different organs and physiological traits (Figure 8). The PC1 explained 36.7% of the variables and PC2 explained 20.4%. The variables on PC1, PD, gs_am, gs_am, and NSC, SS and starch in different organs (leaf, stem and root), were more related to the species with low wood density, *C. leptophloeos*, *A. cearensis* and *S. tuberosa* (Figure 8). For PC2 variables Js and WD were more

related to species with high wood density, *C. pyramidale*, *A. pyrifolium* and *S. joazeiro* (Figure 8).

Discussion

Our results show that species had varied Js and NSC throughout various periods of the year. *C. leptphloeos, A. cearensis*, and *S. tuberosa* (deciduous species with low wood density) present lower Js and have higher concentration of NSC, especially SS, in the rain period in leaves, while in the dry period they present higher amounts of starch in the stem (*C. leptphloeos* and *A. cearensis*) and in the root (*S. tuberosa*). *S. joazeiro* (the evergreen species) presents higher Js in all periods of the year and frequent synthesis of NSC, in addition to a high concentration of NSC in the stem. The species *C. pyramidale* and *A. pyrifolium* have contrasting Js and NSC dynamics. *C. pyramidale* had higher Js throughout the periods. On the other hand, *A. pyrifolium* presents lower Js throughout the periods. Furthermore, the NSC concentration in the organs of these species is comparatively lower than that *C. leptphloeos, A. cearensis*, *S. tuberosa*, and to the starch in the stem of the *S. joazeiro*.

Dynamics of sap velocity in response to seasonality

In the Caatinga, seasonality is well marked, and plants respond to rainfall and VPD (Lima and Rodal 2010; Souza et al. 2016; de Queiroz et al. 2020). Thus, maintaining Js in the rainy season is essential to carry out their gas exchange and secure resources (Hartmann and Trumbore, 2016; Paloschi et al., 2021; Würth et al., 2005). We found that the sap velocity was higher for most species during the two wet period, i.e. rainy and first rains, which is not surprising given higher soil water availability. However, there were species-level differences. Sap velocity was highest for *S. joazeiro*, which likely has a deep root system as evidenced by its lower Ψ_{xylem} in midday (Lima et al., 2012) and seasonal shifts in water isotope signatures (Wright *et al.* 2021). During the dry period, *S. joazeiro*, *C. pyramidale*, and *C. leptophloeos* had higher sap velocity

in November. This is possibly because *S. joazeiro* and *C. pyramidale* are species with high wood density that can tolerate dry conditions and can still initiating leaf sprouting (Poorter *et al.* 2010; Lima *et al.* 2012). On the other hand, *C. leptophloeos* had a high flower production, which requires internally stored water and NSC for this phenophase (Lima et al. 2021; Resco de Dios and Gessler 2021).

The low hourly J_s of *C. leptphloeos, S. tuberosa,* and *A. cearensis* can be due stomatal closure and high xylem capacitance resulting from lower wood density and large water storage capacity (Brito et al., 2022b; Yu et al., 2019). The hourly sap velocity patterns revealed that the species follow a similar diurnal behavior as a response to atmospheric demand. This behavior was expected since many studies shown that high VPD reflects low stomatal conductance (Grossiord et al., 2020; Yu et al., 2019). At the same time, transpiration increases in many species, resulting in numerous consequences for species tolerance, such as failure hydraulics or in other species occur reduced photosynthetic rates and risks of carbon depletion due low stomatal conductance (Grossiord et al., 2020; McDowell et al., 2022; Piper, 2011). In SDTF such as the Caatinga, this becomes a serious problem, as it increases water loss by evapotranspiration and thus contributes to severe drought events and water deficit of trees (Grossiord et al., 2020, 2017; McDowell et al., 2022).

We found that the species *C. leptophloeos* maintained the same sap velocity peak observed between 2018-2019, while *C. pyramidale* presented a later Js peak (12:30 pm) in relation to the results obtained by Wright *et al.*, (2024). This change in peak times in different years possibly occurred because in 2022, there was more rainfall, and these conditions favored transpiration for a longer time in the species *C. pyramidale*.

Responses of species to water availability

C. leptphloeos, S. tuberosa, and *A. cearensis* showed higher Ψ_{xylem} both in predawn and midday during the rainy period, possibly due to greater cell turgidity, that is, greater capacitance which is often observed in species with relatively lower WD (Borchert and Pockman, 2005; Carrasco et al., 2014). While *S. joazeiro, C. pyramidale* and *A. pyrifolium*, which have greater WD, probably have lower capacitance, reflecting their Ψ_{xylem},. Deciduous trees with high wood density with low capacitance, such as *C. pyramidale* and *A. pyrifolium,* may be more tolerant to desiccation, as their tissues support low water potential and saturate quickly after water availability (Borchert and Pockman, 2005). Similar results for this same study site, although for fewer species, can be found in Brito *et al.* (2022) and Medeiros *et al.* (2024). *S. joazeiro* had lower Ψ_{xylem} in the predawn and sharply reduced in the midday, being the lowest compared to the other species in the rainy period. This behavior can be supported by a deep root system that helps uptake water in the deepest layers of the soil (Lima and Rodal, 2010). In addition, the high density of wood itself helps to withstand very negative pressures and consequently promotes greater resistance to cavitation (Lima et al., 2012; Markesteijn et al., 2011b; Poorter et al., 2010), factors that favored high sap velocity for this species during the evaluated period.

Regarding stomatal conductance, there was no significant difference among species or reading intervals for the rainy period. Because there is higher water available in the rainy season, tree may not need to restrict their gas exchange, allowing for generally greater carbon gain (Dalmolin et al., 2015). In the month representing the dry period, g_s was high in species with high wood density and remained similar in the afternoon, especially in *S. joazeiro*. The anomalous rain event in October and November may have promoted gas exchange in species that still had leaf cover (Borchert, 1994; Lima et al., 2021). The presence of leaves in the evergreen species during the dry period and the reduction in VPD in November favored an increase in g_s and, consequently, in Js (Brodribb et al., 2002; Grossiord et al., 2020).

Relationship among NSC concentration, phenology, and sap velocity

The species with low WD (*C. leptophloeos*, *A. cearensis* and *S. tuberosa*) had a higher concentration of total NSC in the rainy period than the species with high WD (*C. pyramidale*, *A. pyrifolium* and *S. joazeiro*). *C. leptophloeos*, *A. cearensis*, and *S. tuberosa* have a drought avoidance mechanism (Blanco-Sánchez et al., 2022), so they lose their leaves earlier to escape excessive water loss by transpiration (Lima et al., 2012; Markesteijn et al., 2011b; Souza et al., 2020). Therefore, they need to maximize their CO_2 assimilation when resources are available and store NSC for use during the dry season to maintain their metabolism and translocate C (Kawai et al., 2022; Würth et al., 2005). In addition, there may be an increase in NSC reserves in specific plant organs, such as stems and roots, which are trees main NSC storage organs (Tomasella et al., 2020). During the dry season, trees can mobilize stored carbohydrates to supply the continuous metabolic demand of the plant (Piper, 2011). Plants that can maintain high amounts and availability of NSC during drought may be more resilient (Tomasella et al., 2020). There is a connection between the parenchyma cells that contain NSC and the xylem vessels, allowing the exchange of water and solutes between these structures. This exchange plays a key role in regulating the metabolism and efficient transport of NSC through the phloem in plants (Kawai et al., 2022; Tomasella et al., 2020).

The highest concentration of starch in the leaves and stem of *S. joazeiro* was essential to maintain high Js and g_s during the dry period. The sugars present in the xylem sap can reduce osmotic potential, and this is important for the plant, as the higher concentration of solute in the xylem allows more significant water transport, increasing the flow (O'Brien et al., 2014). Water tends to flow from the soil, with a higher osmotic potential, towards the xylem, where the osmotic potential is lower (O'Brien et al., 2014; Tomasella et al., 2020). Studies have shown that tropical trees with higher concentration of NSC had higher xylem water potential during the dry period (O'Brien et al., 2014). Furthermore, this higher concentration of NSC and the higher WD of this species may help species in this functional group to withstand negative

pressures and have greater resistance to cavitation (Markesteijn et al., 2011b). Since *S. joazeiro* is an evergreen species, this favored the production of soluble sugar found in the leaves and stem, allowing SS to be available for frequent use (Palacio et al., 2018a; Piper, 2011). This suggests that evergreen species may have greater resistance to cavitation, which maintains J_s and NSC production even in the dry period, which may increase hydraulic security and avoid carbon starvation (Janssen et al., 2020; McDowell et al., 2022), although more representative measurements of various evergreen species are needed to test this

The species that showed the lowest concentration of NSC was *A. pyrifolium*. This behavior corresponded to low Js, which suggests that this species has little NSC production and storage capacity and greater hydraulic control to avoid excessive water loss (Vico et al., 2014; Wang et al., 2016). However, analysis of other traits of this species, such as anatomy and photosynthesis, is necessary for a better understanding of the physiological mechanisms of this species.

The species *C. leptophloeos* showed high concentration of SS in the stem during the dry period. This suggests that, in addition to a high stem water storage capacity, this species is also able to store large amount of SS in its stem, which can become available for early metabolism (Kawai et al., 2022; Palacio et al., 2018a). This finding is unique because it suggests that tree stems play an important role in long and short-term storage of needed resources such as water and SS. Not surprisingly, *S. tuberosa* stored more starch in the root during the drought, which promoting the translocation of sugars necessary for metabolism (Hartmann and Trumbore, 2016). It is well-documented that *S. tuberosa* has an extensive resource capacity in the roots, which are essential for flowering and supporting a high yield of fleshy fruits even at the end of the dry season (Lima Filho et al., 2009). Furthermore, starch storage in the root system may play an important role in leaf sprouting in the next season and in recovery from stress after drought (Resco de Dios and Gessler, 2021; Santos et al., 2021). Starch is the main long-term

storage compound, and deciduous species such as *S. tuberosa* depend on the translocation of stored NSC more so than evergreens like *S. joazeiro*, because deciduous species build a new leaf canopy each season (Lima et al., 2012; Rosell et al., 2021).

Phenology was a good predictor of sap velocity, as flow responded to phenophase intensities, indicating that phenology responds to seasonality (da Silva E Teodoro et al., 2022; Lima et al., 2021). Due species having more than 50% of crown coverage in most species in the rainy month (March 2022), and *C. leptophloeos* and *S. tuberosa* presenting the budding phenophase, the Js was high in the species, especially in *S. joazeiro*, which stood out among them. The specie *A. pyrifolium* did not present the reproductive phenophases (flowering and fruiting) in March (Supporting Information S1: Figure S2a), (which demand greater flow to the drains), resulting lower Js than the other species. Possibly lower Js also occurred because this species presented high leaf fall, low water potential, and low stomatal conductance, more conservative drought tolerance strategies (Markesteijn et al., 2011a).

Many deciduous species with high wood density start sprouting soon after the first rains that mark the end of the dry season. This explains greater sprouting in *C. pyramidale* and *A. pyrifolium* and lower leaf sprouting in deciduous species with low wood density (Lima et al., 2021, 2012). However, *C. leptophloeos* and *S. tuberosa* showed high Fournier intensity in the flowering phenophase, suggesting that greater starch storage in the stem of *C. leptophloeos* and the root of *S. tuberosa* may support the reproductive phenophase of these species (Supporting Information S1: Figure S2b). These species start flowering in the late dry season, regardless of the occurrence of rain (Lima et al., 2021, 2012). Therefore, long-term stored starch could be translocated to these drains (Piper, 2011; Rosell et al., 2021), and the water status in deciduous species with low wood density is kept high.

Conclusions

We found that species have varied water use and allocation of non-structural carbohydrates. *C. leptphloeos, S. tuberosa,* and *A. cearensis* have high stem water storage and NSC storage, and *S. joazeiro* maintains high sap velocity and non-structural carbohydrates production during the wet and dry periods. Considering longer dry periods and irregular rainy periods, deciduous species with low wood density that use stored NSC to resprout and flowering during the dry season may be the most affected by drought due to the risk of depletion of their reserves.

Acknowledgment

We would like to thank the students from the Plant Physiology laboratory (Laboratório de Fisiologia Vegetal, LFV), Department of Botany at UFPE, for their assistance with laboratory analyses, the Study Group of Semiarid Ecohydrology, the Center for Functional Ecology of Plants (Núcleo de Ecologia Funcional de Plantas, NEFPlan), and the Universidade Federal Rural de Pernambuco, Serra Talhada Academic Unit (UFRPE/UAST) for assistance in fieldwork, especially Nielson Brito, Cíntia Amando, and Romário Horas. We also thank the Postgraduate Program in Plant Production at UFRPE/UAST for the availability of equipment and laboratories. We are grateful to professor Dr. José Romualdo de Sousa Lima from Federal University of Agreste de Pernambuco (UFAPE) for the Scholander pressure chamber and Senhor Homem Bom Magalhães for access to the field site. This work was financially supported by FACEPE (Facepe-Pronem-APQ-0336-2.03/14). MM is funded by (FACEPE Fellow-IBPG-0330-2.07/21). The work was also supported by the CAPES/TAMU project (006/2014) for the measures of sap velocity and by the INCT: National Observatory of Water and Carbon Dynamics in the Caatinga Biome – ONDACBC, contributing with meteorological data.

Data Availability Statement

The data that support the findings of this study are available from the corresponding author upon reasonable request.

Authors' Contributions

MM, CLW, and MGS conceived the study. MM, JRIS, and ALJ collected the data. MM and CLW analyzed the data. MM, CLW, ALAL and MGS wrote the first draft with edits from all authors. ALAL, ESS, and MGS provided supervision and resources.

Conflict of Interest

None declared.

References

Allen, K., Dupuy, J.M., Gei, M.G., Hulshof, C., Medvigy, D., Pizano, C., Salgado-Negret, B., Smith, C.M., Trierweiler, A., Van Bloem, S.J., Waring, B.G., Xu, X., Powers, J.S., 2017. Will seasonally dry tropical forests be sensitive or resistant to future changes in rainfall regimes? Environ. Res. Lett. 12. https://doi.org/10.1088/1748-9326/aa5968

Arnan, X., Leal, I.R., Tabarelli, M., Andrade, J.F., Barros, M.F., Câmara, T., Jamelli, D., Knoechelmann, C.M., Menezes, T.G.C., Menezes, A.G.S., Oliveira, F.M.P., de Paula, A.S., Pereira, S.C., Rito, K.F., Sfair, J.C., Siqueira, F.F.S., Souza, D.G., Specht, M.J., Vieira, L.A., Arcoverde, G.B., Andersen, A.N., 2018. A framework for deriving measures of chronic anthropogenic disturbance: Surrogate, direct, single and multi-metric indices in Brazilian Caatinga. Ecol. Indic. 94, 274–282. https://doi.org/10.1016/j.ecolind.2018.07.001

Barros, F. de V., Bittencourt, P.R.L., Brum, M., Restrepo-Coupe, N., Pereira, L., Teodoro, G.S., Saleska, S.R., Borma, L.S., Christoffersen, B.O., Penha, D., Alves, L.F., Lima, A.J.N., Carneiro, V.M.C., Gentine, P., Lee, J.E., Aragão, L.E.O.C., Ivanov, V., Leal,

L.S.M., Araujo, A.C., Oliveira, R.S., 2019. Hydraulic traits explain differential responses of Amazonian forests to the 2015 El Niño-induced drought. New Phytol. 223, 1253–1266. https://doi.org/10.1111/nph.15909

Berenguer, E., Lennox, G.D., Ferreira, J., Malhi, Y., Aragão, L.E.O.C., Barreto, J.R., Del Bon Espírito-Santo, F., Figueiredo, A.E.S., França, F., Gardner, T.A., Joly, C.A., Palmeira, A.F., Quesada, C.A., Rossi, L.C., de Seixas, M.M.M., Smith, C.C., Withey, K., Barlow, J., 2021. Tracking the impacts of El Niño drought and fire in human-modified Amazonian forests. Proc. Natl. Acad. Sci. U. S. A. 118. https://doi.org/10.1073/pnas.2019377118

Bhusal, N., Han, S.G., Yoon, T.M., 2019. Impact of drought stress on photosynthetic response, leaf water potential, and stem sap flow in two cultivars of bi-leader apple trees (Malus × domestica Borkh.). Sci. Hortic. (Amsterdam). 246, 535–543. https://doi.org/10.1016/j.scienta.2018.11.021

Blanco-Sánchez, M., Ramos-Muñoz, M., Pías, B., Ramírez-Valiente, J.A., Díaz-Guerra, L., Escudero, A., Matesanz, S., 2022. Natural selection favours drought escape and an acquisitive resource-use strategy in semi-arid Mediterranean shrubs. Funct. Ecol. 36, 2289–2302. https://doi.org/10.1111/1365-2435.14121

Borchert, R., 1994. Soil and stem water storage determine phenology and distribution of tropical dry forest trees. Ecology 75, 1437–1449. https://doi.org/10.2307/1937467

Borchert, R., Pockman, W.T., 2005. Water storage capacitance and xylem tension in isolated branches of temperate and tropical trees. Tree Physiol. 25, 457–466. https://doi.org/10.1093/treephys/25.4.457

Bosch, D.D., Marshall, L.K., Teskey, R., 2014. Forest transpiration from sap flux density

measurements in a Southeastern Coastal Plain riparian buffer system. Agric. For. Meteorol. 187, 72–82. https://doi.org/10.1016/j.agrformet.2013.12.002

Bréda, N., Huc, R., Granier, A., Dreyer, E., 2006. Temperate forest trees and stands under severe drought: a review of ecophysiological responses, adaptation processes and long-term consequences. Ann. For. Sci. 63, 625–644.

Bretfeld, M., Ewers, B.E., Hall, J.S., 2018. Plant water use responses along secondary forest succession during the 2015–2016 El Niño drought in Panama. New Phytol. 219, 885–899. https://doi.org/10.1111/nph.15071

Brito, N.D. da S., Medeiros, M.J. dos S., Souza, E.S. de, Lima, A.L.A. de, 2022a. Drought response strategies for deciduous species in the semiarid Caatinga derived from the interdependence of anatomical, phenological and bio-hydraulic attributes. Flora Morphol. Distrib. Funct. Ecol. Plants 288. https://doi.org/10.1016/j.flora.2022.152009

Brito, N.D. da S., Medeiros, M.J. dos S., Souza, E.S. de, Lima, A.L.A. de, 2022b. Drought response strategies for deciduous species in the semiarid Caatinga derived from the interdependence of anatomical, phenological and bio-hydraulic attributes. Flora Morphol. Distrib. Funct. Ecol. Plants 288. https://doi.org/10.1016/j.flora.2022.152009

Brodribb, T.J., Cochard, H., 2009. Hydraulic failure defines the recovery and point of death in water-stressed conifers. Plant Physiol. 149, 575–584. https://doi.org/10.1104/pp.108.129783

Brodribb, T.J., Holbrook, N.M., Gutiérrez, M. V., 2002. Hydraulic and photosynthetic co-ordination in seasonally dry tropical forest trees. Plant, Cell Environ. 25, 1435–1444. https://doi.org/10.1046/j.1365-3040.2002.00919.x

Burkhardt, J., Pariyar, S., 2016. How does the VPD response of isohydric and anisohydric

plants depend on leaf surface particles? Plant Biol. 18, 91–100. https://doi.org/10.1111/plb.12402

Cai, W., Wang, G., Santoso, A., Mcphaden, M.J., Wu, L., Jin, F.F., Timmermann, A., Collins, M., Vecchi, G., Lengaigne, M., England, M.H., Dommenget, D., Takahashi, K., Guilyardi, E., 2015. Increased frequency of extreme La Niña events under greenhouse warming. Nat. Clim. Chang. 5, 132–137. https://doi.org/10.1038/nclimate2492

Calbi, M., Boenisch, G., Boulangeat, I., Bunker, D., Catford, J.A., Changenet, A., Culshaw, V., Dias, A.S., Hauck, T., Joschinski, J., Kattge, J., Mimet, A., Pianta, M., Poschlod, P., Weisser, W.W., Roccotiello, E., 2024. A novel framework to generate plant functional groups for ecological modelling. Ecol. Indic. 166, 112370. https://doi.org/10.1016/j.ecolind.2024.112370

Cardoso, A.A., Batz, T.A., McAdam, S.A.M., 2020. Xylem embolism resistance determines leaf mortality during drought in persea americana. Plant Physiol. 182, 547–554. https://doi.org/10.1104/pp.19.00585

Carrasco, O.L., Bucci, S.J., Di Francescantonio, D., Lezcano, O.A., Campanello, P.I., Scholz, F.G., Rodríguez, S., Madanes, N., Cristiano, P.M., Hao, G.Y., Holbrook, N.M., Goldstein, G., 2014. Water storage dynamics in the main stem of subtropical tree species differing in wood density, growth rate and life history traits. Tree Physiol. 35, 354–365. https://doi.org/10.1093/treephys/tpu087

Cavaleri, M.A., Coble, A.P., Ryan, M.G., Bauerle, W.L., Loescher, H.W., Oberbauer, S.F., 2017. Tropical rainforest carbon sink declines during El Niño as a result of reduced photosynthesis and increased respiration rates. New Phytol. 216, 136–149. https://doi.org/10.1111/NPH.14724

Chave, J., Coomes, D., Jansen, S., Lewis, S.L., Swenson, N.G., Zanne, A.E., 2009. Towards a worldwide wood economics spectrum. Ecol. Lett. 12, 351–366. https://doi.org/10.1111/j.1461-0248.2009.01285.x

Chuste, P.A., Maillard, P., Bréda, N., Levillain, J., Thirion, E., Wortemann, R., Massonnet, C., 2020. Sacrificing growth and maintaining a dynamic carbohydrate storage are key processes for promoting beech survival under prolonged drought conditions. Trees - Struct. Funct. 34, 381–394. https://doi.org/10.1007/s00468-019-01923-5

da Silva E Teodoro, É.D.M., da Silva, A.P.A., Brito, N.D. da S., Rodal, M.J.N., Shinozaki-Mendes, R.A., de Lima, A.L.A., 2022. Functional traits determine the vegetative phenology of woody species in riparian forest in semi-arid Brazil. Plant Ecol. 223, 1137–1153. https://doi.org/10.1007/s11258-022-01264-3

Dalmolin, Â.C., de Almeida Lobo, F., Vourlitis, G., Silva, P.R., Dalmagro, H.J., Antunes, M.Z., Ortíz, C.E.R., 2015. Is the dry season an important driver of phenology and growth for two Brazilian savanna tree species with contrasting leaf habits? Plant Ecol. 216, 407–417. https://doi.org/10.1007/s11258-014-0445-5

de Alcântara, L.R.P., Coutinho, A.P., Neto, S.M.D.S., de Gusmão da Cunha Rabelo, A.E.C., Antonino, A.C.D., 2021. Computational modeling of the hydrological processes in caatinga and pasture areas in the brazilian semi-arid. Water (Switzerland) 13. https://doi.org/10.3390/w13131877

De Guzman, M.E., Santiago, L.S., Schnitzer, S.A., Álvarez-Cansino, L., 2017. Trade-offs between water transport capacity and drought resistance in neotropical canopy liana and tree species. Tree Physiol. 37, 1404–1414. https://doi.org/10.1093/treephys/tpw086

de Medeiros, F.J., de Oliveira, C.P., 2021. Dynamical Aspects of the Recent Strong El Niño

Events and Its Climate Impacts in Northeast Brazil. Pure Appl. Geophys. 178, 2315–2332. https://doi.org/10.1007/s00024-021-02758-3

de Oliveira, C.C., Zandavalli, R.B., de Lima, A.L.A., Rodal, M.J.N., 2015. Functional groups of woody species in semi-arid regions at low latitudes. Austral Ecol. 40, 40–49. https://doi.org/10.1111/aec.12165

Decarsin, R., Guillemot, J., le Maire, G., Blondeel, H., Meredieu, C., Achard, E., Bonal, D., Cochard, H., Corso, D., Delzon, S., Doucet, Z., Druel, A., Grossiord, C., Torres-Ruiz, J.M., Bauhus, J., Godbold, D.L., Hajek, P., Jactel, H., Jensen, J., Mereu, S., Ponette, Q., Rewald, B., Ruffault, J., Sandén, H., Scherer-Lorenzen, M., Serrano-León, H., Simioni, G., Verheyen, K., Werner, R., Martin-StPaul, N., 2024. Tree drought–mortality risk depends more on intrinsic species resistance than on stand species diversity. Glob. Chang. Biol. 30. https://doi.org/10.1111/gcb.17503

Dubois, M., Gilles, K.A., Hamilton, J.K., Rebers, P.A., Smith, F., 1956. Colorimetric Method for Determination of Sugars and Related Substances. Anal. Chem. 28, 350–356. https://doi.org/10.1021/ac60111a017

Farrar, J.F., 1993. Carbon partitioning, in: Photosynthesis and Production in a Changing Environment. Springer Netherlands, Dordrecht, pp. 232–246. https://doi.org/10.1007/978-94-011-1566-7_15

Fletcher, L.R., Scoffoni, C., Farrell, C., Buckley, T.N., Pellegrini, M., Sack, L., 2022. Testing the association of relative growth rate and adaptation to climate across natural ecotypes of Arabidopsis. New Phytol. 236, 413–432. https://doi.org/10.1111/nph.18369

Fontes, C.G., Dawson, T.E., Jardine, K., McDowell, N., Gimenez, B.O., Anderegg, L., Negrón-Juárez, R., Higuchi, N., Fine, P.V.A., Araújo, A.C., Chambers, J.Q., 2018. Dry

and hot: The hydraulic consequences of a climate change–type drought for Amazonian trees. Philos. Trans. R. Soc. B Biol. Sci. 373. https://doi.org/10.1098/rstb.2018.0209

Fournier, L.A., 1974. Un método cuantitativo para la medición de características fenológicas en árboles. Turrialba 24, 422–423.

Frappart, F., Biancamaria, S., Normandin, C., Blarel, F., Bourrel, L., Aumont, M., Azemar, P., Vu, P.L., Le Toan, T., Lubac, B., Darrozes, J., 2018. Influence of recent climatic events on the surface water storage of the Tonle Sap Lake. Sci. Total Environ. 636, 1520–1533. https://doi.org/10.1016/j.scitotenv.2018.04.326

Furze, M.E., Huggett, B.A., Aubrecht, D.M., Stolz, C.D., Carbone, M.S., Richardson, A.D., 2019. Whole-tree nonstructural carbohydrate storage and seasonal dynamics in five temperate species. New Phytol. 221, 1466–1477. https://doi.org/10.1111/nph.15462

Gimenez, B.O., Jardine, K.J., Higuchi, N., Negrón-Juárez, R.I., Sampaio-Filho, I. de J., Cobello, L.O., Fontes, C.G., Dawson, T.E., Varadharajan, C., Christianson, D.S., Spanner, G.C., Araújo, A.C., Warren, J.M., Newman, B.D., Holm, J.A., Koven, C.D., McDowell, N.G., Chambers, J.Q., 2019. Species-specific shifts in diurnal sap velocity dynamics and hysteretic behavior of ecophysiological variables during the 2015–2016 el niño event in the amazon forest. Front. Plant Sci. 10, 1–16. https://doi.org/10.3389/fpls.2019.00830

Granier, A., 1985. Une nouvelle méthode pour la mesure du flux de sève brute dans le tronc des arbres. Ann. des Sci. For. 42, 193–200. https://doi.org/10.1051/forest:19850204

Grossiord, C., Buckley, T.N., Cernusak, L.A., Novick, K.A., Poulter, B., Siegwolf, R.T.W., Sperry, J.S., McDowell, N.G., 2020. Plant responses to rising vapor pressure deficit. New Phytol. 226, 1550–1566. https://doi.org/10.1111/nph.16485

Grossiord, C., Sevanto, S., Borrego, I., Chan, A.M., Collins, A.D., Dickman, L.T., Hudson, P.J., McBranch, N., Michaletz, S.T., Pockman, W.T., Ryan, M., Vilagrosa, A., McDowell, N.G., 2017. Tree water dynamics in a drying and warming world. Plant Cell Environ. 40, 1861–1873. https://doi.org/10.1111/pce.12991

Hartmann, H., Trumbore, S., 2016. Understanding the roles of nonstructural carbohydrates in forest trees - from what we can measure to what we want to know. New Phytol. 211, 386–403. https://doi.org/10.1111/nph.13955

Intergovernmental Panel on Climate Change (IPCC), 2023. Climate Change 2022 – Impacts, Adaptation and Vulnerability, Climate Change 2022 – Impacts, Adaptation and Vulnerability. Cambridge University Press. https://doi.org/10.1017/9781009325844

IPCC (Intergovernmental Panel on Climate Change), n.d.

Janssen, T.A.J., Hölttä, T., Fleischer, K., Naudts, K., Dolman, H., 2020. Wood allocation trade-offs between fiber wall, fiber lumen, and axial parenchyma drive drought resistance in neotropical trees. Plant Cell Environ. 43, 965–980. https://doi.org/10.1111/pce.13687

Jiao, L., Lu, N., Fu, B., Wang, J., Li, Z., Fang, W., Liu, J., Wang, C., Zhang, L., 2018. Evapotranspiration partitioning and its implications for plant water use strategy: Evidence from a black locust plantation in the semi-arid Loess Plateau, China. For. Ecol. Manage. 424, 428–438. https://doi.org/10.1016/j.foreco.2018.05.011

Kannenberg, S.A., Phillips, R.P., 2020. Non-structural carbohydrate pools not linked to hydraulic strategies or carbon supply in tree saplings during severe drought and subsequent recovery. Tree Physiol. 40, 259–271. https://doi.org/10.1093/treephys/tpz132

Kawai, K., Waengsothorn, S., Ishida, A., 2022. Sapwood density underlies xylem hydraulics

and stored carbohydrates across 13 deciduous tree species in a seasonally dry tropical forest in Thailand. Trees - Struct. Funct. 37, 485–495. https://doi.org/10.1007/s00468-022-02364-3

Liang, X., Ye, Q., Liu, H., Brodribb, T.J., 2021. Wood density predicts mortality threshold for diverse trees. New Phytol. 229, 3053–3057. https://doi.org/10.1111/nph.17117

Lima, A.L.A., Rodal, M.J.N., 2010. Phenology and wood density of plants growing in the semi-arid region of northeastern Brazil. J. Arid Environ. 74, 1363–1373. https://doi.org/10.1016/j.jaridenv.2010.05.009

Lima, A.L.A. de, Rodal, M.J.N., Castro, C.C., Antonino, A.C.D., Melo, A.L. de, Gonçalves-Souza, T., Sampaio, E.V. de S.B., 2021. Phenology of high- and low-density wood deciduous species responds differently to water supply in tropical semiarid regions. J. Arid Environ. 193. https://doi.org/10.1016/j.jaridenv.2021.104594

Lima, A.L.A. de, Sá Barretto Sampaio, E.V. de, Castro, C.C. de, Rodal, M.J.N., Antonino, A.C.D., Melo, A.L. de, 2012. Do the phenology and functional stem attributes of woody species allow for the identification of functional groups in the semiarid region of Brazil? Trees - Struct. Funct. 26, 1605–1616. https://doi.org/10.1007/s00468-012-0735-2

Lima Filho, P.J.M., Santos, F., Antônio, C., 2009. Avaliações fenotípicas e fisiológicas de espécies de Spondias tendo como porta enxerto o umbuzeiro (Spondias tuberosa Cam.). Rev. Caatinga 22, 59–63.

Lima, T.R.A., Carvalho, E.C.D., Martins, F.R., Oliveira, R.S., Miranda, R.S., Müller, C.S., Pereira, L., Bittencourt, P.R.L., Sobczak, J.C.M.S.M., Gomes-Filho, E., Costa, R.C., Araújo, F.S., 2018. Lignin composition is related to xylem embolism resistance and leaf life span in trees in a tropical semiarid climate. New Phytol. 219, 1252–1262.

https://doi.org/10.1111/nph.15211

Mantova, M., Herbette, S., Cochard, H., Torres-Ruiz, J.M., 2022. Hydraulic failure and tree mortality: from correlation to causation. Trends Plant Sci. 27, 335–345. https://doi.org/10.1016/j.tplants.2021.10.003

Markesteijn, L., Poorter, L., Bongers, F., Paz, H., Sack, L., 2011a. Hydraulics and life history of tropical dry forest tree species: Coordination of species' drought and shade tolerance. New Phytol. 191, 480–495. https://doi.org/10.1111/j.1469-8137.2011.03708.x

Markesteijn, L., Poorter, L., Paz, H., Sack, L., Bongers, F., 2011b. Ecological differentiation in xylem cavitation resistance is associated with stem and leaf structural traits. Plant, Cell Environ. 34, 137–148. https://doi.org/10.1111/j.1365-3040.2010.02231.x

McDowell, N., Pockman, W.T., Allen, C.D., Breshears, D.D., Cobb, N., Kolb, T., Plaut, J., Sperry, J., West, A., Williams, D.G., Yepez, E.A., 2008a. Mechanisms of plant survival and mortality during drought: why do some plants survive while others succumb to drought? New Phytol. 178, 719–739. https://doi.org/10.1111/j.1469-8137.2008.02436.x

McDowell, N., Pockman, W.T., Allen, C.D., Breshears, D.D., Cobb, N., Kolb, T., Plaut, J., Sperry, J., West, A., Williams, D.G., Yepez, E.A., 2008b. Mechanisms of plant survival and mortality during drought: Why do some plants survive while others succumb to drought? New Phytol. 178, 719–739. https://doi.org/10.1111/j.1469-8137.2008.02436.x

McDowell, N.G., Sapes, G., Pivovaroff, A., Adams, H.D., Allen, C.D., Anderegg, W.R.L., Arend, M., Breshears, D.D., Brodribb, T., Choat, B., Cochard, H., De Cáceres, M., De Kauwe, M.G., Grossiord, C., Hammond, W.M., Hartmann, H., Hoch, G., Kahmen, A., Klein, T., Mackay, D.S., Mantova, M., Martínez-Vilalta, J., Medlyn, B.E., Mencuccini, M., Nardini, A., Oliveira, R.S., Sala, A., Tissue, D.T., Torres-Ruiz, J.M., Trowbridge,

A.M., Trugman, A.T., Wiley, E., Xu, C., 2022. Mechanisms of woody-plant mortality under rising drought, CO2 and vapour pressure deficit. Nat. Rev. Earth Environ. 3, 294–308. https://doi.org/10.1038/s43017-022-00272-1

Medeiros, M., Lima, A.L.A. de, Silva, J.R.I., Jesus, A.L.N. de, Wright, C.L., Souza, E.S. De, Santos, M.G., 2025. Seasonal Shifts in Tree Water Use and Non - Structural Carbohydrate Storage in a Tropical Dry Forest. Plant Cell Environ. 48, 1–15. https://doi.org/10.1111/pce.15449

Medeiros, M., Wright, C.L., de Lima, A.L.A., da Silva Brito, N.D., Souza, R., Silva, J.R.I., Souza, E., 2024. Divergent hydraulic strategies of two deciduous tree species to deal with drought in the Brazilian semi-arid region. Trees 38, 681–694. https://doi.org/10.1007/s00468-024-02506-9

Meinzer, F.C., Johnson, D.M., Lachenbruch, B., McCulloh, K.A., Woodruff, D.R., 2009. Xylem hydraulic safety margins in woody plants: Coordination of stomatal control of xylem tension with hydraulic capacitance. Funct. Ecol. 23, 922–930. https://doi.org/10.1111/j.1365-2435.2009.01577.x

Mencuccini, M., Manzoni, S., Christoffersen, B., 2019. Modelling water fluxes in plants: from tissues to biosphere. New Phytol. 222, 1207–1222. https://doi.org/10.1111/nph.15681

Mendes, K.R., Campos, S., da Silva, L.L., Mutti, P.R., Ferreira, R.R., Medeiros, S.S., Perez-Marin, A.M., Marques, T. V., Ramos, T.M., de Lima Vieira, M.M., Oliveira, C.P., Gonçalves, W.A., Costa, G.B., Antonino, A.C.D., Menezes, R.S.C., Bezerra, B.G., Santos e Silva, C.M., 2020. Seasonal variation in net ecosystem CO2 exchange of a Brazilian seasonally dry tropical forest. Sci. Rep. 10, 1–16. https://doi.org/10.1038/s41598-020-66415-w

Meng, L., Chambers, J., Koven, C., Pastorello, G., Gimenez, B., Jardine, K., Tang, Y., McDowell, N., Negron-Juarez, R., Longo, M., Araujo, A., Tomasella, J., Fontes, C., Mohan, M., Higuchi, N., 2022. Soil moisture thresholds explain a shift from light-limited to water-limited sap velocity in the Central Amazon during the 2015-16 El Niño drought. Environ. Res. Lett. 17. https://doi.org/10.1088/1748-9326/ac6f6d

Nardini, A., Salleo, S., Jansen, S., 2011. More than just a vulnerable pipeline: xylem physiology in the light of ion-mediated regulation of plant water transport. J. Exp. Bot. 62, 4701–4718. https://doi.org/10.1093/jxb/err208

O'Brien, M.J., Leuzinger, S., Philipson, C.D., Tay, J., Hector, A., 2014. Drought survival of tropical tree seedlings enhanced by non-structural carbohydrate levels. Nat. Clim. Chang. 4, 710–714. https://doi.org/10.1038/nclimate2281

Oliveira, C.C., Zandavalli, R.B., de Lima, A.L.A., Rodal, M.J.N., 2015. Functional groups of woody species in semi-arid regions at low latitudes. Austral Ecol. 40, 40–49. https://doi.org/10.1111/aec.12165

Oliveira, C.C. de, Zandavalli, R.B., de Lima, A.L.A., Rodal, M.J.N., 2015. Functional groups of woody species in semi-arid regions at low latitudes. Austral Ecol. 40, 40–49. https://doi.org/10.1111/aec.12165

Oliveira, R.S., Costa, F.R.C., van Baalen, E., de Jonge, A., Bittencourt, P.R., Almanza, Y., Barros, F. de V., Cordoba, E.C., Fagundes, M. V., Garcia, S., Guimaraes, Z.T.M., Hertel, M., Schietti, J., Rodrigues-Souza, J., Poorter, L., 2019. Embolism resistance drives the distribution of Amazonian rainforest tree species along hydro-topographic gradients. New Phytol. 221, 1457–1465. https://doi.org/10.1111/nph.15463

Oliveira, R.S., Dawson, T.E., Burgess, S.S.O., Nepstad, D.C., 2005. Hydraulic redistribution

in three Amazonian trees. Oecologia 145, 354–363. https://doi.org/10.1007/s00442-005-0108-2

Oliveira, R.S., Eller, C.B., Barros, F. de V., Hirota, M., Brum, M., Bittencourt, P., 2021a. Linking plant hydraulics and the fast–slow continuum to understand resilience to drought in tropical ecosystems. New Phytol. 230, 904–923. https://doi.org/10.1111/nph.17266

Oliveira, R.S., Eller, C.B., Barros, F. de V., Hirota, M., Brum, M., Bittencourt, P., 2021b. Linking plant hydraulics and the fast–slow continuum to understand resilience to drought in tropical ecosystems. New Phytol. https://doi.org/10.1111/nph.17266

Palacio, S., Camarero, J.J., Maestro, M., Alla, A.Q., Lahoz, E., Montserrat-Martí, G., 2018a. Are storage and tree growth related? Seasonal nutrient and carbohydrate dynamics in evergreen and deciduous Mediterranean oaks. Trees - Struct. Funct. 32, 777–790. https://doi.org/10.1007/s00468-018-1671-6

Palacio, S., Jesús, ·, Camarero, J., Melchor, ·, Alla, A.Q., Lahoz, E., Montserrat-Martí, G., 2018b. Are storage and tree growth related? Seasonal nutrient and carbohydrate dynamics in evergreen and deciduous Mediterranean oaks 32, 777–790. https://doi.org/10.1007/s00468-018-1671-6

Paloschi, R.A., Ramos, D.M., Ventura, D.J., Souza, R., Souza, E., Morellato, L.P.C., Nóbrega, R.L.B., Coutinho, Í.A.C., Verhoef, A., Körting, T.S., Borma, L.D.S., 2021. Environmental drivers of water use for caatinga woody plant species: Combining remote sensing phenology and sap flow measurements. Remote Sens. 13, 1–18. https://doi.org/10.3390/rs13010075

Pereira, P.D.C., Da Silva, T.G.F., Zolnier, S., De Morais, J.E.F., Dos Santos, D.C., 2015. Morfogênese da palma forrageira irrigada por gotejamento. Rev. Caatinga 28, 184–195.

Pérez-Harguindeguy, N., Díaz, S., Garnier, E., Lavorel, S., Poorter, H., Jaureguiberry, P., Bret-Harte, M.S., Cornwell, W.K., Craine, J.M., Gurvich, D.E., Urcelay, C., Veneklaas, E.J., Reich, P.B., Poorter, L., Wright, I.J., Ray, P., Enrico, L., Pausas, J.G., De Vos, A.C., Buchmann, N., Funes, G., Quétier, F., Hodgson, J.G., Thompson, K., Morgan, H.D., Ter Steege, H., Van Der Heijden, M.G.A., Sack, L., Blonder, B., Poschlod, P., Vaieretti, M. V., Conti, G., Staver, A.C., Aquino, S., Cornelissen, J.H.C., 2013. New handbook for standardised measurement of plant functional traits worldwide. Aust. J. Bot. 61, 167–234. https://doi.org/10.1071/BT12225

Pineda-García, F., Paz, H., Meinzer, F.C., 2012. Drought resistance in early and late secondary successional species from a tropical dry forest: The interplay between xylem resistance to embolism, sapwood water storage and leaf shedding. Plant, Cell Environ. 36, 405–418. https://doi.org/10.1111/j.1365-3040.2012.02582.x

Piper, F.I., 2011. Drought induces opposite changes in the concentration of non-structural carbohydrates of two evergreen Nothofagus species of differential drought resistance. Ann. For. Sci. 68, 415–424. https://doi.org/10.1007/s13595-011-0030-1

Poorter, L., Castilho, C. V., Schietti, J., Oliveira, R.S., Costa, F.R.C., 2018. Can traits predict individual growth performance? A test in a hyperdiverse tropical forest. New Phytol. 219, 109–121. https://doi.org/10.1111/nph.15206

Poorter, L., McDonald, I., Alarcon, A., Fichtler, E., Licona, J.-C., Peña-Carlos, M., Sterck, F., Villegas, Z., Sass-klaassen, U., 2010. The importance of wood traits and hydraulic conductance for the performance and life history strategies of 42 rainforest tree species - Poorter - 2009 - New Phytologist - Wiley Online Library. New Phytol. 481–492.

Poorter, L., Rozendaal, D.M.A., Bongers, F., de Almeida-Cortez, J.S., Almeyda Zambrano, A.M., Álvarez, F.S., Andrade, J.L., Villa, L.F.A., Balvanera, P., Becknell, J.M., Bentos,

T. V., Bhaskar, R., Boukili, V., Brancalion, P.H.S., Broadbent, E.N., César, R.G., Chave, J., Chazdon, R.L., Colletta, G.D., Craven, D., de Jong, B.H.J., Denslow, J.S., Dent, D.H., DeWalt, S.J., García, E.D., Dupuy, J.M., Durán, S.M., Espírito Santo, M.M., Fandiño, M.C., Fernandes, G.W., Finegan, B., Moser, V.G., Hall, J.S., Hernández-Stefanoni, J.L., Jakovac, C.C., Junqueira, A.B., Kennard, D., Lebrija-Trejos, E., Letcher, S.G., Lohbeck, M., Lopez, O.R., Marín-Spiotta, E., Martínez-Ramos, M., Martins, S. V., Massoca, P.E.S., Meave, J.A., Mesquita, R., Mora, F., de Souza Moreno, V., Müller, S.C., Muñoz, R., Muscarella, R., de Oliveira Neto, S.N., Nunes, Y.R.F., Ochoa-Gaona, S., Paz, H., Peña-Claros, M., Piotto, D., Ruíz, J., Sanaphre-Villanueva, L., Sanchez-Azofeifa, A., Schwartz, N.B., Steininger, M.K., Thomas, W.W., Toledo, M., Uriarte, M., Utrera, L.P., van Breugel, M., van der Sande, M.T., van der Wal, H., Veloso, M.D.M., Vester, H.F.M., Vieira, I.C.G., Villa, P.M., Williamson, G.B., Wright, S.J., Zanini, K.J., Zimmerman, J.K., Westoby, M., 2019. Wet and dry tropical forests show opposite successional pathways in wood density but converge over time. Nat. Ecol. Evol. 3, 928–934. https://doi.org/10.1038/s41559-019-0882-6

Poyatos, R., Granda, V., Flo, V., Adams, M.A., Adorján, B., Aguadé, D., Aidar, M.P.M., Allen, S., Alvarado-Barrientos, M.S., Anderson-Teixeira, K.J., Aparecido, L.M., Altaf Arain, M., Aranda, I., Asbjornsen, H., Baxter, R., Beamesderfer, E., Berry, Z.C., Berveiller, D., Blakely, B., Boggs, J., Bohrer, G., Bolstad, P. V., Bonal, D., Bracho, R., Brito, P., Brodeur, J., Casanoves, F., Chave, J., Chen, H., Cisneros, C., Clark, K., Cremonese, E., Dang, H., David, J.S., David, T.S., Delpierre, N., Desai, A.R., Do, F.C., Dohnal, M., Domec, J.C., Dzikiti, S., Edgar, C., Eichstaedt, R., El-Madany, T.S., Elbers, J., Eller, C.B., Euskirchen, E.S., Ewers, B., Fonti, P., Forner, A., Forrester, D.I., Freitas, H.C., Galvagno, M., Garcia-Tejera, O., Ghimire, C.P., Gimeno, T.E., Grace, J., Granier, A., Griebel, A., Guangyu, Y., Gush, M.B., Hanson, P.J., Hasselquist, N.J., Heinrich, I.,

Hernandez-Santana, V., Herrmann, V., Hölttä, T., Holwerda, F., Irvine, J., Na Ayutthaya, S.I., Jarvis, P.G., Jochheim, H., Joly, C.A., Kaplick, J., Kim, H.S., Klemedtsson, L., Kropp, H., Lagergren, F., Lane, P., Lang, P., Lapenas, A., Lechuga, V., Lee, M., Leuschner, C., Limousin, J.M., Linares, J.C., Linderson, M.L., Lindroth, A., Llorens, P., López-Bernal, Á., Loranty, M.M., Lüttschwager, D., MacInnis-Ng, C., Maréchaux, I., Martin, T.A., Matheny, A., McDowell, N., McMahon, S., Meir, P., Mészáros, I., Migliavacca, M., Mitchell, P., Mölder, M., Montagnani, L., Moore, G.W., Nakada, R., Niu, F., Nolan, R.H., Norby, R., Novick, K., Oberhuber, W., Obojes, N., Oishi, A.C., Oliveira, R.S., Oren, R., Ourcival, J.M., Paljakka, T., Perez-Priego, O., Peri, P.L., Peters, R.L., Pfautsch, S., Pockman, W.T., Preisler, Y., Rascher, K., Robinson, G., Rocha, H., Rocheteau, A., Röll, A., Rosado, B.H.P., Rowland, L., Rubtsov, A. V., Sabaté, S., Salmon, Y., Salomón, R.L., Sánchez-Costa, E., Schäfer, K.V.R., Schuldt, B., Shashkin, A., Stahl, C., Stojanović, M., Suárez, J.C., Sun, G., Szatniewska, J., Tatarinov, F., TesaÅ™, M., Thomas, F.M., Tor-Ngern, P., Urban, J., Valladares, F., Van Der Tol, C., Van Meerveld, I., Varlagin, A., Voigt, H., Warren, J., Werner, C., Werner, W., Wieser, G., Wingate, L., Wullschleger, S., Yi, K., Zweifel, R., Steppe, K., Mencuccini, M., Martínez-Vilalta, J., 2021. Global transpiration data from sap flow measurements: The SAPFLUXNET database, Earth System Science Data. https://doi.org/10.5194/essd-13-2607-2021

Quentin, Audrey G., Pinkard, E.A., Ryan, M.G., Tissue, D.T., Baggett, L.S., Adams, H.D., Maillard, P., Marchand, J., Landhäusser, S.M., Lacointe, A., Gibon, Y., Anderegg, W.R.L., Asao, S., Atkin, O.K., Bonhomme, M., Claye, C., Chow, P.S., Clément-Vidal, A., Davies, N.W., Dickman, L.T., Dumbur, R., Ellsworth, D.S., Falk, K., Galiano, L., Grünzweig, J.M., Hartmann, H., Hoch, G., Hood, S., Jones, J.E., Koike, T., Kuhlmann, I., Lloret, F., Maestro, M., Mansfield, S.D., Martínez-Vilalta, J., Maucourt, M.,

McDowell, N.G., Moing, A., Muller, B., Nebauer, S.G., Niinemets, Ü., Palacio, S., Piper, F., Raveh, E., Richter, A., Rolland, G., Rosas, T., Joanis, B. Saint, Sala, A., Smith, R.A., Sterck, F., Stinziano, J.R., Tobias, M., Unda, F., Watanabe, M., Way, D.A., Weerasinghe, L.K., Wild, B., Wiley, E., Woodruff, D.R., 2015. Non-structural carbohydrates in woody plants compared among laboratories. Tree Physiol. 35, 1146–1165. https://doi.org/10.1093/treephys/tpv073

Quentin, Audrey G, Pinkard, E.A., Ryan, M.G., Tissue, D.T., Scott Baggett, L., Adams, H.D., Maillard, P., Marchand, J., Landhäusser, S.M., Muller, B., Nebauer, S.G., Niinemets, Ü., Palacio, S., Piper, F., Raveh, E., Richter, A., Rolland, G., Rosas, T., Saint Joanis, B., Sala, A., Smith, R.A., Sterck, F., Stinziano, J.R., Tobias, M., Unda, F., Watanabe, M., Way, D.A., Weerasinghe, L.K., Wild, B., Wiley, E., Woodruff, D.R., 2015. Shinichi Asao 3,4 , Owen K. Atkin 15, 16 , Marc Bonhomme 10, 11 , Caroline Claye 17 , Pak S. Jordi Martínez-Vilalta 35, 13. https://doi.org/10.1093/treephys/tpv073

Reich, P.B., Wright, I.J., Cavender-Bares, J., Craine, J.M., Oleksyn, J., Westoby, M., Walters, M.B., 2003. The evolution of plant functional variation: Traits, spectra, and strategies. Int. J. Plant Sci. 164.

Resco de Dios, V., Gessler, A., 2021. Sink and source co-limitation in the response of stored non-structural carbohydrates to an intense but short drought. Trees - Struct. Funct. 1–4. https://doi.org/10.1007/s00468-021-02116-9

Rito, K.F., Arroyo-Rodríguez, V., Queiroz, R.T., Leal, I.R., Tabarelli, M., 2017. Precipitation mediates the effect of human disturbance on the Brazilian Caatinga vegetation. J. Ecol. 105, 828–838. https://doi.org/10.1111/1365-2745.12712

Rosell, J.A., Piper, F.I., Jiménez-Vera, C., Vergílio, P.C.B., Marcati, C.R., Castorena, M., Olson, M.E., 2021. Inner bark as a crucial tissue for non-structural carbohydrate storage

across three tropical woody plant communities. Plant Cell Environ. 44, 156–170. https://doi.org/10.1111/pce.13903

Rosner, S., Heinze, B., Savi, T., Dalla-Salda, G., 2019. Prediction of hydraulic conductivity loss from relative water loss: new insights into water storage of tree stems and branches. Physiol. Plant. 165, 843–854. https://doi.org/10.1111/ppl.12790

Sala, A., Piper, F., Hoch, G., 2010. Physiological mechanisms of drought-induced tree mortality are far from being resolved. New Phytol. 186, 274–281. https://doi.org/10.1111/j.1469-8137.2009.03167.x

Santana-Vieira, D.D.S., Freschi, L., Da Hora Almeida, L.A., Moraes, D.H.S. De, Neves, D.M., Dos Santos, L.M., Bertolde, F.Z., Soares Filho, W.D.S., Coelho Filho, M.A., Gesteira, A.D.S., 2016. Survival strategies of citrus rootstocks subjected to drought. Sci. Rep. 6, 1–12. https://doi.org/10.1038/srep38775

Santos, V.A.H.F. dos, Ferreira, M.J., Rodrigues, J.V.F.C., Garcia, M.N., Ceron, J.V.B., Nelson, B.W., Saleska, S.R., 2018. Causes of reduced leaf-level photosynthesis during strong El Niño drought in a Central Amazon forest, Global Change Biology. https://doi.org/10.1111/gcb.14293

Santos, W.R. dos, Jardim, A.M. da R.F., Souza, L.S.B. de, Souza, C.A.A. de, Morais, J.E.F. de, Alves, C.P., Araujo Júnior, G. do N., Silva, M.J. da, Salvador, K.R. da S., Silva, M.V. da, Morellato, L.P.C., Silva, T.G.F. da, 2024. Can changes in land use in a semi-arid region of Brazil cause seasonal variation in energy partitioning and evapotranspiration? J. Environ. Manage. 367. https://doi.org/10.1016/j.jenvman.2024.121959

Santos, M., Barros, V., Lima, L., Frosi, G., Santos, M.G., 2021. Whole plant water status and

non-structural carbohydrates under progressive drought in a Caatinga deciduous woody species. Trees. https://doi.org/10.1007/s00468-021-02113-y

Santos, M.G., Oliveira, M.T., Figueiredo, K. V., Falcão, H.M., Arruda, E.C.P., Almeida-Cortez, J., Sampaio, E.V.S.B., Ometto, J.P.H.B., Menezes, R.S.C., Oliveira, A.F.M., Pompelli, M.F., Antonino, A.C.D., 2014. Caatinga, the Brazilian dry tropical forest: Can it tolerate climate changes? Theor. Exp. Plant Physiol. 26, 83–99. https://doi.org/10.1007/s40626-014-0008-0

Schenk, H.J., Steppe, K., Jansen, S., 2015. Nanobubbles: A new paradigm for air-seeding in xylem. Trends Plant Sci. 20, 199–205. https://doi.org/10.1016/j.tplants.2015.01.008

Scoffoni, C., Albuquerque, C., Brodersen, C.R., Townes, S. V., John, G.P., Cochard, H., Buckley, T.N., McElrone, A.J., Sack, L., 2017. Leaf vein xylem conduit diameter influences susceptibility to embolism and hydraulic decline. New Phytol. 213, 1076–1092. https://doi.org/10.1111/nph.14256

Sevanto, S., Mcdowell, N.G., Dickman, L.T., Pangle, R., Pockman, W.T., 2014. How do trees die? A test of the hydraulic failure and carbon starvation hypotheses. Plant, Cell Environ. 37, 153–161. https://doi.org/10.1111/pce.12141

Silva, P.F. da, Lima, J.R. de S., Antonino, A.C.D., Souza, R., de Souza, E.S., Silva, J.R.I., Alves, E.M., 2017. Seasonal patterns of carbon dioxide, water and energy fluxes over the Caatinga and grassland in the semi-arid region of Brazil. J. Arid Environ. 147, 71–82. https://doi.org/10.1016/j.jaridenv.2017.09.003

Silva, K.A., de Souza Rolim, G., de Oliveira Aparecido, L.E., 2022. Forecasting El Niño and La Niña events using decision tree classifier. Theor. Appl. Climatol. 148, 1279–1288. https://doi.org/10.1007/s00704-022-03999-5

Smith, M.G., Miller, R.E., Arndt, S.K., Kasel, S., Bennett, L.T., 2018. Whole-tree distribution and temporal variation of non-structural carbohydrates in broadleaf evergreen trees. Tree Physiol. 38, 570–581. https://doi.org/10.1093/treephys/tpx141

Souza, B.C. de, Carvalho, E.C.D., Oliveira, R.S., de Araujo, F.S., de Lima, A.L.A., Rodal, M.J.N., 2020. Drought response strategies of deciduous and evergreen woody species in a seasonally dry neotropical forest. Oecologia 1, 221–236. https://doi.org/10.1007/s00442-020-04760-3

Souza, B.C. de, Oliveira, R.S., De Araújo, F.S., De Lima, A.L.A., Rodal, M.J.N., 2015. Divergências funcionais e estratégias de resistência à seca entre espécies decíduas e sempre verdes tropicais. Rodriguesia 66, 21–32. https://doi.org/10.1590/2175-7860201566102

Sperry, J.S., 2000. Hydraulic constraints on plant gas exchange. Agric. For. Meteorol. 104, 13–23. https://doi.org/10.1016/S0168-1923(00)00144-1

Steppe, K., Vandegehuchte, M.W., Tognetti, R., Mencuccini, M., 2015. Sap flow as a key trait in the understanding of plant hydraulic functioning. Tree Physiol. 35, 341–345. https://doi.org/10.1093/treephys/tpv033

Tomasella, M., Petrussa, E., Petruzzellis, F., Nardini, A., Casolo, V., 2020. The possible role of non-structural carbohydrates in the regulation of tree hydraulics. Int. J. Mol. Sci. 21. https://doi.org/10.3390/ijms21010144

Tonet, V., Brodribb, T., Bourbia, I., 2024. Variation in xylem vulnerability to cavitation shapes the photosynthetic legacy of drought. Plant Cell Environ. 47, 1160–1170. https://doi.org/10.1111/pce.14788

Venturas, M.D., Sperry, J.S., Hacke, U.G., 2017. Plant xylem hydraulics: What we

understand, current research, and future challenges. J. Integr. Plant Biol. 59, 356–389. https://doi.org/10.1111/jipb.12534

Vico, G., Thompson, S.E., Manzoni, S., Molini, A., Albertson, J.D., Almeida-Cortez, J.S., Fay, P.A., Feng, X., Guswa, A.J., Liu, H., Wilson, T.G., Porporato, A., 2014. Climatic, ecophysiological, and phenological controls on plant ecohydrological strategies in seasonally dry ecosystems. Ecohydrology 8, 660–681. https://doi.org/10.1002/eco.1533

Wang, L., Dai, Y., Guo, J., Gao, R., Wan, X., 2016. Interaction of hydraulic failure and carbon starvation on Robinia pseudoacacia seedlings during drought. Linye Kexue/Scientia Silvae Sin. 52, 1–9. https://doi.org/10.11707/j.1001-7488.20160601

Westoby, M., Falster, D.S., Moles, A.T., Vesk, P.A., Wright, I.J., 2002. Plant ecological strategies: Some leading dimensions of variation between species. Annu. Rev. Ecol. Syst. 33, 125–159. https://doi.org/10.1146/annurev.ecolsys.33.010802.150452

Will, R.E., Wilson, S.M., Zou, C.B., Hennessey, T.C., 2013. Increased vapor pressure deficit due to higher temperature leads to greater transpiration and faster mortality during drought for tree seedlings common to the forest-grassland ecotone. New Phytol. 200, 366–374. https://doi.org/10.1111/nph.12321

Wright, C.L., de Lima, A.L.A., de Souza, E.S., West, J.B., Wilcox, B.P., 2021. Plant functional types broadly describe water use strategies in the Caatinga, a seasonally dry tropical forest in northeast Brazil. Ecol. Evol. 11, 11808–11825. https://doi.org/10.1002/ece3.7949

Wright, C.L., West, J.B., de Lima, A.L.A., Souza, E.S., Medeiros, M., Wilcox, B.P., 2023. Contrasting water-use strategies revealed by species-specific transpiration dynamics in the Caatinga dry forest. Tree Physiol. 1–15. https://doi.org/10.1093/treephys/tpad137

Würth, M.K.R., Peláez-Riedl, S., Wright, S.J., Körner, C., 2005. Non-structural carbohydrate pools in a tropical forest. Oecologia 143, 11–24. https://doi.org/10.1007/s00442-004-1773-2

Yang, B., Peng, C., Harrison, S.P., Wei, H., Wang, H., Zhu, Q., Wang, M., 2018. Allocation mechanisms of non-structural carbohydrates of Robinia pseudoacacia L. Seedlings in response to drought and waterlogging. Forests 9, 1–16. https://doi.org/10.3390/f9120754

Yu, T., Feng, Q., Si, J., Pinkard, E.A., 2019. Coordination of stomatal control and stem water storage on plant water use in desert riparian trees. Trees - Struct. Funct. 33, 787–801. https://doi.org/10.1007/s00468-019-01816-7

Zhang, T., Cao, Y., Chen, Y., Liu, G., 2015a. Non-structural carbohydrate dynamics in Robinia pseudoacacia saplings under three levels of continuous drought stress. Trees - Struct. Funct. 29, 1837–1849. https://doi.org/10.1007/s00468-015-1265-5

Zhang, T., Cao, Y., Chen, Y., Liu, G., 2015b. Non-structural carbohydrate dynamics in Robinia pseudoacacia saplings under three levels of continuous drought stress. Trees - Struct. Funct. 29, 1837–1849. https://doi.org/10.1007/s00468-015-1265-5

Zuidema, P.A., Babst, F., Groenendijk, P., Trouet, V., Abiyu, A., Acuña-Soto, R., Adenesky-Filho, E., Alfaro-Sánchez, R., Aragão, J.R.V., Assis-Pereira, G., Bai, X., Barbosa, A.C., Battipaglia, G., Beeckman, H., Botosso, P.C., Bradley, T., Bräuning, A., Brienen, R., Buckley, B.M., Camarero, J.J., Carvalho, A., Ceccantini, G., Centeno-Erguera, L.R., Cerano-Paredes, J., Chávez-Durán, Á.A., Cintra, B.B.L., Cleaveland, M.K., Couralet, C., D'Arrigo, R., del Valle, J.I., Dünisch, O., Enquist, B.J., Esemann-Quadros, K., Eshetu, Z., Fan, Z.X., Ferrero, M.E., Fichtler, E., Fontana, C., Francisco, K.S., Gebrekirstos, A., Gloor, E., Granato-Souza, D., Haneca, K., Harley, G.L., Heinrich, I., Helle, G., Inga, J.G., Islam, M., Jiang, Y. mei, Kaib, M., Khamisi, Z.H., Koprowski, M., Kruijt, B.,

Layme, E., Leemans, R., Leffler, A.J., Lisi, C.S., Loader, N.J., Locosselli, G.M., Lopez, L., López-Hernández, M.I., Lousada, J.L.P.C., Mendivelso, H.A., Mokria, M., Montóia, V.R., Moors, E., Nabais, C., Ngoma, J., Nogueira Júnior, F. de C., Oliveira, J.M., Olmedo, G.M., Pagotto, M.A., Panthi, S., Pérez-De-Lis, G., Pucha-Cofrep, D., Pumijumnong, N., Rahman, M., Ramirez, J.A., Requena-Rojas, E.J., Ribeiro, A. de S., Robertson, I., Roig, F.A., Rubio-Camacho, E.A., Sass-Klaassen, U., Schöngart, J., Sheppard, P.R., Slotta, F., Speer, J.H., Therrell, M.D., Toirambe, B., Tomazello-Filho, M., Torbenson, M.C.A., Touchan, R., Venegas-González, A., Villalba, R., Villanueva-Diaz, J., Vinya, R., Vlam, M., Wils, T., Zhou, Z.K., 2022. Tropical tree growth driven by dry-season climate variability. Nat. Geosci. 15, 269–276. https://doi.org/10.1038/s41561-022-00911-8

Table and Figures

Table 1. Characteristics for the selected species, including stem-specific wood density (WD), diameter close to the ground (D), and tree height (HT). *Denotes species which we observed to be multi-stemmed. [a]Values obtained from Lima et al (2012).

Species	Family	WD (g cm^{-3})	D (cm)	HT (cm)
Commiphora leptophloeos (Mart.) J.B.Gillett	Burseraceae	0.32±0.06	30.3±9.3	5.46±0.95
Spondias tuberosa Arruda*	Anacardiaceae	0.49±0.02[a]	78.9±37.8	5.63±0.95
Amburana cearensis (Allemao) A.C.Sm.	Fabaceae	0.51±0.09	13.84±3.4	4.00±0.90
Sarcomphalus joazeiro (Mart.) Hauenshild*	Rhamnaceae	0.62±0.01[a]	21.0±6.4	5.45±0.44
Cenostigma pyramidale (Tul.) Gagnon & G. P. Lewis	Fabaceae	0.69±0.09	12.0±2.0	5.84±1.35
Aspidosperma pyrifolium Mart. & Zucc.	Apocynaceae	0.74±0.04	9.3±2.1	2.90±0.15

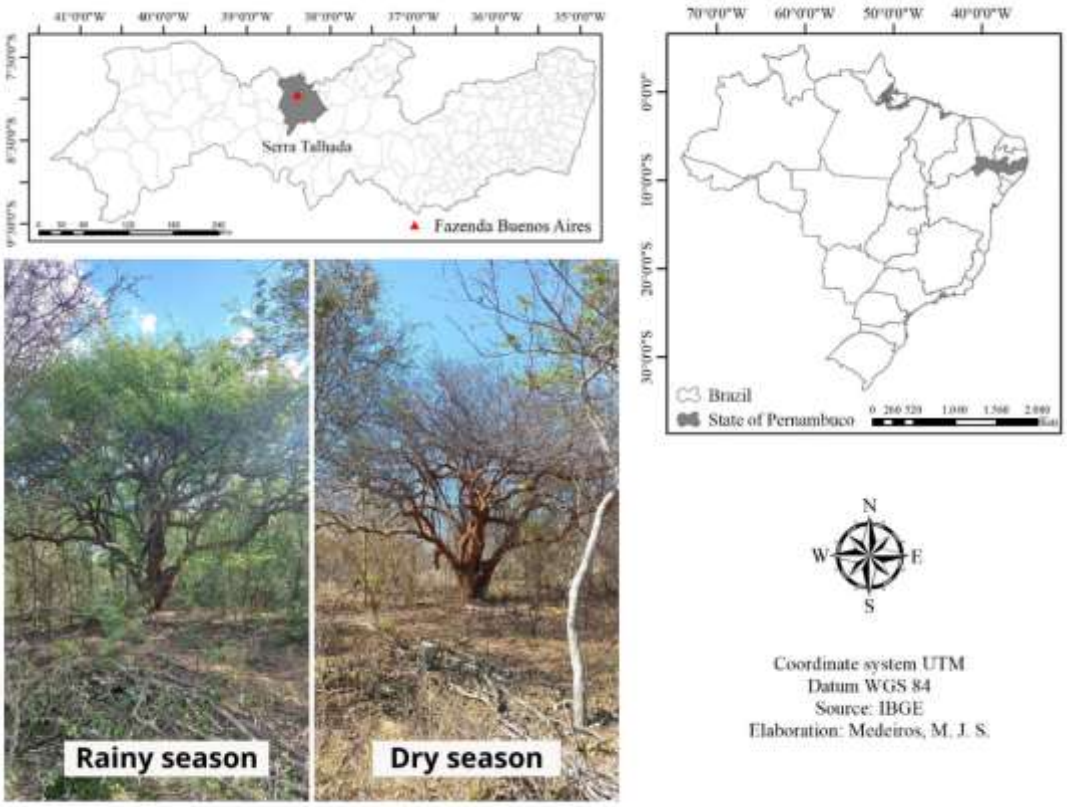

Figure 1. Map of the study area and photos of *Commiphora leptophloeos* taken at Fazenda Buenos Aires Farm, Serra Talhada-PE, Brazil during the rainy season (left; photo taken in January) and the dry seasons (right; photo taken in September). Photo credit: M. Medeiros.

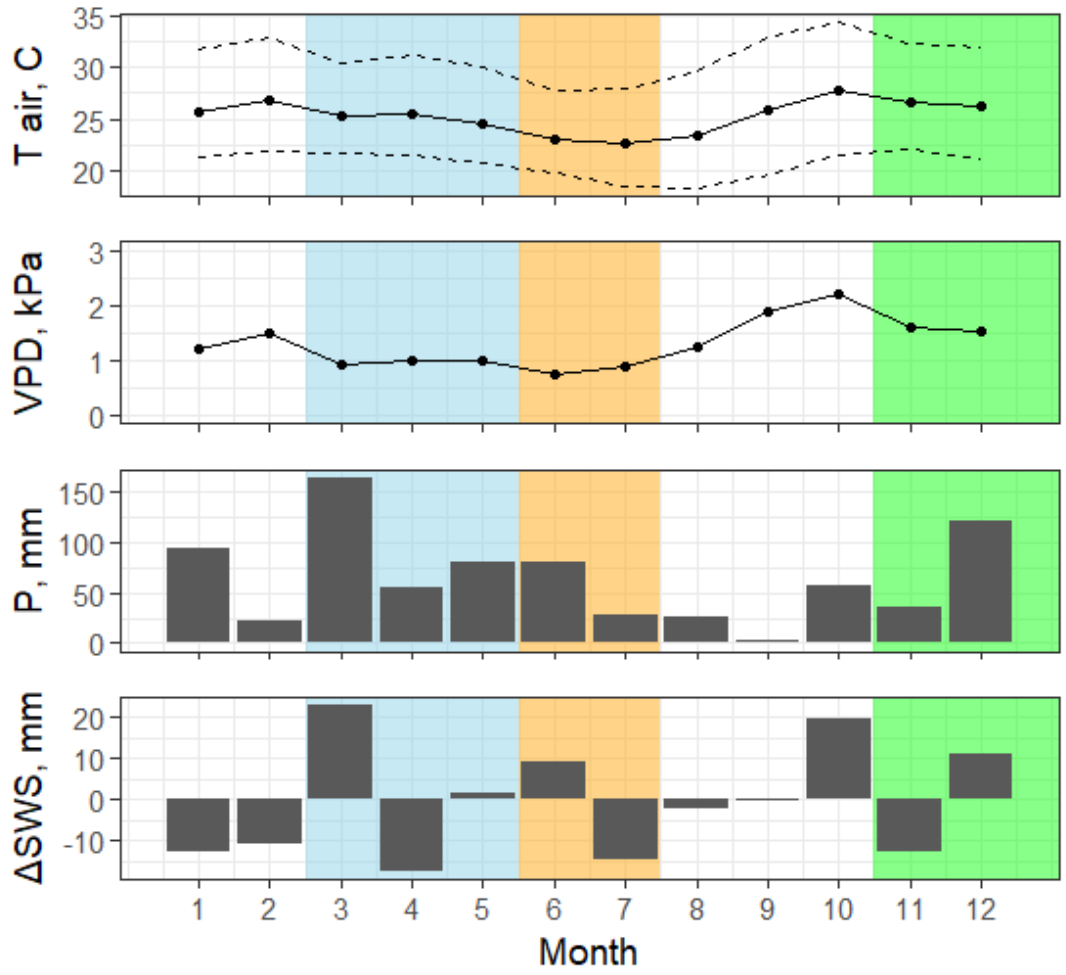

Figure 2. Monthly average air temperature (T air, C) with average daily minimum and maximum (dashed lines), monthly average vapor pressure deficit (VPD, kPa), monthly total change in soil water storage (ΔSWS, mm) in the top 40 cm, and monthly total precipitation (P, mm) from January to December 2022 at Fazenda Buenos Aires near Serra Talhada, PE, Brazil. Periods are denoted as: rainy in blue, transition in orange, and first rains in green.

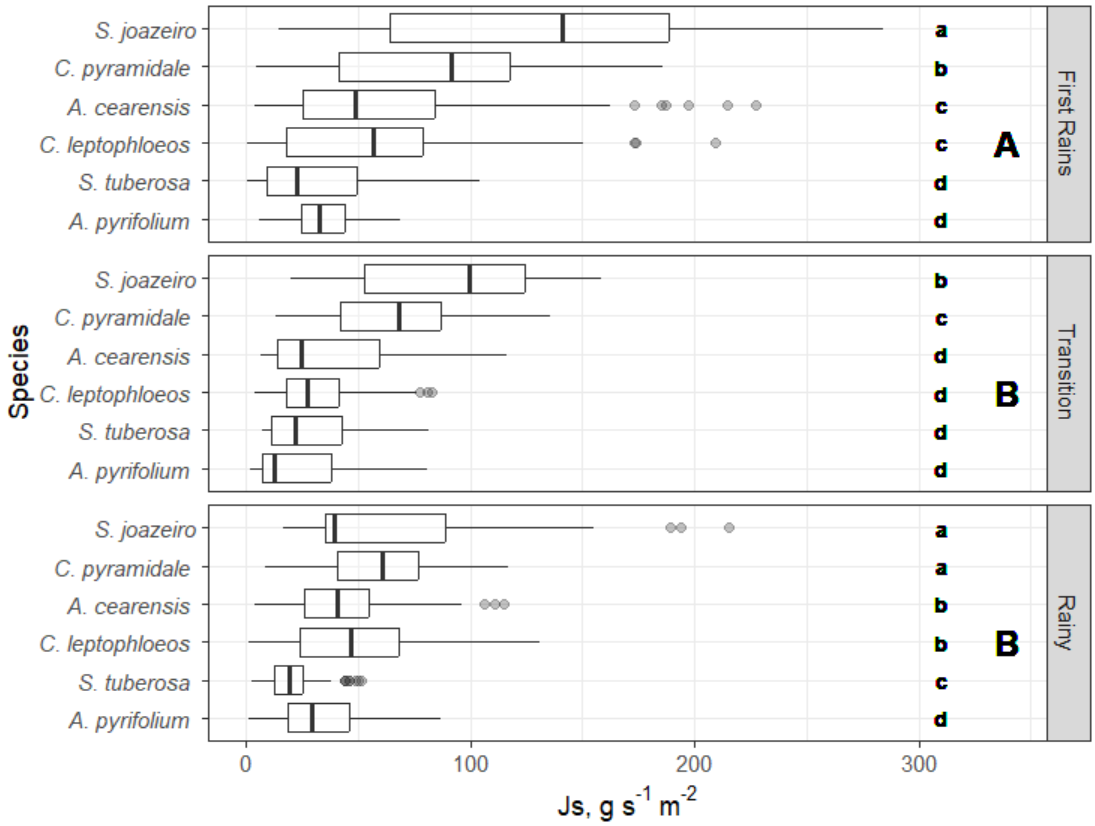

Figure 3. Daily peak average of sap velocity (Js) from the time window 11:00 to 15:00 in individuals of each species during the periods: rainy (Mar. 19 to May 31, 2022), transition to dry season (Jun. 1 to Jul. 19, 2022), and the first rains of the next rainy (Nov. 9 to Dec. 31, 2022). Significant differences between species within each period are denoted by small. Significant differences between the three periods are denoted by larger letters. Statistical results are summarized in Supporting Information S1: Table S1.

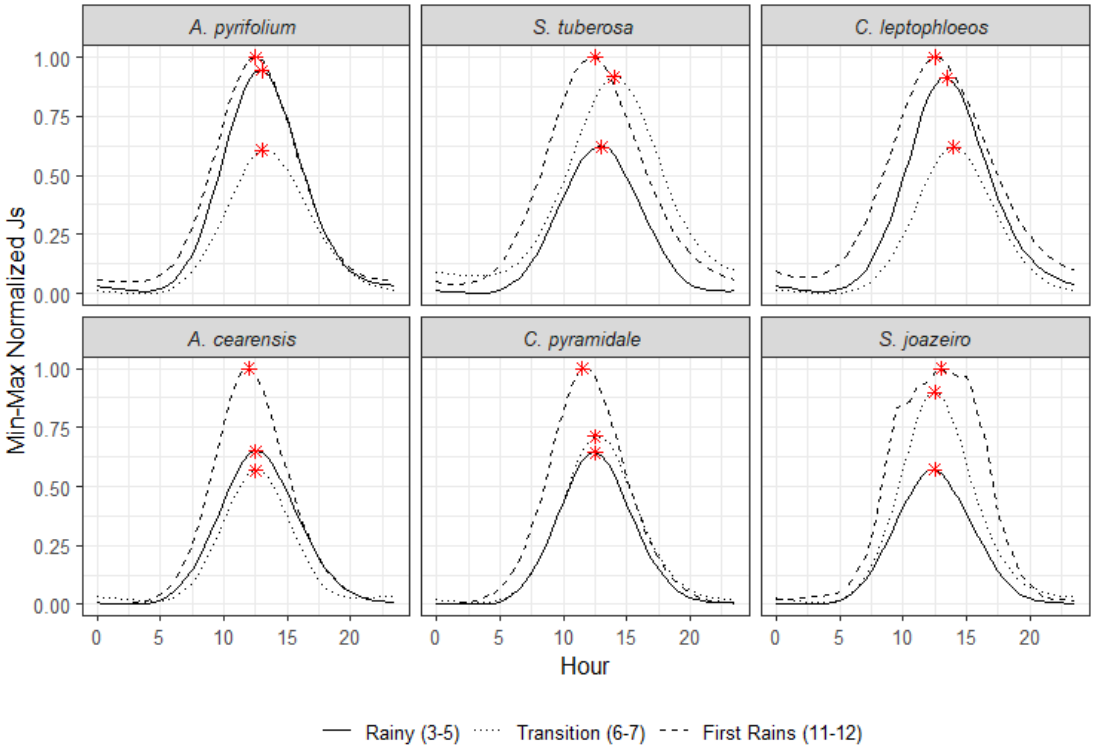

Figure 4. Average diurnal pattern of min-max normalized sap velocity by species during the periods: rainy (Mar. 19 to May 31, 2022), transition to dry season (Jun. 1 to Jul. 19, 2022), and the first rains of the next rainy (Nov. 9 to Dec. 31, 2022). The red star denotes the timing of peak sap velocity, as noted in Supporting Information S1: Table S2.

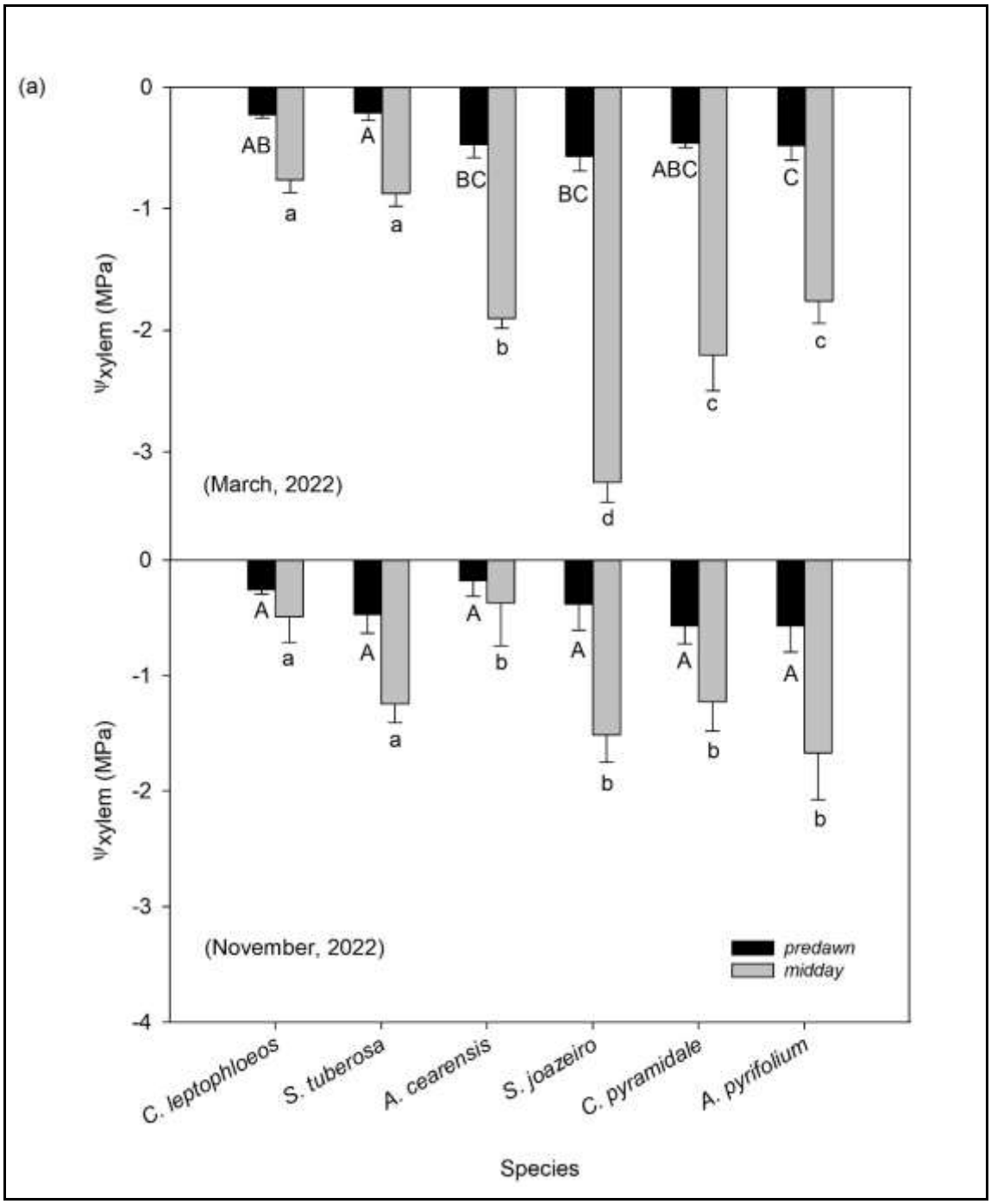
(a)
Ψxylem (MPa)
0
-1
-2
-3
AB
a
A
a
BC
b
BC
d
ABC
c
C
c
(March, 2022)
0
-1
-2
-3
-4
A
a
A
a
A
b
A
b
A
b
A
b
(November, 2022)
predawn
midday
C. leptophloeos
S. tuberosa
A. cearensis
S. joazeiro
C. pyramidale
A. pyrifolium
Species

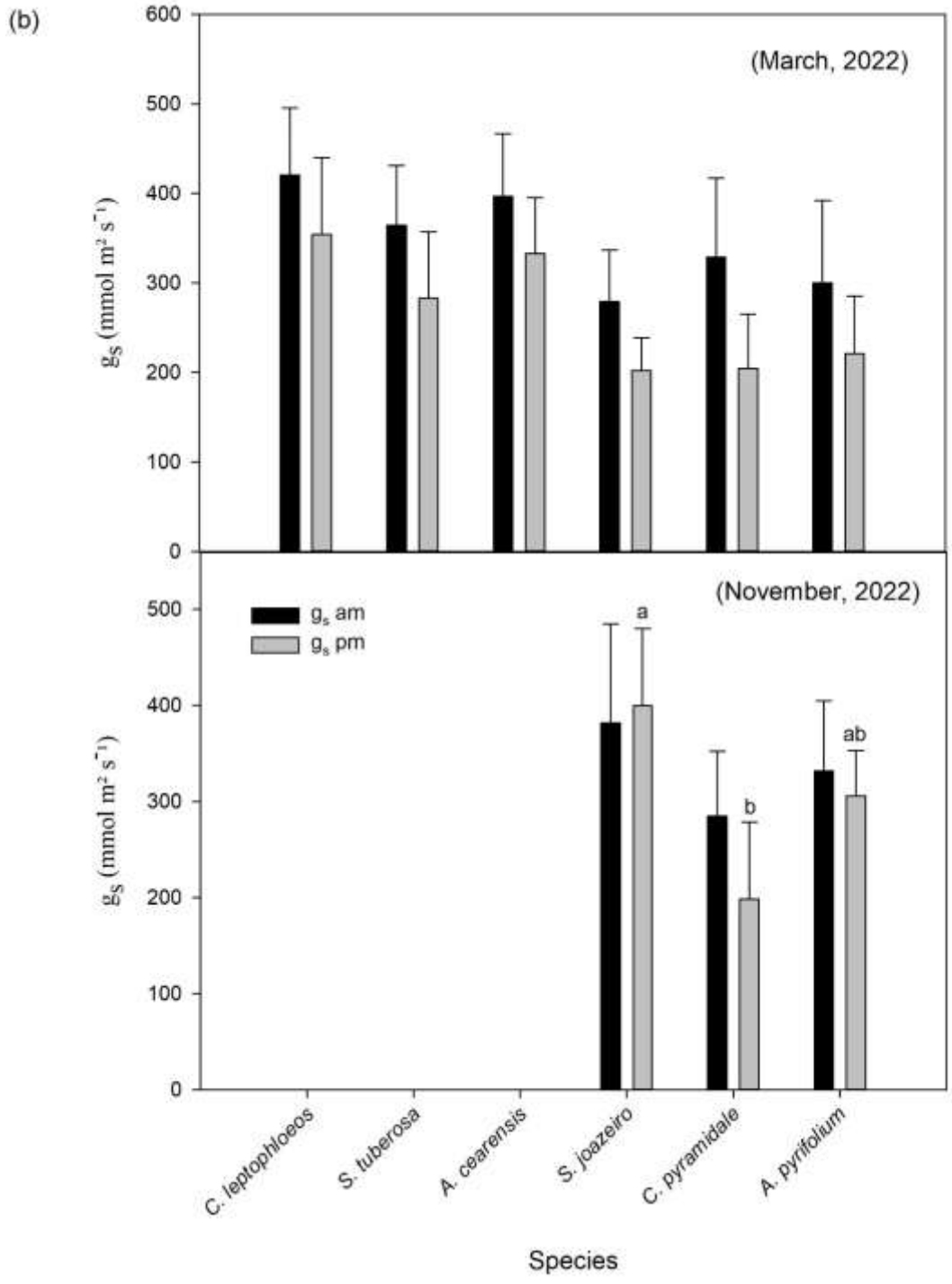

Figure 5. (a) Xylem water potential (Ψ_{xylem}) of species in predawn and midday, and (b) Stomatal conductance (g_s) of the species in the am (9:00 to 10:00) and pm (14:00 to 15:00) on March 25, 2022 (rainy period) and November 3, 2022 (dry period), 2022, municipality of Serra Talhada-Pernambuco, Brazil. Uppercase letters compare predawn and lowercase letters compare midday values between species, at the 5% level of probability by Tukey's test.

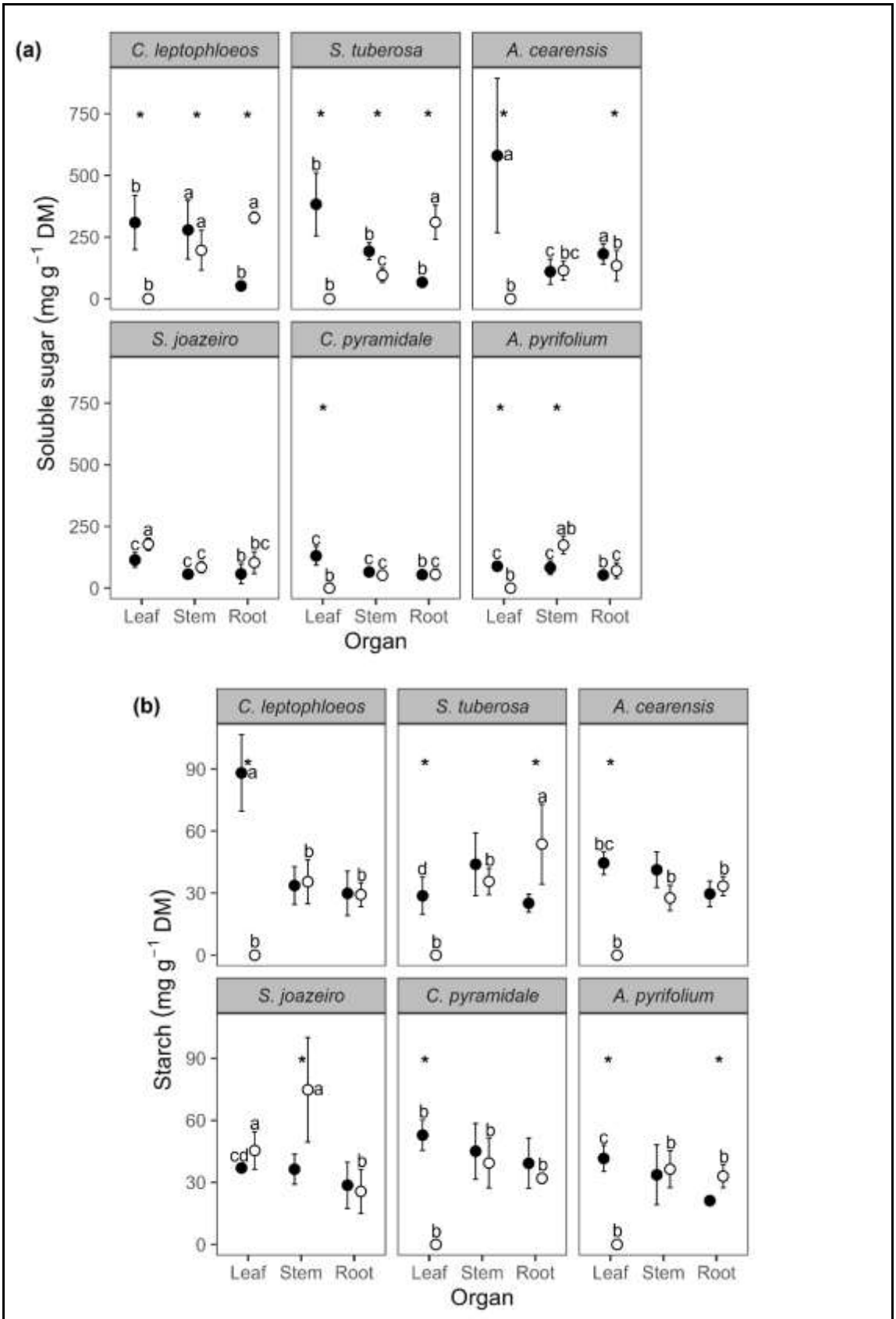

Figure 6. (a) Concentration of Soluble sugar (SS), and (b) starch in different plant organs

(leaf, stem, root) measured on April 9, 2022 (rainy period) and Oct 19, 2022 (dry period), in Serra Talhada, State of Pernambuco, Brazil. Filled points represent rainy period and unfilled points represent dry period. * Denotes difference between periods for each species and small letters denotes difference between species within each organ and in each period by Tukey's test ($p<0.05$).

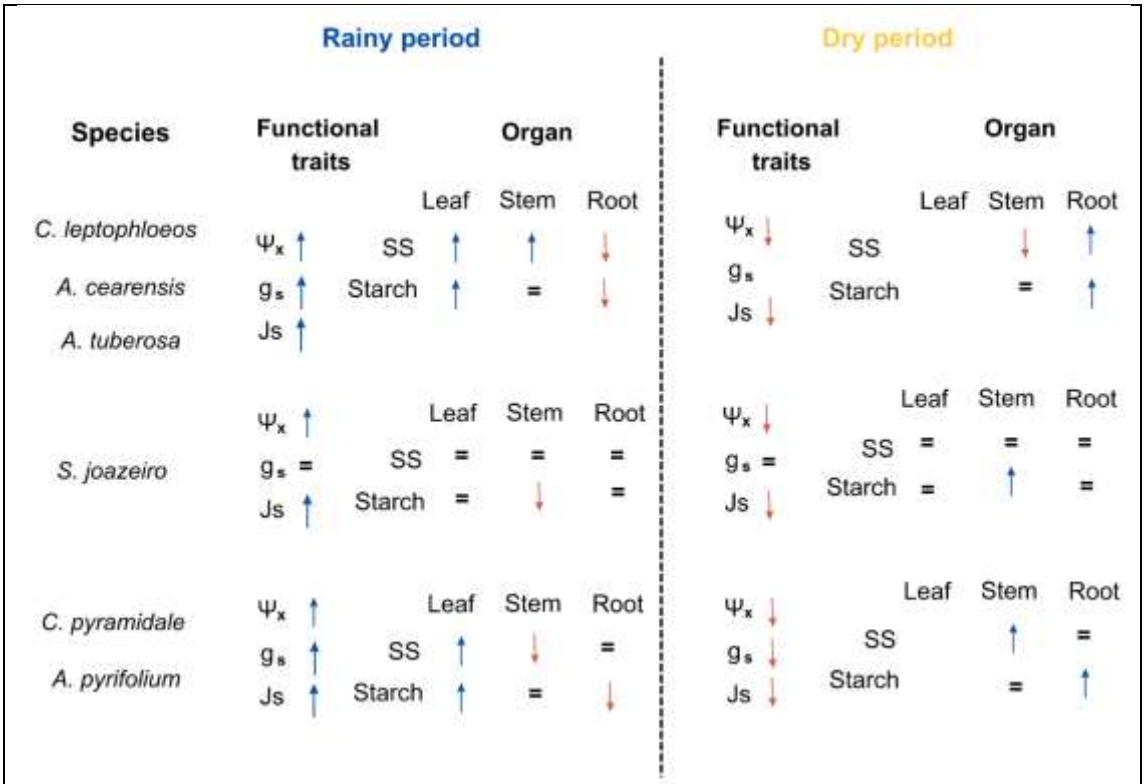

Summary of functional traits in each species and between the rainy and dry periods in the year 2022 in the Caatinga dry forest. Blue arrow pointing up indicates it was higher; red down arrow indicates that it was smaller, and '=' sign indicates that there is no difference between the seasons. Absence of arrow or '=' sign indicates that these traits were not measured in the dry period due to leaf loss. Ψx , xylem water potential; gs, stomatal conductance; J s, sap velocity; SS, soluble sugar.

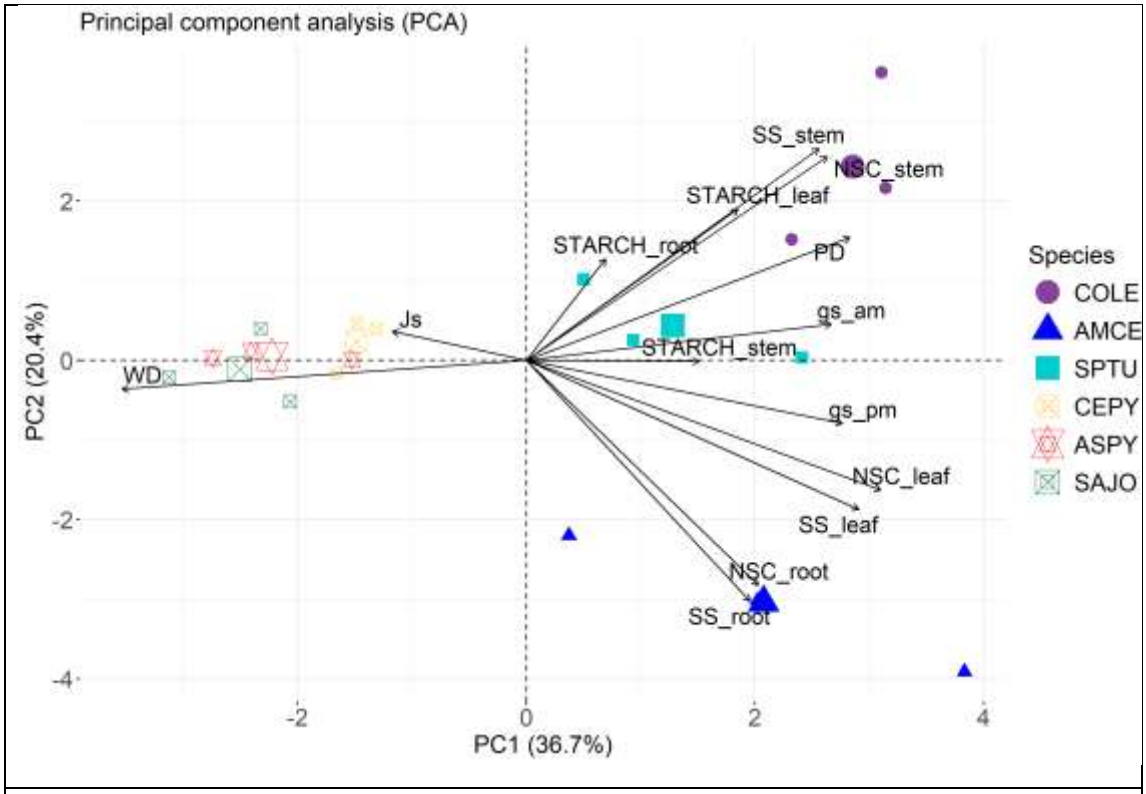

Figure 8. Principal Component Analysis - PCA by species: *C. leptophloeos* (COLE), *A. cearensis* (AMCE), *S. tuberosa* (SPTU), *C. pyramidale* (CEPY), *A. pyrifolium* (ASPY), *S. joazeiro* (SAJO). Js: average sap velocity, WD: wood density; gs_am: Stomatal Conductance in the morning; gs_pm: Stomatal Conductance in the afternoon; PD: xylem water potential in predawn; NSC_leaf: Leaf non-structural carbohydrates; NSC_stem: Stem non-structural carbohydrates; NSC_root: Root non-structural carbohydrates; SS_leaf: Leaf Soluble sugar; SS_Stem: Stem Soluble sugar; SS_root: Root Soluble sugar; STARCH_leaf: Leaf Starch; STARCH_stem: Stem Starch; STARCH_root: Root Starch.

Supporting Information

Table S1. Linear mixed effect model results.

Table S2. Timing of maximum sap velocity (Js) during the period (Mar 19 to May 31, 2022);

Species	**Js peak, rainy season (h:m)**	**Shift, transition (h)**	**Shift, first rains (h)**
A. cearensis	12:30 PM	0.0	0.5
C. leptophloeos	1:30 PM	-0.5	1.0
S. tuberosa	1:30 PM	-1.0	0.5
S. joazeiro	12:30 PM	0.0	-0.5
C. pyramidale	12:30 PM	0.0	1.0
A. pyrifolium	1:00 PM	0.0	0.5

in hour:minutes), and average temporal shifts (in hours) in subsequent transition to transition to dry period (Jun 1 to Jul 19, 2022), and the first rains of the next rainy period (Nov 9 to Dec 31, 2022).

Model	F-statistic	p-value
Js ~ Sps, Rainy season only	79.5	<0.0001
Js ~ Sps, Transition season only	109.6	<0.0001
Js ~ Sps, First Rains season only	102.9	<0.0001
Js ~ Season (across seasons)	110.0	<0.0001

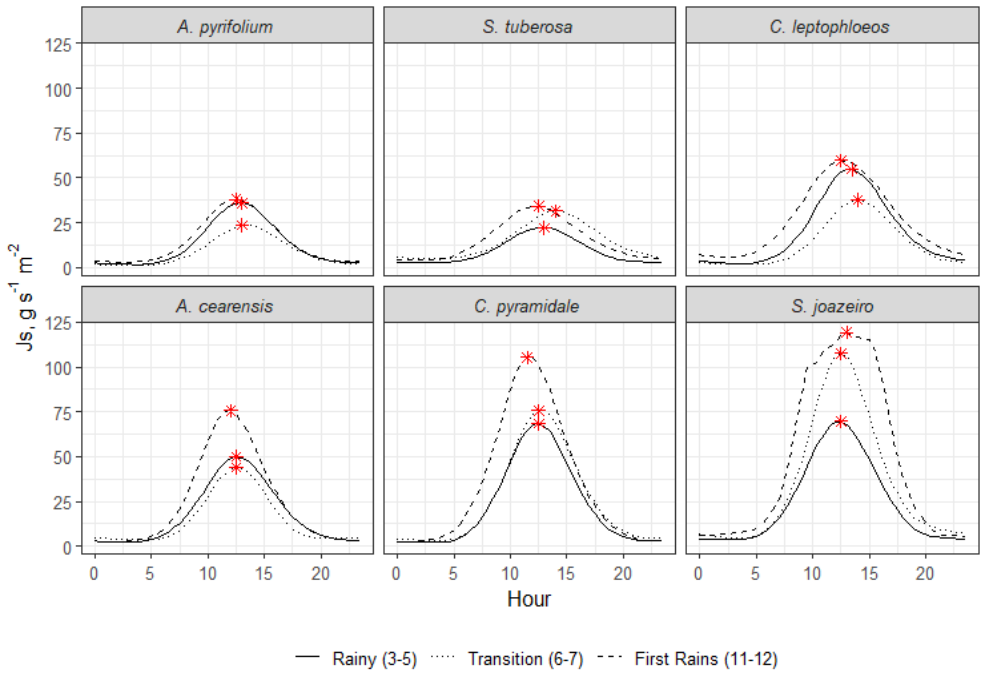

Figure S1. Average diurnal pattern of absolute sap velocity by species during the periods: rainy (Mar. 19 to May 31, 2022), transition to dry season (Jun. 1 to Jul. 19, 2022), and the first rains of the next rainy (Nov. 9 to Dec. 31, 2022). The red star denotes the timing of peak sap velocity, as noted in Supporting Information S1: Table S2.

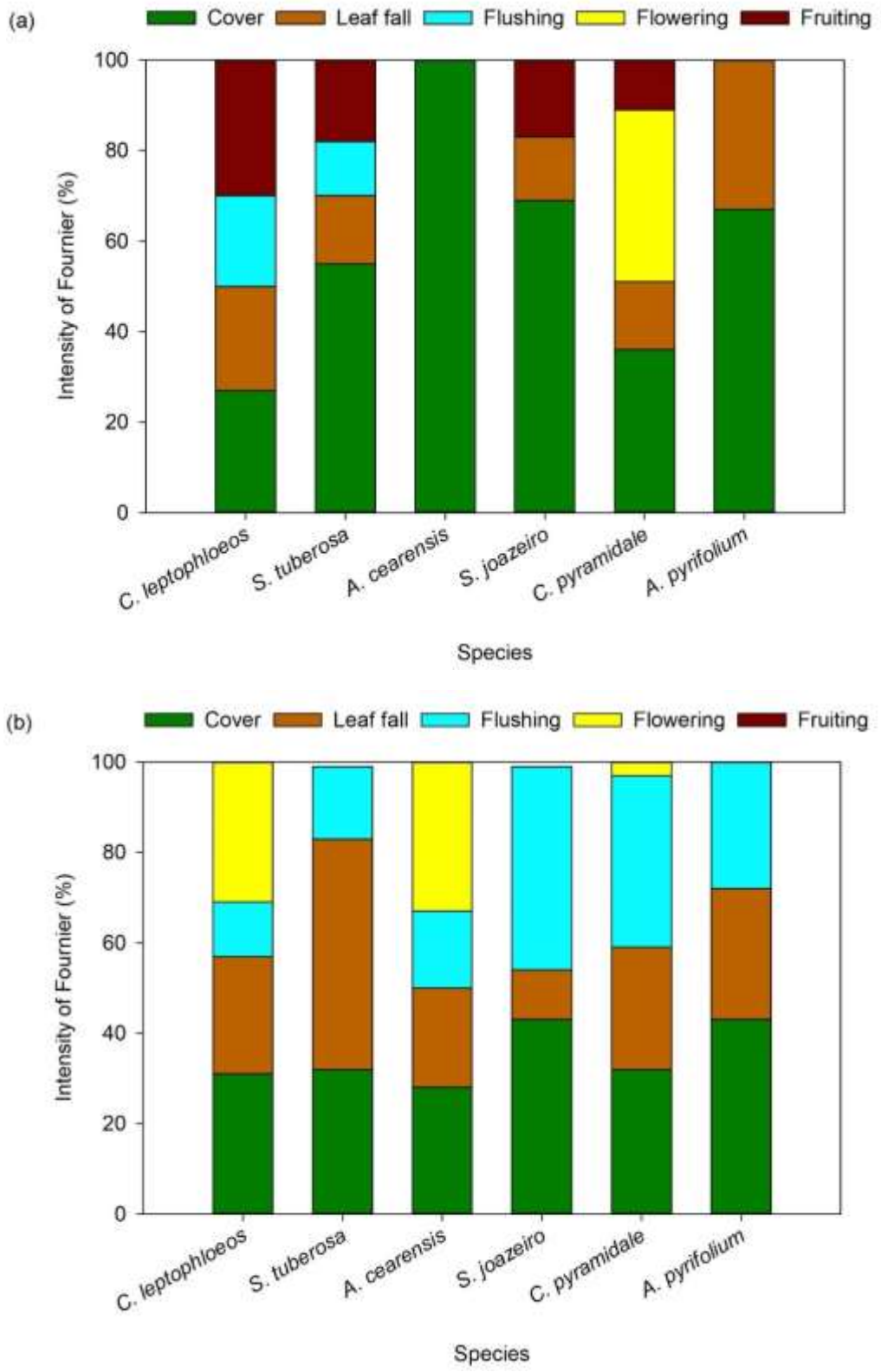

Figure S2. Fournier intensity for species. (a) March 25, 2022 (rainy period) and November 3, 2022 (dry period), near the municipality of Serra Talhada-Pernambuco, Brazil.

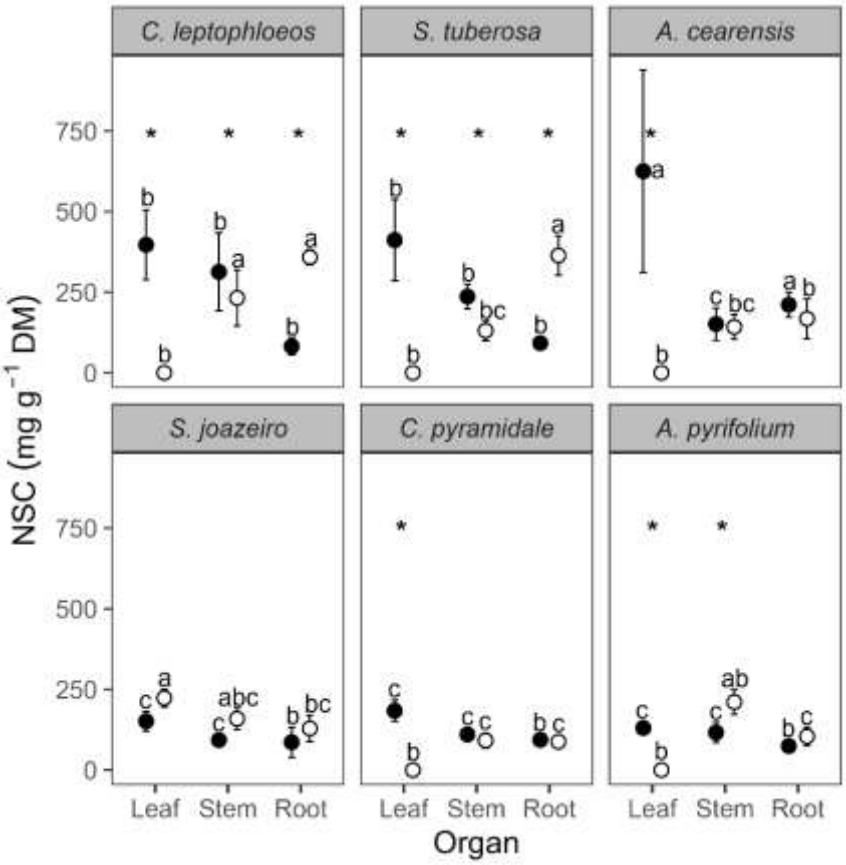

Figure S3. Concentration of non-structural carbohydrates (NSC) in different plant organs. Data were collected on March 25, 2022 (rainy period) and November 3, 2022 (dry period), near the municipality of Serra Talhada-Pernambuco, Brazil. Filled points represent rainy period and unfilled points represent dry period. * Denotes difference between periods for each species and different letters denotes difference between species within each organ and in each period by Tukey's test ($p<0.05$).